UNIVERSITA' DEGLI STUDI DI MILANO – BICOCCA

SCUOLA DI DOTTORATO DI SCIENZE

Facoltà di Scienze Matematiche, Fisiche e Naturali

Corso di Dottorato di Ricerca in Scienze Chimiche XIX ciclo

Development of new potential antitumor drugs based on Ras protein inhibition

Tutor: Prof. Francesco Nicotra
Co-Tutor: Dott. Francesco Peri

Cristina Airoldi

Dipartimento di Biotecnologie e Bioscienze

Anno Accademico 2005-2006

INDEX

INTRODUCTION AND GENERAL BACKGROUND

_____

EXPERIMENTAL SECTION

_____

Index

_____

INTRODUCTION

AND GENERAL BACKGROUND

1. Ras proteins, cell cycle and tumorigenesis

1.1. Ras proteins

1.1.1. Ras proteins are small GTP-binding proteins

Ras proteins are ubiquitarian in eukaryotic species. They belong to a superfamily of intracellular molecules named **small GTP-binding proteins** (SGP). Nowadays, almost 100 members of this superfamily are known, presenting a high degree of both structural and functional correlations.[1] The main feature of G proteins is their capability of binding the nucleotide GTP and, thanks to their *intrinsic GTPasic activity*, hydrolyzing it to GDP. Ras proteins are therefore able to pass from an active GTP-bound form to an inactive GDP-bound form. The self-turn-off mechanism, a sort of intramolecular negative feed-back, allows the activated protein to return to its inactive state. Their possibility to alternate quickly between the active and the inactive state makes Ras proteins *molecular switches* for different transduction pathways. The different signaling pathways proceed from specific trans-membrane *growth factor receptors*. These receptors, once activated through their extracellular domain interaction with specific ligands (such as PDGF, EGF, IL2), make dimers and undergo to auto-phosphorylation (each subunit is responsible for the trans-phosphorylation of the other on specific cytoplasmic domain tyrosin residues) by their *intrinsic*

---

[1] Shurmann A., Brauers A., Maβmann S., Becker W., Joost h. G., "Cloning a new family of mammalian GTP-binding proteins with remote similarity to the Ras-related GTPases", *J. Biol. Chem.*, **1996**, 270, 28, 982-988.

tyrosine-kinasic activity. The new phosphorylated residues are sites of recruitment for *adaptor proteins*, such as Gbr2.[2] Gbr2, like other proteins of this class, contains an SH2 (SRC homology region 2) domain that recognizes and binds the phosphorilated sequence pTyr-X-Asn-Val. Gbr2 also presents two SH3 (SRC homology region 3) domains, able to bind sequences rich in proline residues with high affinity; these domains are responsible for Gbr2 binding to **GEFs** (Guanine Nucleotide Exchange Factors) proteins, requested for Ras protein activation (Fig. 1-1).[3]
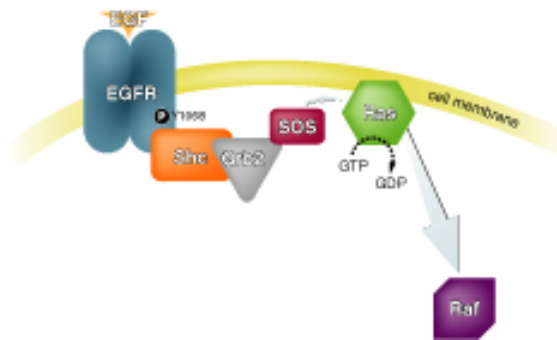
Figure 1-1. The activated membrane-spanning epidermal growth factor receptor (EGFR) becomes a platform for the assembly of a signaling complex that includes the cytoplasmic growth factor receptor bound protein 2 (Grb2) and son of sevenless (SOS), which activates the membrane-bound GTPase, Ras.

As Ras affinity for GDP is higher than for GTP, the inactive Ras-GDP complex accumulates inside the cell. GEFs are citoplasmatic proteins that act as GDP/GTP exchangers, promoting the conversion of the GDP-bound form into the GTP-bound form. In particular, they allow GDP release and consequent Ras binding to GTP, whose intracellular concentration is higher. Among mammalian GEFs, Sos is the most characterised. According to the proposed

---

[2] Van Blesen T., Hawes B. E., Luttrell D. K., Krueger K. M., Touhara K., Porfflri E., Sakaue M., Luttrell L. M., Lefkowitz R. J., "Receptor tyrosin-kinase- and G beta gamma-mediated MAP kinase activation by a common signaling pathway", *Nature*, **1995**, 376, 781-784.

[3] Rozakis-Adcock M., Fernley R., Wade J., Pawson T., Bowtell D., "The SH2 and SH3 domains of mammalian Gbr2 couple the EGF receptor to the Ras activator mSos1", *Nature*, **1993**, 363,83-85.

_____

model, Gbr2 and Sos are thought to be pre-associated into cytoplasm; receptor phosphorylation recruits Gbr2-Sos complex at the cytoplasmic membrane; as Ras is anchored to the membrane inner side through an hydrophobic tail (its C-terminus is usually farnesylated), Gbr2-Sos complex recruiment is fundamental because it promotes the interaction between Sos and Ras, interaction that allows Ras activation. After the binding to GTP, Ras hydrolizes the nucleotide slowly, turning off the signalling pathway. Ras enzymatic activity is increased by GTPase activating proteins called **GAPs** (GTPasi Activating Proteins), that promote GTP hydrolysis to GDP (Fig. 1-2).[4]
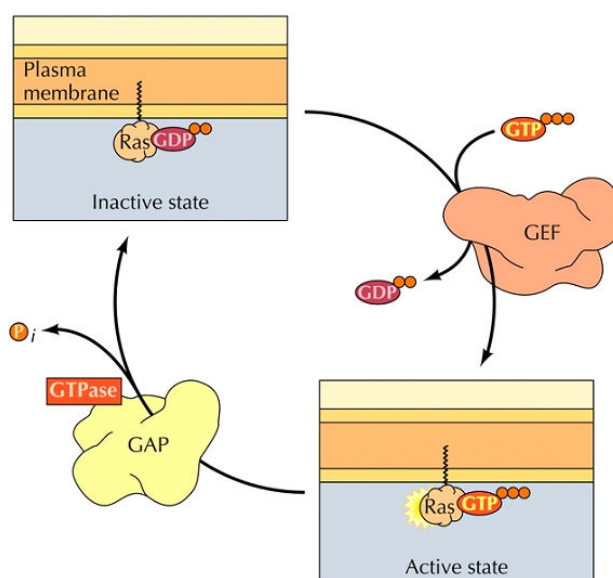
Figure 1-2. The Ras protein function of "molecular switches" takes play through the reversible passage between the active state bound to GTP (on) and that inactive one bound to GDP (off). Their activity is specifically regulated by GEFs proteins, that promote the nucleotide exchange GTP/GDP and therefore Ras activation, and by GAPs proteins, that stimulate GTP hydrolysis and then Ras inactivation.

Several Ras effectors have been so far identified. The most characterized pathway is mediated by the protein-kinase **Raf**; it consists in an activation cascade of serine/threonine kinases: Raf contains an N-terminal binding site

_____

[4] Boguski M.S., McCormick F., "Proteins regulating Ras and its relatives", *Nature*, **1993**, 366, 643-654.

_____

(CR1) with which binds the activated form of Ras and a C-terminal serine/threonine kinase domain (CR2) through which it phopsphorylates and activates the MEK kinase (Mitogen-activated Extracellular receptor-regulated Kinase), a MAP kinase kinase, that, in turn, phopsphorylates and activates the MAP chinase ERK. ERK finally moves to the nucleus and interacts with various physiological targets, among which the transcriptional factors codified by proto-oncogens such as **Myc**, **Jun** and **Fos**. The final result is the expression of genes responsible for the overcoming of the restriction point between the G1 phase and the S phase of the cellular cycle, that alllows DNA duplication and therefore cell proliferation.[5] During the last few years, however, it has been demonstrated that Ras can also activate the phosphatidylinositol-3-kinase (PI-3K) signaling pathway, interfere with Rac and Rho pathways, causing cytoskeleton changes, bind the Ral-guanine nucleotide dissociation stimulator.[6,7,8]

Moreover, recent hypotheses support the possibility that Ras is activated by receptors coupled to trimeric G proteins, through a mechanism that involves their βγ subunits.

Therefore, Ras can be considered a crucial signaling point at which informations from a great number of sources (several growth factors) reach, are transformed in signals and transmitted to many transduction pathways, generating multiple intracellular answers. For this reason, mutations in Ras genes have deep effects on cell growth and proliferation.

---

[5] Zhang X. F., Settleman J., Kyriakis J., Takeuchi-Suzuki E., Elledge S. J., Marshall M. S., Bruder J. T., Rapp U. R. & Avruch J., "Normal and oncogenic p21ras proteins bind to the amino-terminal regulatory domain of c-Raf-1", *Nature*, **1993**, 364, 308-3013.

[6] Rodriguez-Viciana P., Downward J. , "Activation of PI-3-kinase by interaction with Ras and by point mutation", *EMBO J.*, **1996**, 15, 2442-2451.

[7] Kikuchi A., Demo S. D., Ye Z. H., Chen Y. W., and Williams L. T., et al., "RalGDS family members interact with the effector loop of Ras", *Mol. Cell. Biol.*, **1994**, 14, 7483-7491.

[8] Wittinghofer A. and Herrmann C., "Ras-effector interactions, the problem of specificity", *Fedn Eur. biochem. Socs. Lett.*, **1995**, 369, 52-56.

1.1.2. Mammalian Ras proteins isoforms

Three Ras genes are translated in four proteins, having a molecular weight of 21 kDa (**p21Ras**), **Harvey-Ras** (**H-Ras**), **Neuroblastoma-Ras** (**N-Ras**), **Kirsten-Ras** (**K-Ras 4A**, **K-Ras 4B**), being the last two splicing variants of a single gene. With the exception of K-Ras 4B, that it is constituted of 189 amino acids, the Ras proteins are composed by 188 residues.[9] Sequences are identical for the first 86 amino acids, that include effector binding site, and present a high homology degree until residue 165. Differences in the sequence are present in the C-terminal region, that in consequence of this is called *iper-variability region*. Each of these proteins presents however the **CAAX-box** (with C = Cys, A = aliphatic amino acid, X = Met/Ser) that is farnesylated during the post-translational processing. The post-translational farnesylation is responsible for Ras localization at the cytoplasmic membrane (Fig. 1-3).

Structure of Ras isoforms. ◖= regions responsible for guanine nucleotide binding. ● = effector binding site. □ = Effector/GAP interaction site. ▨ = GEF interaction site.
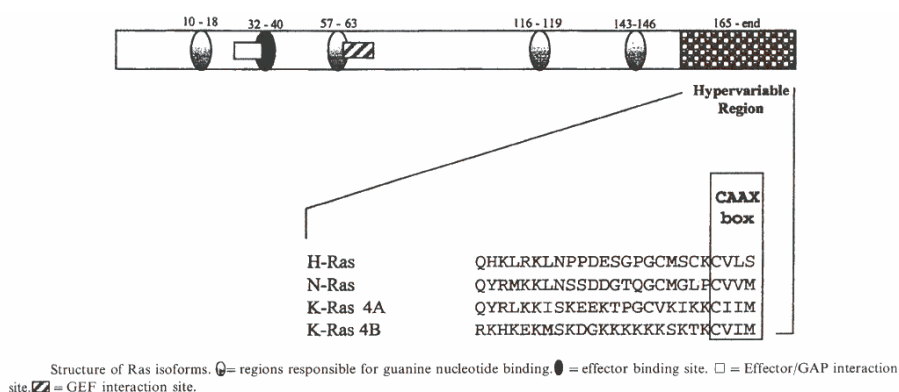
Figure 1-3. Sequence comparation between the different Ras isoforms. Regionis involved in the binding to nucleotidea, effectora and regulator protein GEFs and GAPs present a high homology degree like the CAAX-box in C-terminal [from ref. 10].

---

[9] Lowy D.R., Willumsen B.M., "Function and regulation of Ras", *Annu. Rev. Biochem.*, **1993**, 62, 851-891.

[10] Midgley R.S., Kerr D.J., "Ras as a target in cancer therapy", *Critical Reviews in*

_____

H-, N- and K-Ras can also undergo to *palmitoylation* of one or two cysteine located upstream CAAX sequence. This modification seems to be request to allow Ras localization to cytoplasmic membrane regions rich in cholesterol. K-Ras 4B, that does not present cysteine residues at the C-terminal, seems to associate to the membrane in a cholesterol-independent way, taking advantage of its short polybasic sequence constituted of lysine residues. Recent studies in fact have demonstrated that K-Ras has membrane localization different from K- and N-Ras: this difference can influence the signaling transduction downstream Ras.[11] N-Ras and K-Ras, moreover, when are not farnesilated, can undergo to *geranylgeranylation*. There are then important differences concerning the three Ras gene expression levels both from the temporal point of view, that is in the different stages of development, and from the spatial point of view, that is in the various tissues. In rat, for example, the level of H-Ras is prevailing in brain, muscle and skin, K-Ras transcript is instead more abundant in gut, lungs and thymus, N-Ras transcript is very copious in testicles and thymus.[12] Analyzing rats knock-out rat phenotype it was demonstrated that N-Ras gene is indispensable for regular organism development, rat growth and the fertility, K-Ras is fundamental for processes such as hemopoiesis, myocardium cell proliferation, neuronal cell survival;[13] instead, both H-Ras deletion, and H- and N-Ras double deletion do not show any visible effect.[14] In the light of these considerations, it can be deduced that K-Ras possesses a unique function, necessary and sufficient for rat development.[15]

_____

oncology/Hematology, **2001**, 44, 109-120.

[11] Olsen M. F., Marias R., "Ras protein signalling", Semin. Immunol., 2000, 12, 63-73.

[12] Koera K., Nakamura K., Nakao K., Miyoshi j., Toyoshima K., Hatta T., Otani H., Aiba A., Katsuki M., "K-Ras is essential for the development of the mouse embryo", *Oncogene*, **1997**, 15, 1151-1159.

[13] Johnson L., Greenbaum d., Cichowski K., Mercer K., Murphy E., Chmitt E., Bronson R., Umanoff H., Eldelmann W., Kucherlapati R., Jacks T., "K-ras is an essential gene in the mouse with a partial functional overlap with N-ras", *Genes Dev.*, **1997**, 11, 2468-2481.

[14] Esteban, L. M. et al, "Ras-guanine nucleotide exchange factor Sos2 is dispensable for mouse growth and development" *Mol. Cell Biol.*, **2000**, 20, 6410-6413.

[15] Bar-Sagi, D. et al, "Microinjection of the Ras incogene protein into PC12 cells

The frequency with which different oncogenic mutants of Ras isoforms are present in human tumors follows the order K>N>H.[16] Also the type of Ras mutation correlates with the tumor type, although it is not possible to observe an absolute specificity.

1.1.3. Catalytic mechanism of Ras proteins

The mechanism of Ras GTP-hydrolysis is still under investigation. Two models have been proposed: according to the first, Ras assumes the conformation able to hydrolyze GTP only after the binding to GAP protein, that, therefore, is needed exclusively in order to stabilize the catalitically-active form of Ras; according to the second, instead, it is GAP that directly cuts the phosphate bond.[17] The reaction catalyzed from the complex is the following:

$$\text{GTP}_{\text{bound}} + \text{H}_2\text{O} \rightarrow \text{GDP}_{\text{bound}} + \text{P}_{\text{i}}$$
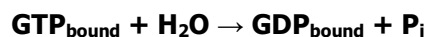
It consists in the hydrolysis of the **phosphoanhydridic bond** between phosphates β and γ of GTP. Likewise other proteins able to hydrolize GTP and ATP, Ras requires the presence of divalent cations as enzymatic cofactors and in particular of Mg^{2+}, (although it has been experimentally demonstrated the possibility to replace Mg^{2+} with Mn^{2+}).[18] The real substrate of this reaction is therefore the Mg^{2+} GTP complex, and the product is the

induces morphological differentiation" *Cell*, **1985**, 42, 841-848.

[16] Hermann C. and Nassar N., "Ras and its effectors", *Prog. Biophys. molec. Biol.*, **1996**, 66, 1, 1-41.

[17] Scheffzek K., Reza Ahmadian M., Kabsch W., Wiesmuller L., Lautwein A., Scmitz F., Wittinghofer A. . "The Ras-RasGAP complex: structural basis for GTPase activation end its loss in oncogenyc ras mutants", *Science*, **1997**, 277, 5324, 333-338.

[18] Schweins T., Scheffzek K., Abheuer R., Wittinghofer A., "The Role of the Metal Ion in the p21[ras] Catalysed GTP-hydrolysis: Mn^{2+} versus Mg^{2+}", *J. Mol. Biol.*, **1997**, 266, 847-856.

Mg^{2+}GDP complex, in which the metallic ion masks partially the negative charges and influences the conformation of the phosphoric groups.
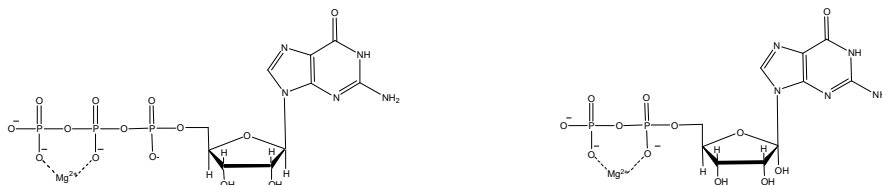
Figure 1-4. Mg^{2+}GTP e Mg^{2+}GDP complexes. The metallic ion interacts with the phosphoric group negative charges masking them partially.

Crystallografic studies allowed the identification a molecule of H$_2$O (*Wat175*) in a position that is compatible with the role of *nucleophile* for the hydrolysis reaction; the reaction substrate, the GTP, seems to act as base (Fig. 1-5).
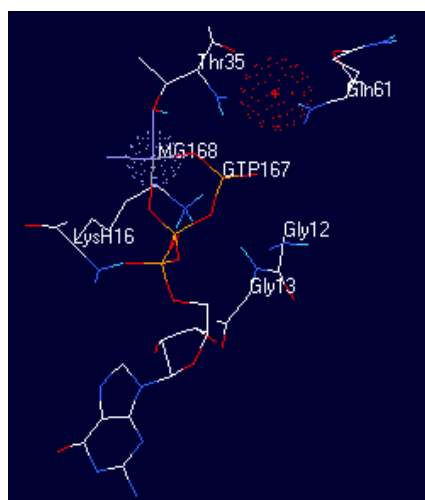
Figure 1-5. Spatial disposition of Wat175 (red), Mg^{2+} ion (grey), GTP and Ras residues required for catalysis.

According to the most probable mechanism, the hydrolysis would proceed through the following steps: (1) the γ phosphate of GTP tears a proton from the H$_2$O molecule that acts as nucleophile; (2) the so generated hydroxide ione attacks the protonated γ phosphate, giving rise to the transition state that is thought to have trigonal pyramidal geometry; (3) the pentacovalent

_____

intermediate is formed, that looses the P_i, acting as leaving group. Schematically:
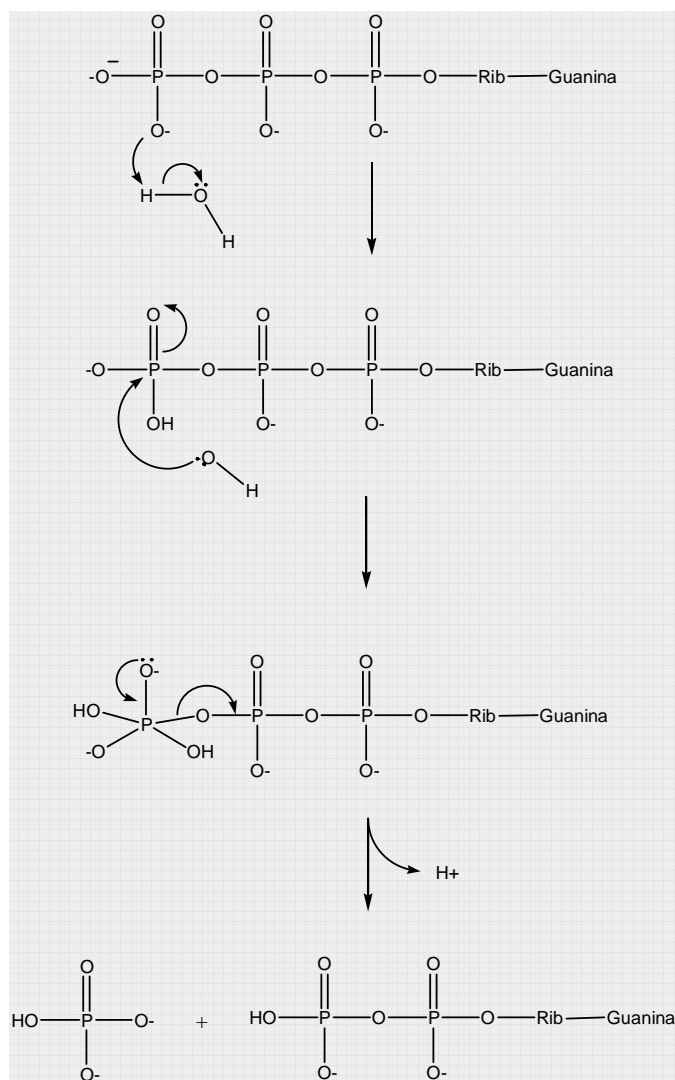
Scheme 1-1. The most probable mechanism for the hydrolisis reaction that converts GTP into GDP catalyzed by Ras proteins.

Alternative to this **associative mechanism**, is a second **dissociative mechanism,** according to which *Gln 61* acts as base and the amidic group of Gly13, disposed in a functional way for the formation of an hydrogen

bond with the oxygen between GTP β and γ phpsphates, is crucial for catalysis:
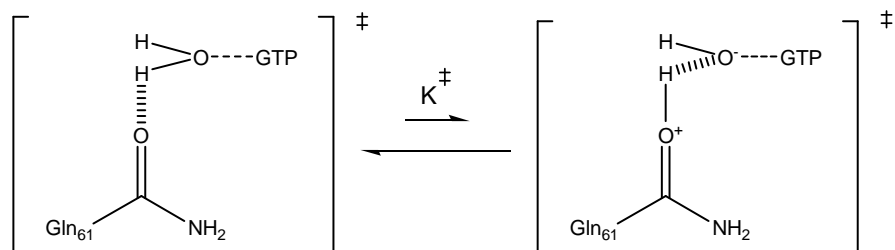
Scheme 1-2. Transition state hypothesized for thedissociative mechanism of GTP hydrolisis reaction.
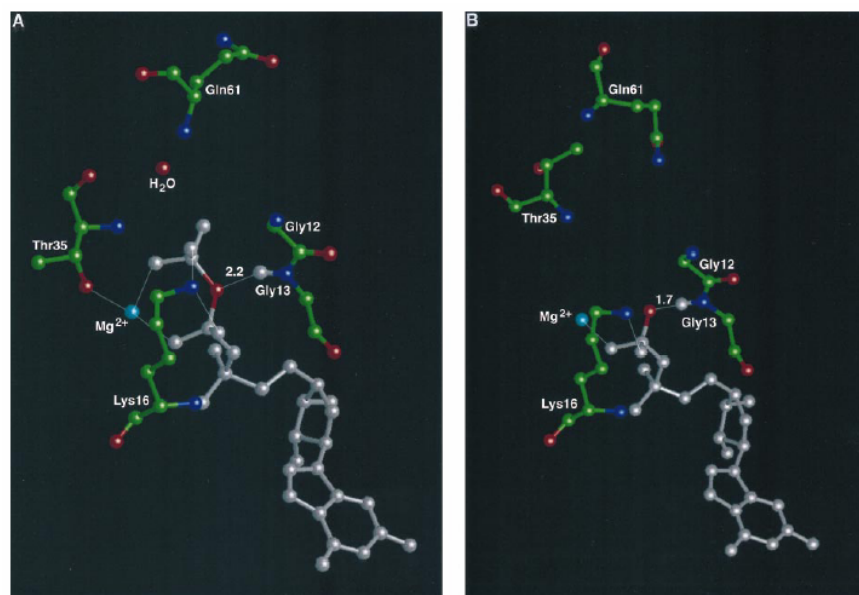
Figure 1-6. Cristallografic structure of Ras active site with GMPPNP (a GTP analog) (A) and with GDP (B) [from ref. 19].

This amide is highly conserved in G proteins and the hydrogen bond is present both in the GTP bound form and in the GDP bound form, therefore, more probably, also in the transition state; such bond seems to be able to stabilizing the leaving group.

The dissociative transition state is characterized by complete, or almost

complete, hydrolisis of oxygen-phosphorus bond, while the formation of the bond with the nucleophile is not complete again; on the contrary, in the associative transition state -O-P bond begins to being hydrolized after the formation of the bond with the nucleophile (Scheme 1-2).[19]
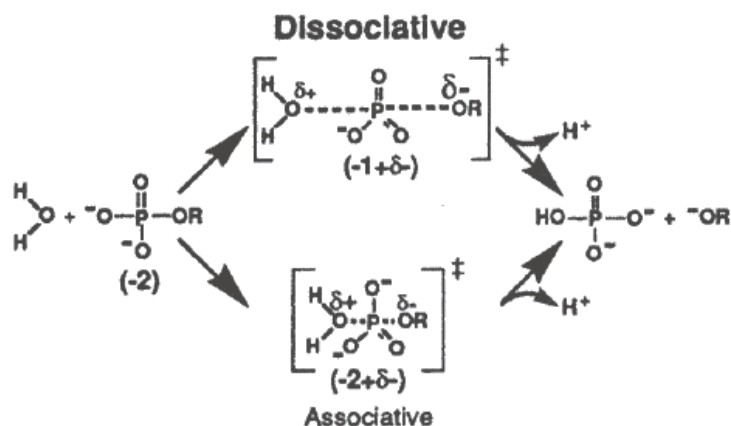
Scheme 1-3. Associative mechanism vs dissociative mechanism [from ref. 19].

1.1.4. Structural characteristics of Ras proteins

From the topologic point of view, Ras protein structure is constituted by 5 α-helixs and 6 β-strands (Fig. 1-8). Segments (**32 - 40**) and (**60 -76**), called respectively **Switch 1** and **Switch 2**, are of particular importance, being the only protein regions that change in meaningful way their conformation passing from the active form to the inactive one. Switch 1 comprises loop 2 and β-sheet 3 (Fig. 1-9), while Switch 2 comprises loop 4 and α-helix 2 (Fig. 1-10). It is interesting that these regions are involved in the binding with regulating GAP and GEF proteins and with effector proteins.[17, 20]

---

[19] Maegley K. A., Admiraal S. J., Herschlag D., "Ras-catalysed hydrolysis of GTP: A new perspective from model studies", *Pro. Natl. Acad. Sci. USA*, **1996**, 93, 8160-8166.
[20] Quilliam L. A., Hisaka M. M., Zhong S., Lowry A., Mosteller R. D., Han J., Drugan J.

Figure 1- 7. Ribbon rappresentation of p21H-Ras tridimensional structure (red for α-helixes, yellow for β-strands).
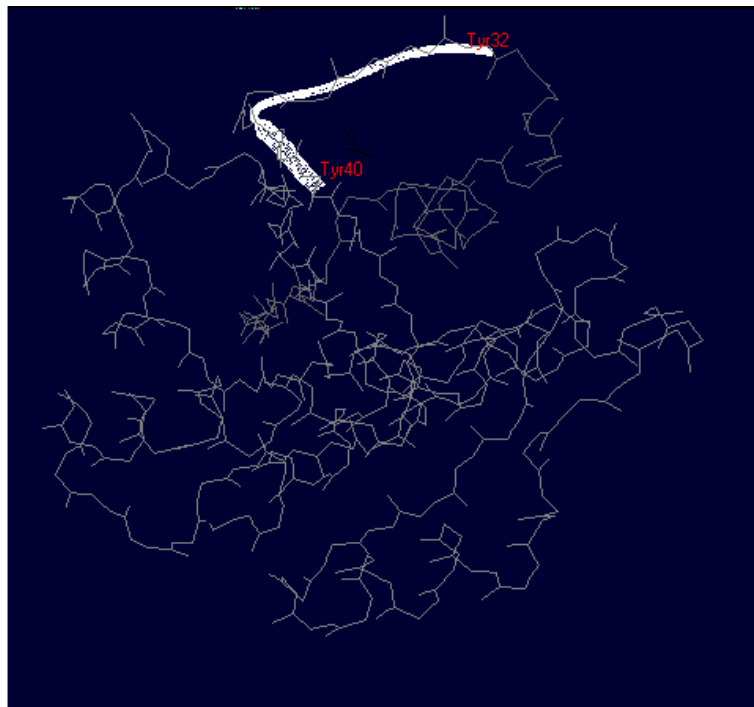
Figure 1-8. Rappresentation of H-Ras switch 1 (ribbons, white) when the protein is bound to GTP.

K., Broek D., Campbell S. L. and Der C. J., "Involvment of the Switch 2 domain of Ras in its interaction with Guanine Nucleotide Exchange Factors", *The journal of Biological Chemistry*, **1996**, 271, 11076.

_____
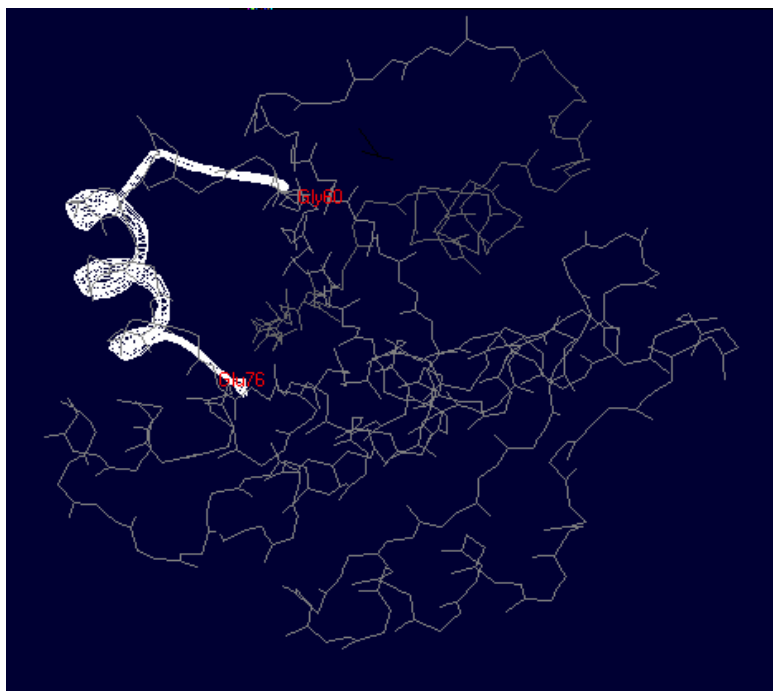
Figure 1-9. Rappresentation of H-Ras switch 2 (ribbons, white) when the protein is bound to GTP.

Both the regions contain a loop and are located on the external surface of the protein; their conformation changes meaningfully according to the nature of the nucleotide bound to Ras. In fact, overlapping the structures of p21H-Ras-Mg^{2+}-GDP and p21H-Ras-Mg^{2+}-GTP it can be noticed that the protein regions with the greatest RMSD are just segments (30-36) and (59-72) (Fig. 1-10).

A lot of proteins able to bind nucleotides such as ATP and GTP possess a *motive rich in glycines*, that generally form a very flexible loop among a β-sheet and an α-helix. This loop interacts with one of the nucleotide phosphate groups and is called **P-loop** (Fig. 1-11). This motive is characterized by the sequence: **AG-x(4)-GK [ST]**.

In H-Ras amino acid sequence a similar motive can be identified; it is placed in a very important region for the interaction with the nucleotide (res. 11-17).
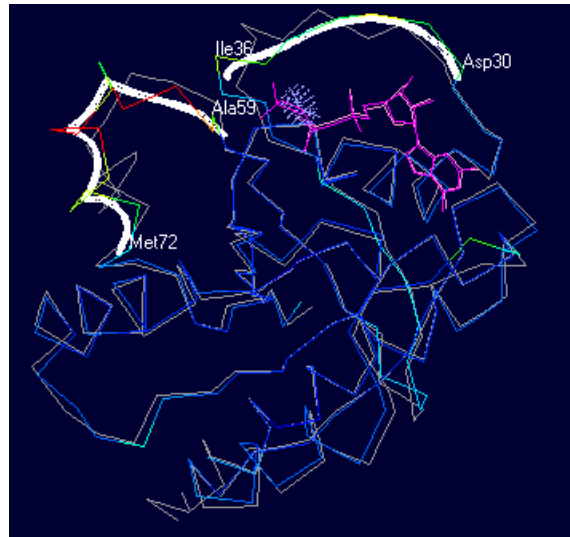
Figure 1-10. Structural overlapping of p21^{H-ras}-Mg^{++}-GDP (white) e p21^{H-ras}-Mg^{++}-GTP (colored, according to RMSD values: blue = very low RMSD, red = hight RMSD) complexes.

MTEYKLVVVG**AGGVGKS**ALTIQLIQNHFVDEYDPTIEDSYRKQVVIDGETCLLDILD

TAGQEEYSAMRDQYMRTGEGFLCVFAINNTKSFEDIHQYREQIKRVKDSDDVPMVL

VGNKCDLAARTVESRQAQDLARSYGIPYIETSAKTRQGVEDAFYTLVREIRQHKLRK

LNPPDESGPGCMSCKCVLS
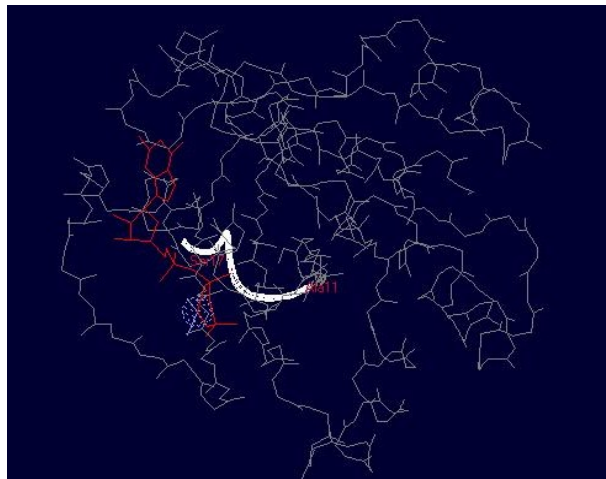
Figure 1-11. Ras P-loop di Ras, motive rich in glycines and very flexible that interacts with one of the GTP / GDP phosphate groups; characterized by the pattern AG-x (4) - GK [St], it is common to proteins that bind nucleotides.

1.1.4.1. Post-traslational modifications

In order to assolve to their function, Ras proteins have to be anchored to the inner side of cytoplasmic membrane. For this reason, they undergo to a farnesylation process (addition of lipidic chains of 15 C atoms from the *farnesyldiphosphate*) of their C-terminal portion, where the signal sequence **CAAX**, recognized by the enzyme farnesyltransferase (**FTasi**), is present.

MTEYKLVVVGAGGVGKSALTIQLIQNHFVDEYDPTIEDSYRKQVVIDGETCLLDILDT
AGQEEYSAMRDQYMRTGEGFLCVFAINNTKSFEDIHQYREQIKRVKDSDDVPMVLV
GNKCDLAARTVESRQAQDLARSYGIPYIETSAKTRQGVEDAFYTLVREIRQHKLRKL
NPPDESGPGCMSCK**CVLS** (H-Ras sequence).

After farnesylation, the removal of the last 3 amino acids is made by a protease and the methylation of cysteine residue that located at the C-terminal extremity of the sequence. In absence of farnesiylation, in the case of K-Ras and N-Ras, the geranylgeranylation (addition of lipidic chains of 20 C atoms C from the *geranylgeranyldiphosphate*) takes place; the reaction is catalyzed by the enzyme geranylgeranyltransferase (**GGTasi**).

1.1.4.2. Interactions with other proteins

1.1.4.2.1. Interactions with p120GAP

The tridimensional structure of the complex formed by H-Ras-GDP and p120Gap has been obtained with a resolution of 2.5 Å.[17]

Switch 1 is directly involved in the interaction. It contains 5 acidic residues (Asp30, Glu31, Asp33, Glu37 and Asp38) that create a negative charged surface used for interacting with GAP and effectors. In fact, the amino acid Lys949, located in a loop of GAP particularly exposed, interacts with this surface, particularly with **Asp33** and **Asp38** and with **Thr35**. Also Switch 2 region takes part to this interaction. Unlike what observed in the structure of isolated Ras, where it appears very mobile, in the complex with GAP it seems very stable. Ras **Tyr64** participates to the formation of the

hydrophobic interface and interacts with the amidic carbonyl of GAP Leu902. **Gln61**, fundamental for the catalysis, binds through an hydrogen bridge the amidic carbonyl of GAP Arg789.

Also the P-loop is involved in the interaction; in fact, **Gly12** interacts with Arg798 through a Van der Waals interaction (Fig. 1-12).
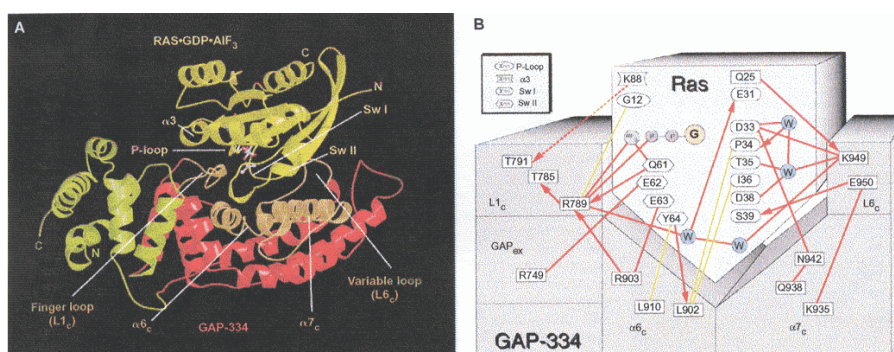
Figure 1-12. (A) Structural motives present in the interaction region between Ras and p120GAP: GAP regions in contact with Ras are rappresented in light brown, Ras in yellow. (B) Schematic rappresentationof Ras-GAP interaction: polar interactions (red lines), contacts between side chain atoms and backbone atoms (red arrows), hydrofobic interactions or Van der Waals interazioni (yellow lines) [from ref. 17].

1.1.4.2.2. Interactions with GEF proteins

The most important mutations that alter Ras ability to bind to the nucleotide exchanger GEF concern residues belonging to Switch 1 and 2; the most dramatic effects are obtained in the cases T35A, D38A, D38E, Q61H, Q61L, E62H and E63H. In particular, mutations E62H and E63H do not alter the interaction with GAP but only with GEF, while the mutant Y64W responds to GEF but not to GAP: evidently Switch 2 interacts with Ras regulators through several amino acids. A lot of other mutations of switch regions do not modify the affinity for GEF, but they perturb nucleotide exchange mechanism stimulated by GEF.[21]

---

[21] McCormick F., Polakis P., "Structural requirements for the interaction of p21Ras with GAP, exchange factors, and its biological effector target", _The Journal of Biological Chemistry_, **1993**, 268, 13, 9157-9160.

_____

1.1.4.2.3. Interactions with effectors

Only in the active form, that is when they bind to GTP, Ras proteins are able to bind to their effectors. Ras effectors do not show neither sequence nor function homology, but they are characterized by a common Ras binding domain (**RBD**), composed by 10/20 amino acids, and by a common topology that is ubiquitin tertiary structure (ββααββα).[22] Ras residues 32-40 are directly involved in the binding with effectors: mutation D38A, for example, prevents all these interactions.

GTP hydrolysis causes a reduction of Ras affinity for its effectors of about 1300 times. Probably, after the hydrolysis of the phosphate group, Tyr 32 ana Tyr 35 side chains change their orientation and this change makes Asp38s and Glu31 loosing important contacts with the effector molecule, reducing the affinity.[17]

1.1.4.3. Mg^{2+} binding site

Proteins involved in phosphate group transfer need divalent cations as Mg^{+2}, whose presence increases protein affinity for nucleotides. The ion is coordinated by six oxygen atoms (both for Ras-GTP and for Ras-GDP) forming a perfect double trigonal pyramid, as shown in the Scheme 1-4. Two of these oxygen atoms belong to β and γ phosphate groups; two other oxygen atoms belong to **Ser17** and **Thr35** side chains, highly conserved in all the proteins that bind guanylic nucleotids. The two octahedron apical positions are rappresented the oxygen atoms of two water molecules: one of these are coordinated to α phosphate, the other one is coordinated to **Asp57** residue.

Mutagenesis experiments to have shown that mutations S17A and D57A cause a decrease in Ras affinity for the nucleotide, showing the importance of the cation for the interaction with GTP or GDP. Mutant T35A does not

_____

[22] Herrmann C., "Ras-effector interactions: after one decade", *Current opinion in structural biology*, **2003**, 13, 122.

have effects; an explanation could be that threonine oxygen of can easily be replaced by a water molecule in the coordination of the cation, while this does not happen for the serine.[23]
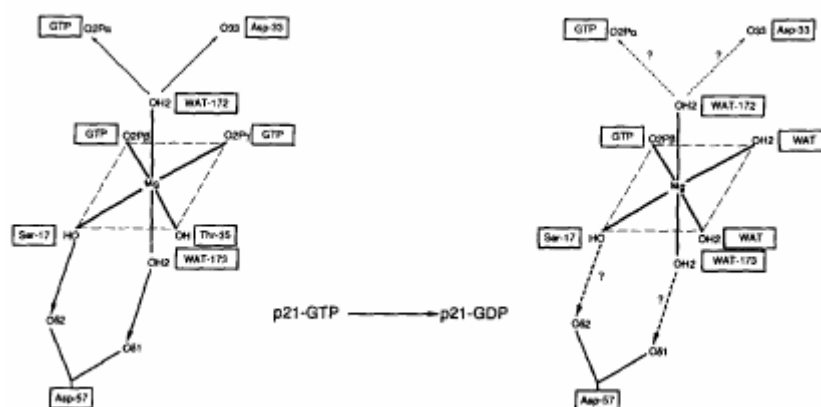
Scheme 1-4. Mg^{2+} coordination on p21-Gpp(NH) and GDP complex, as determinated by crystallography (Pai et al., EMBO J., 1990, 9, 2351-2359) [from ref. 23].

1.1.4.4. Nucleotide binding site

The most important interactions between Ras and nucleotides involve the guanine on nucleotide and the following amino acids on Ras:

▪ **Asp119** that with one of the two oxygens of the side chain forms an hydrogen bond with the hydrogen in position N1 of the guanina, while with the other oxygen interacts with the aminic group in position N2;

▪ **Asn116** that interacts with the position N7 of the guanina;

▪ **Ala146** that, through the oxygen, form a bond hydrogen with the hydroxyl bound to the position C6;

▪ **Lys117** and **Phe28** that present Van der Waals interactions with the base.

Residues 116, 117 and 119 and residue 146 respectively belong to the

---

[23] John J., Rensland H., Schlinchting I., Vetter I., Borasio G. D., Goody R. S., Wittinghofer A., "Kinetics and Structural Analysis of the Mg^{2+}-binding site f the Guanine nucleotide-biding Protein p21[H-ras]", _The Journal of Biological Chemistry_, **1993**, 268, 2, Issue of January 15, 923-929.

motives **NKXD** and **SAK**, both highly conserved in proteins that bind guanylic nucleotides.[16]

Evolution made Ras proteins, and other proteins involved in the processes of signal trasdution that bind GTP / GDP, highly specific for the nucleotide type, discriminating between GTP / GDP and ATP / ADP and less sensitive to chemical modifications on phosphate chain and ribose unit. The binding affinity of Ras for GTP is very similar to that for GDP. The affinity do not change in a relevant way by modifying the bond among the groups phosphate (for instance with the insertion of a phosphamide bond **GppNHp**), or by adding a group such the methylantranyloil in postion 3' of ribose.

The reasons for this could depend on the fact that adeninic nucleotides are already involved in a great number of cellular processes of energy generation and transfer, making therefore ADP / ATP turnover too slow too. From the chemical point of view, GTP offers more hydrogen bond donor and acceptors groups than the ATP to interact with the protein, giving a more stable complex. Ras protein binding to adeninic nucleotides, in fact, is much less stable, since important interactions miss, especially in the positions N2 and C6 of the nucleotide.[24]

1.1.4.5. Structural basis of mutant oncogenicity

The knowledge of Ras structure and function helps to understand the reasons that make tumorigenic some variations of these proteins. **Gln61**, besides to be fundamental for Ras inactivation also results important for the interaction with GAP: in fact, its substitution with any other amino acid, with the exception of glutamate, results in the loss of GTP hydrolysis promoted

---

[24] Rensland H., John J., Linke R., Simon I., Schlichting I., Wittinghofer A., and Goody R.S., "Substrate and product structural requirements for binding of nucleotides to H-Ras p21: the mechanism of discrimination between guanosine and adenosine nucleotides", *Biochemistry*, **1995**, 34, 593.

by GAP and in cell tumoral transformation. **Gly12** can be replaced only by proline without causing tumorigenicity; the other aminoacids, being more bulky, prevent the interaction with the GAP Arg789 residue. This does not totally inhibit the contact between the two proteins, but obstructs the catalytic mechanism of hydrolysis of the phosphate group. The mutant G12P, on the contrary, show an unexpected increase of the rate of GTP hydrolysis.
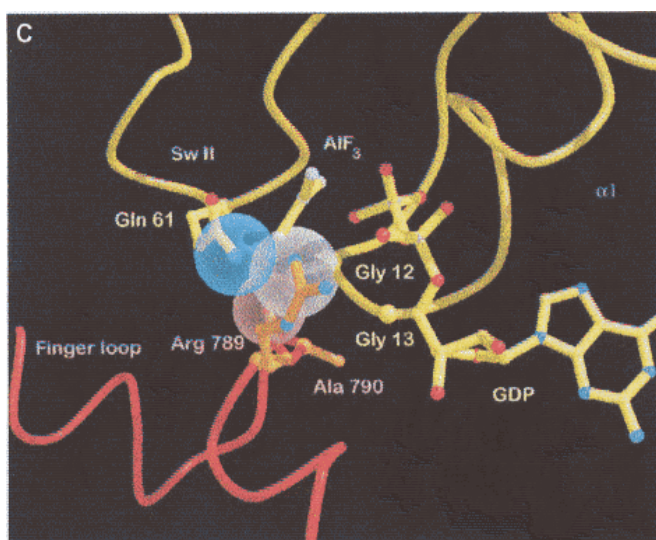
Figure 1-13. Gly 12, Gly 13 e Gln 61, the three most frequently mutated Ras residues in the oncogenic protein variants [from ref. 17].

Gly13 does not participate directly in the interaction with regulating proteins or with effectors, but it is located in a critical region, the P-loop, where the glycines are highly required for the interaction with the nucleotide. Mutations of this residue can alter the affinity for GAP or the catalytic activity.

The mutations described above lead to a costutively active Ras protein, that is present in about the 30% of human tumors. It is therefore of great pharmacological importance the search of molecules that show Ras inhibitory activity. The process of Ras activation can be blocked or reduced by inhibiting: (1) the protein expression, (2) the anchorage to cytoplasmic membrane, (3) the GTPasic activity, (4) the interaction with the effectors.[17]

1.2. Ras proteins and tumorigenesis

1.2.1. Cancer

Tumors are animal pathologies characterized by an uncontrolled, irreversible and progressive proliferation of abnormal and irregular cells (for dimensions, form and number of chromosome), that brings to formation of a malignant neoplasia (malignant tumor, leukemia or linfoma). Carcinogenic formation can invade and to destroy the adjacent tissues making metastasis and so to compromising the functionality of organs different from that in which the tumoral transformation is originated.

Cancer etiology is a complex process still unknown in its details; different factors can promote it, and they can be both endogenous (for instance hormones), and exogenus (viruses, ionizing radiations, mutagenic chemical substances), whose effects can be combined.[25]

Fundamental feature of every tumoral cell is that, after division, they give origin, to two new cancerous cells, suggesting that neoplastic phenotype is genetically determined, or rather is codified in cancerous cell DNA. Every tumoral cell transmits then its genetic patrimony to its progeny, and, in effects, it is possible to demonstrate that many tumors are clonal.[26, 27]

In general, transformation of normal cells in tumoral cells is a multi-step process and demands a number of key events that include the acquisition of cell self-sufficiency to growth signals. This factor is probably a consequence

---

[25] Paoletti R., Nicosia S., Clementi F., Fumagalli G., "Farmacologia generale e molecolare", second edition, **1999**, UTET.
[26] Lewin B., "Il gene VI", **1999**, Zanichelli.
[27] Watson J. D., Gilman M., Witkowski J., Zoller M., "DNA ricombinante", first italian edition, **1994**, Zanichelli.

of proliferation stimulation by autocrin growth signals, of the over-expression of growth factor receptors, of the over-expression or the activation of cytoplasmic component of signaling pathways.

Inside the genetic patrimony, two classes of genes are present whose level the mutations of which are cause of neoplastic transformation:[26]

- **oncogenes**: they were initially identified as genes brought by virus (viral oncogenes, v-onc) that cause the transformation of target cells. It was then demonstrated that one of the principal classes have cellular (cellular oncogenes, c-onc) counterparts, involved in regulation of normal cellular functions. These cellular genes are called **proto-oncogenes** and, sometimes, their mutations or aberrant activation are associated to the formation of a tumor. Oncogene generation represents a purchase of function, in which a cellular proto-oncogene is activated in an incorrect way, because of a mutation in the corresponding protein, or of a constitutive activation, or the lack of expression disactivation.

- **tumor suppressors**: they are genes that normally impose some restriction to cellular cycle and cell growth; loss of restrictions is obviously tumorigenic, because it has as result the impossibility to correctly check cell progression the cycle.

1.2.2. The "Ras network", cell cycle and tumorigenesis

As discussed above, Ras proteins are molecular switches that have a crucial role in transmission of signal mediated by tyrosine-kinasic receptors.

They are activated by wide variety of extracellular stimuli and are able, to activate several effector enzymes, feeding therefore different pathways of signal transduction [1.1.1] (Scheme 1-5).

The Ras effectors more studied and characterized so far are the

serine/threonine kinases **Raf** (c-Raf1, bRaf, aRaf).[28] After interaction with Ras, Raf localizes at the cytoplasmic membrane, and this event seems to be fundamental for its activity. Raf phosphorylates and so activates protein-kinases activated by mitogen 1 and 2 (*Mek 1* and *2*), able to phosphorilate and to activate in turn protein-kinases *Erk1* and *2*.[29, 30] These two proteins are activated by the binding of cytoplasmic factors and, once activated, move inside the nucleus, where they phosphorylate transcription factors among which the products of the proto-oncogenes *Jun* and *Fos*. These events bring the transcription factor AP-1, constituted by Jun-Fos heterodimers, to be activated. This factor is responsible for expression of key proteins for cellular cycle regulation, that is type D cyclines, which promote the overcoming of the restriction point between G1 phase and S phase[31] and therefore cell progression in the cycle and its duplication.

Another Ras effector is represented by the *phosphatidylinositol-3-kinases* (**PI3K**), that are activated upon interaction with Ras. PI3K phosphorilate the *phosphatidylinositol-4,5-diphosphate*, producing the *phosphatidylinositol-3,4,5-triphosphate*, a second messenger that binds a wide range of other proteins.[6] Very important is the activation of the kinases *PDK1* and *AKT* (or *PKB*); the first activates in turn a lot of proteins of the AGC family, while the second has a strong anti-apoptotic function.[32] PI3Ks, moreover, stimulate Rac, a protein Rho family member involved in regulation of actin expression, a cytoskeleton fundamental component, and of some transcription factors among which *NF-kB*.

A third family of Ras effectors includes three exchange factors (RalGDS,

---

[28] Marais R., Light Y., Paterson H. F., Marshall C. J., "Ras recruits Raf-1 to the plasma membrane for activation by tyrosin phosphorylation", *EMBO J.*, **1995**, 14, 3136-3145.

[29] Kolch W., "Coordinating ERK/MAPK signalling through scaffolds and inhibitors", *Nat. Rev.*, **2005**, 827-837

[30] Mor A. and Philips M. R., "Compartmentalized Ras/MAPK Signaling", *Ann. Rev. Immunol.*, **2006**, 771-800.

[31] Yordy J. S., Muise-Helmericks R. C., "Signal transduction and Ets family of transcription factors", *Oncogene*, **2000**, 19, 6503-6513.

[32] Datta S. R., Brunet A., Greenberg M. E., "Cellular survival: to play in three Akts", *Genes Dev.*, **1999**, 13, 2905-2927.

Rgl/Rsb2, Rgl2/Rlf) through which the stimulation of **Ral** proteins takes place. This event has as consequence *phopspholipase D1* and *Ralbp1* activation; this pathway is, together with AKT / PKB one, responsible for the inhibition of the transcription factor *Forkhead*, implicated in cellular cycle arrest, through the induction of *CKI p27*, and in apoptosis, through the expression of *Fas-ligand*.[33]

Phospholipase C is a further Ras effector; this enzyme catalyses the hydrolysis of *phosphatidylinositol-4,5-diphosphate* to *diacyl glycerol* (DAG) and *inositol-1,4,5-triphosphate*. This pathway is responsible for protein-kinases C activation and for intracellular mobilization Ca^{2+}.[34,35]
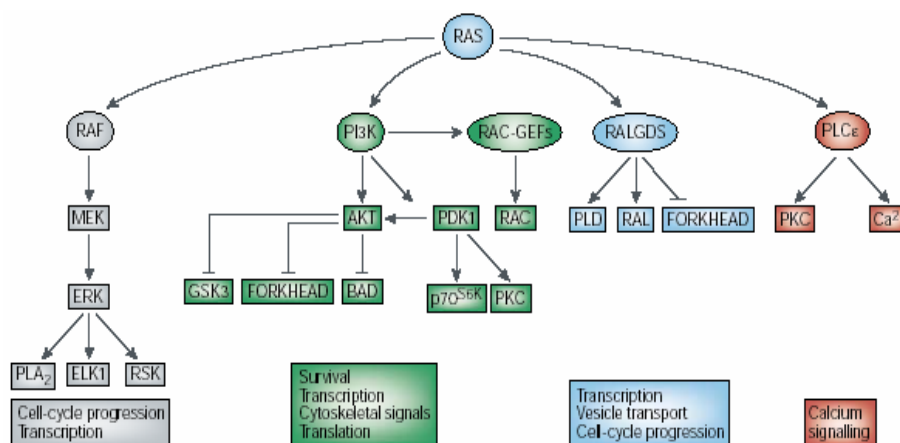
Scheme 1-5. Trasduction pathways downstream Ras [from ref. 36].

In the light of these data, it appears evident that Ras proteins, more than in a pathway, is rather involved in a complex *metabolic network*, which has a fundamental and decisive role to in the cellular cycle regulation. Through

[33] De Ruiter N. D., Burgering B. M. and Bos J. L., "Regulation of the Forkhead transcription factor AFX by Ral-dependent phosphorylation of threonines 447 and 451", *Mol. Cell. Biol.*, **2001**, 21, 8225-8235.

[34] Kelley G. G., Reks S. E., Ondrako J. M., Smrcka A. V., "Phospholipase C: a novel Ras effector", *EMBO J.*, **2001**, 20, 743-754.

[35] Bos J. L., "Ras oncogenes in human cancer: a review", *Cancer Res.*, **1989**, 49, 4682-4689.

[36] Downward J., "Targeting Ras signalling pathways in cancertherapy", *Natures Reviews / Cancer*, **2003**, 3, Issue of January, 11-22.

combination of a lot of trasduction pathways responsive to them, in fact, the expression inside the cell of Ras mutants constitutively active can promote different modifications of the cellular phenotype, that are characteristic of the tumoral transformation: 1) *increase of proliferation rate* caused by induction of regulators of the cellular cycle as D1 cycline, that brings to Rb pathway inactivation, and to suppression of inhibitors of cell cycle progression such as Kip1, 2) *desensitization to apoptosis* through AKT / PKB, 3) *induction of angiogenesis* through transcriptional up-regulation, mainly mediated by ERK proteins, of angiogenic factors, 4) *increase of invasivness*, due to expression of metal-protease of matrix and to Rac-dependent modifications of cytoskeleton.

Ras genes are therefore **proto-oncogenes**. As a consequence of the introduction of some mutations in their sequence, such genes can codify for constitutively active proteins (Ras **oncogenic variants**) that, are constantly in the GTP-bound active state, because of their acquisition of resistance to GAP activation of the GTPasic function.

Ras mutations generally associated to tumoral transformation take place mainly in **codons 12** and **61**, more rarely codon **13**; this is not casual, since amino acidic residues 12 and 61 are fundamental for the interaction with GAP and for Ras catalytic activity, while residue 13 takes part to P-loop, important for the interaction with the nucleotide [1.1.4.3.]. These mutations are associated approximately to the 30% of human tumors,[10, 18] although the frequency with which they appear varies according to tumor type. Extremely different is then the incidence with which such mutations interest the possible isoformes of Ras proteins: K-Ras is the more frequently changed isoform in human tumors, followed then by N-Ras, while oncogenic variants of H-Ras are very rare.

To support the experimental evidences that want different biological roles for Ras isoformes there is the fact that mutations in different isoforms result associated to different types of tumors.

2. Ras proteins: a new target for anti-tumor therapy

In a high percent of human tumors mutated Ras oncogenes have been found and the contribution of their aberrant functions to neoplastic cell transformation is higher than that one indicated from the percentage of mutation, (in fact the over-expression of many tyrosine-kinasic receptors for growth factors brings to an increase of Ras-dependent signalling). Inhibition of these proteins is therefore a promising approach for the development of new antitumor drugs.[37, 38]

2.1. Strategies for the inhibition of Ras-mediated mitogenic signals

With the aim to avoid that constitutively active Ras proteins induce tumoral cell transformation, it is fundamental to prevent that every kind of signal reach effectors located downstream to Ras. For this reason, the ideation of new strategies leading to selective Ras inhibition required a deep knowledge of its biochemistry. The most important strategies of Ras inhibition consist: (1) in the inhibition of Ras anchorage to the membrane; (2) in the block of Ras expression; (3) in the inhibition of the interactions with effectors; (4) in the selective targeting of cells in which Ras signalling is active; (5) in the

---

[37] Kloog Y., Cox A. D., "Ras inhibitors: potential for cancer therapeutics", *Molecular medicine Today*, **2000**, 6, 398-402.
[38] Friday B. B., Adjei A. A., "K-Ras as a target for cancer therapy", *Biochimica et Biophysica Acta*, **2005**, 1756, 127 – 144.

_____

restoration of mutant defective GTPasic activity; (6) in the immunotherapic treatment of cells containing Ras oncogenic variants by cytotoxic T cells.[39, 40] These strategies are schematically represented in the following scheme and analyzed in details in next paragraph.
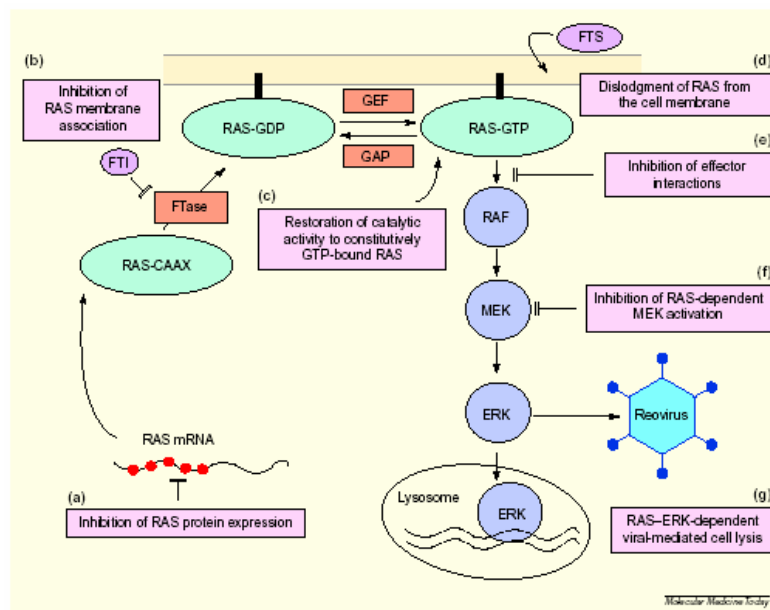
Scheme 5-1. Ras inhibition strategies [from ref. 37].

2.1.1. Inhibition of Ras anchorage to the cytoplasmic membrane

It is essential for its biological function that Ras moves from the cytoplasm to the plasma membrane; only when anchored to the membrane inner side, in fact, it reaches its appropriate sub-cellular localization that allows it to

_____

[39] Pruitt K., Der C. J., "Ras and Rho regulation of the cell cycle and oncogenesis", *Cancer Letters*, **2001**, 171, 1-10.
[40] Beaupre D. M., Kurzrock R., "Ras inhibitors in hematologic cancers: biologic considerations and clinical applications", *Investigational New Drugs*, **1999**, 17, 137-143.

interact with effector molecules. The binding to the membrane requires a protein post-translational processing that involves farnesylation of its C-terminal extremity, reaction catalyzed by the enzyme farnesyltransferase (FTasi), that uses the substrate _farnesyldiphosphate_ (FDP) [1.1.2.; 1.1.4.1.]. As this process is indispensable for Ras functionality, it has become one of the most important target in rational design of Ras inhibitors.

The first approach to prevent Ras anchorage to the plasmatic membrane consists in the use of **farnesyltransferase inhibitors** (**FTIs**) (Fig. 2-1).

Physioligical FTPase substrate

farnesyldiphosphate (FDP)

CAAX box

Examples of FTPase inhibitors that are substrate analogues

alpha-hydroxyfarnesyl-phosphonic acid

L-739,750

A bisubstrate analogue

BMS185878
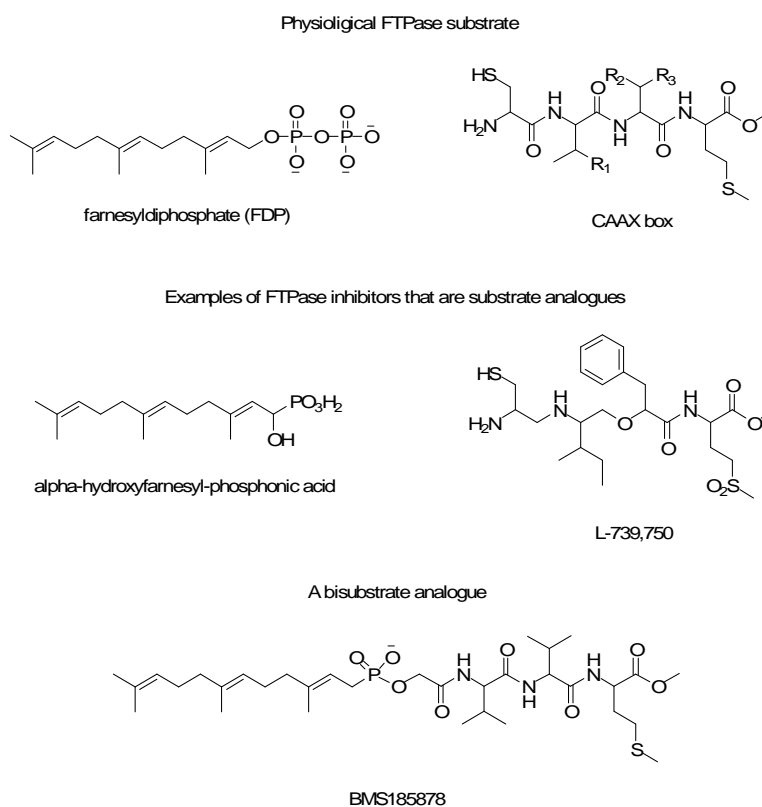
Figure 2-1. Natural analogous and synthetic inhibitors of FTPase [from ref. 10].

Such inhibitors can be divided in three groups: (1) **FDP analogous**, that compete with the natural substrate of the enzyme, (2) **CAAX mimetics**, that compete with Ras CAAX box recognized by FTasi, (3) **bisubstrate**

analogues that mimic both the mechanisms and the transition state of the farnesylation process. Both natural FTIs , as limonene, and FTIs of synthetic origin, as **SCH66336** (Sarasar) or **R115777** (Zanestra), exist. [10, 29, 40, 41, 42] These compounds show the ability to inhibit in an efficient way H-Ras farnesylation in cell cultures and to promote the reversion of mammalian carcinomas in transgenic rats that express activated H-Ras proteins. Moreover, they present very low toxicity and these results are promising in the perspective to use these compounds in the treatment of different human tumors. Unfortunately, these expectations have been disregarded; that is consequence of the fact that, with the exception of H-Ras, that is only farnesylated, K- and N-Ras, the Ras isoforms more frequently mutated in human tumors, can, in alternative, be geranylgeranylated by the enzyme geranylgeranyltransferase (GGTasi), overcoming the farnesyltransferase inhibition. The attempt to employ a combination of FTIs and GGTIs failed because of the high toxicity of this mixture. It is possible that FTI low toxicity is due just to their inability to inhibit the function of all endogenous Ras proteins, which result to be essential for cellular growth.[29, 40] Recent studies[43] have demonstrated FTI ability to cause growth arrest in G2/M in some circumstances and to induce apoptosis in others, without passing, through the inhibition of Ras processing.

Ras anchorage to the cytoplasmic membrane is also targeted by another class of molecules. Some compounds that mimic Ras farnesylcysteine have been developed. Among these, **farnesylthiosalisylic acid** (FTS) is the most studied.

---

[41] Gibbs J. B., Graham S. L., Hartamn G. D., Koblan K., S., Kohl N. E., Omer C. A. and Oliff A., "Farnesyl transferase inhibitors versus Ras inhibitors", *Curr. Opinion in Chem. Biol.*, **1997**, 1, 197-203.

[42] Santagada V., Caliendo G., Severino B., Lavecchia A., Perissutti E., Fiorino F., Zampella A., Sepe V., Califano D., Santelli G., and Novellino E., "Synthesis, Pharmacological Evaluation, and Molecular Modelling Studies of Novel Peptidic CAAX Analogues as Farnesyl-Protein-Transferase Inhibitors", *J. Med. Chem.*, **2006**, 49, 1882-1890.

[43] Prendergast G. C., "Actin up: RhoB in cancer and apoptosis", *Nature Reviews Cancer*, **2001**, 1, 162-168.
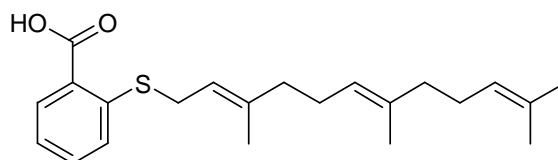
Figure 2-2. Structure of S-*trans,trans*-farnesylthiosalisylic acid (FTS).

In vitro this compound acts as inhibitor of Ras S-prenylcysteine methylation, *in vivo* it inhibits the growth of human cells expressing oncogenic variants of H-Ras, reverting their transformed morphology in a dose-dependent way and at concentrations (0,1-10 μM) lower than those required for methylation inhibition. The lack of cytotoxicity at these concentration values suggests moreover that such compound is not able to prevent the correct process of isoprenylation in the intact cells.[44] It has been demonstrated experimentally that this molecule is able to block the growth of human melanoma cells.[45] FTS is thought to be a Ras antagonist, since the main consequence of its action consists in the decrease of the levels of the protein in membrane and in the accumulation of complete processed Ras molecules in the cytoplasm. FTS seems to be able to compete with Ras for the anchorage sites to the membrane, and to promote Ras removal from the membrane, making it therefore susceptible to proteolytic degradation and carrying to a reduction of its total level inside cell. On the base of its mechanism of action, FTS is capable of acting as antagonist of whichever Ras isoform, provided that farnesylated.[29,36,46,47]

---

[44] Marom M., Haklai R., Ben-Baruch G., Marciano D., Egozi Y., and Kloog Y., "Selective inhibition of Ras-dependent Cell Growth by Farnesylthiosalisylic Acid", *The Journal of biological Chemistry*, **1995**, 38, Issue of September 22, 22263-22270.

[45] Jansen B., Schlagbauer-Wadl H., Kahr H., Heere-Ress E., Mayer B. X., Eichler H.-G., Pehamberger H., Gana-Weisz M., Ben-David E., Kloog Y., and Wolff K., "Novel Ras antagonist blocks human melanoma growth", *PNAS*, **1999**, 96, 24, 14019-14024.

[46] Haklai R., Weisz M. G., Elad G., Paz A., Marciano D., Egozi Y., Ben-baruch G., and Kloog Y., "Dislodgment and Accelerated Degradation of Ras", *Biochemistry*, **1998**, 37, 1306-1314.

2.1.2. Inhibition of Ras expression

Another Ras inhibition strategy is represented by the downregulation of its expression. The more efficient approach is that based on **antisense oligonucleotides** specific for sequences of **Ras** and **c-Raf1**, one of its main effectors. Binding cRNA, these oligonucleotides can inhibit protein production mainly through two mechanisms: (1) mRNA degradation through the Rnase H activity directed against RNA-DNA duplex, (2) interfering with DNA transcription. Some compounds have been tested *in vivo* on animal models, in particular nude mice, showing the ability to reduce tumoral lung cell growth K-Ras-transformed and they are now on clinical trial phase for druf development. However, several difficulties related to the use of these substances as antitumor agents exist, depending in particular on toxicity phenomena.[29, 37, 48]

2.1.3. Inhibition of Ras interaction with effectors

Ras aberrant forms ability to transduce signals can be inhibited interferring with the "communication" between the protein and its downstream effector molecules. Studies that have concurred to deepen the knowledge of the structure of Ras-effector complexes, identifying in particular the protein

---

[47] Gana-Weisz M., Halaschek-Wiener J., Jansen B., Elad G., Haklai R., and Kloog Y., "The Ras Inhibitor *S*-trans,*trans*-Farnesylthiosalisylic Acid Chemosensitizes Human Tumor Cells Without Causing Resistance", *Clinical Cancer Research*, **2002**, Vol. 8, 555–565.

[48] Ross P. J., George M., Cunningham D., Di Stefano F., Andreyev H. J. N., Workman P., and Clerke P. A., "Inhibition of Kirsten-Ras Expression in Human Colorectal Cancer Using Rationally Selected Kirsten-Ras Antisense Oligonucleotides", *Molecular Cancer Therapeutics*, **2001**, 1, 29-41.

_____

regions indispensable for the different interactions, have been fundamental to this purpose. Just such regions are the main targets of this strategy, consisting in the use of **peptides mimicking the Ras-binding domain** of some its main effectors. Peptides that reproduce the Ras-binding domain of Raf1, for example, can inhibit Ras-induced proliferation in NIH3T3 cells.[37]

2.1.4. Selective targeting of cells in which Ras signalling is active

Human **reovirus** requires that the Ras transduction pathway is active in order to be able to infect cell culture. For this reason, it is possible to direct reovirus infection selectively towards cells in which Ras protein is active, without therefore to damage cells in which instead Ras-dependent proliferation is turned-off. This type of approach has been demonstrated effective in culture and in some animal models: a single intra-tumoral reovirus injection in immune deficient mice carrying tumoral v-ErbB-transformed NIH3T3 cells, in human U87 glioblastoma cells or Ras-transformed 10T1/2 cells, resulted in deep regression of tumor (65-80%). As reovirus is not dangerous for man, it could be used for the therapy of tumors that express constituent active Ras protein.[37, 49]

2.1.5. Restoration of mutant defective GTPasic activity

Oncogenic Ras proteins are not able to generate a stable transition state for the GTP hydrolysis reaction and then they can't hydrolyze GTP to GDP. As a

_____

[49] Coffey M. C., Strong J. E., Forsyth P. A., Lee P. W. K., "Reovirus Therapy of Tumors with Activated Ras Pathway", *Science*, **1998**, 282, 1332-1334.

_____

consequence, these mutants remain constitutively in the active state, that is responsible for tumoral transformation. A valid strategy of inhibition of these variants consists in the design of compounds capable of restoring Ras GTPasic activity. Such molecules take advantage of the phenomenon named **substrate-assisted catalysis**, which consists in the restoration of the defective catalytic activity, in virtue of the substrate ability to supply, in the correct position and direction, those catalytic functional groups lost as a result of the mutation. Prototype of this compound family is the **GTP-diaminobenzophenone-phosphoroamidate** (**DABP-GTP**), a GTP analogues. DABP-GTP furnishes the aminic group, essential for catalysis, lost because of mutations in Gln-61 residue and in this way it restores Ras GTPasic activity.
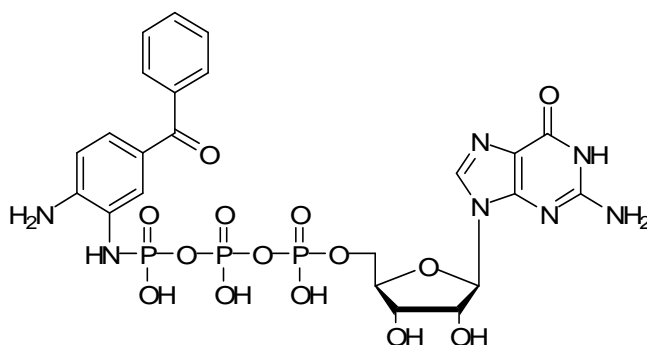
Figure 2-3. Structure of GTP-diaminobenzophenone-phosphoroamidate (DABP-GTP).

Gly12 and Gly13 were identified as the small hydrofobic region that repairs the aromatic aminic group of this molecule.

The DABP-GTP can act as substrate also for the wild-type Ras proteins, but it is hydrolyzed more efficiently by the mutants; for this reason, it is extremely selective for the down-regulation of the Ras oncogenic forms, rather than for those normal ones, and, therefore, the signalling of the Ras proteins wild type would not be altered by this type of inhibitors. Another obvious advantage is the fact that Ras oncogenic mutants can be inactivated reversibly.[29, 37, 50]
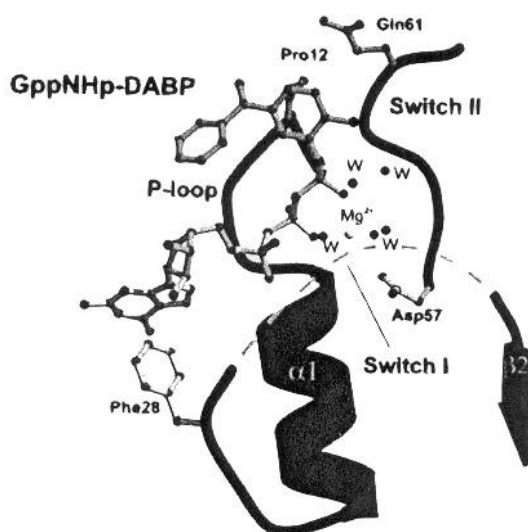
Figure 2-4. Ras(G12P)-DABP-GppNHp complex active site [from ref. 50].

2.1.6. Immunotherapic treatment of oncogenic Ras variants

Cytotoxic T cells CD8+ are able to contribute to recognition and to elimination of tumoral cells. Preclinical studies[10] indicate that T cells-mediated immune response, specific for individual Ras mutations, can be obtained through the _in vitro_ stimulation with synthetic peptides corresponding to the different mutations. Similarly, these responses take place _in vivo_ after immunization with antigen presenting cells (APCs) treated _ex vivo_ with the same peptides. Generated T cells (both CD4+ and CD8+) recognize and kill tumoral cells that carry the correspondent mutations. Such immunotherapic approach is object of clinical trials for various types of tumor treatment.

---

[50] Ahmadian M. R., Zro T., Vogt D., Kabsch W., Selinger Z., Wittinghofer A., and Scheffzek K., "Guanosine triphosphatase stimulation of oncogenic Ras mutants", _Proc. Natl. Acad. Sci. USA - Pharmacology_, **1999**, 96, 7065-7070.

_____

2.2. A new class of Ras inhibitors able to prevent GDP/GTP nucleotide exchange

The inhibition of GDP/GTP nucleotide exchange, consisting in the release of GDP from Ras and in the consequent binding to GTP, is essential for protein activation and can represent a target of anti-tumor drug development.

Few years ago, the Schering-Plough Research Institute laboratories obtained a small library of compounds with the capability of inactivating Ras, preventing the nucleotide exchange. These molecules present a common structural base, represented in Fig. 2-5, and differ for the nature of the group R bound to the sulphonamidic nitrogen.
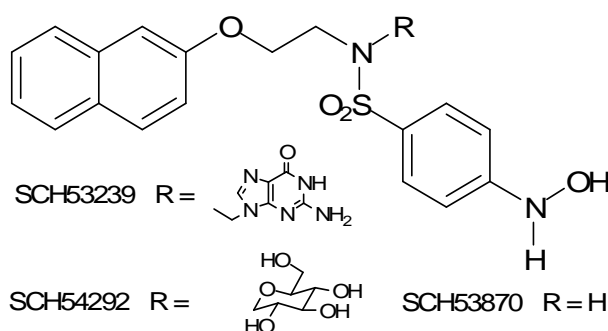
Figure 2-5. Schering–Plough inhibitor structures.

Their biological activity was tested *in vitro* by nucleotide exchange assays. The entity of the exchange between ^{32}P-GDP and not marked GDP on the Ras oncogenic mutant G12V was measured in presence of every inhibitor. In these conditions, GDP has an IC_{50} of 0.5 µM. **SCH53239**, designed in order to compete with GDP for the binding to Ras nucleotide binding site, and **SCH53870** show the same IC_{50} value, while **SCH54292** inhibits at higher concentrations (IC_{50} of 0.7 µM). It was also claimed that the latter

compound is more water soluble than the other, important characteristic for inhibitor pharmacokinetic.

Scatchard kinetic analyses demonstrated that inhibitors **SCH53870** and **SCH54292** do not compete with GDP for binding to Ras.[51] In order to clarify which was the nature of the interaction between such compounds and the Ras-GDP complex, a deepened analysis has been executed, taking advantage of various analytical techniques, in particular mass spectrometry and NMR, and a computational approach, the molecular modelling. ESI mass spectra of solutions containing the Ras-GDP complex and one of the two inhibitors **SCH53870** and **SCH54292** showed, in both cases, a peak corresponding to the mass of the ternary complex Ras-GDP-inhibitor, without the presence the mass corresponding to the dimeric species Ras-inhibitor. This result therefore confirmed the 1:1 stoichiometry of the ternary complex (Ras-GDP: inhibitor) and the non-covalent nature of the bond. It has also been observed that the complex stability is dependent from pH (it diminishes decreasing the pH) and on solvent nature (addition of organic solvents to solution promotes the dissociation). In addition, the Ras region involved in the binding to inhibitors was mapped through the covalent modification of the protein by treatment with succinic anhydride. Succinic anhydride reacts with the amino groups of exposed lysine exposed on the protein surface. Comparison of mass spectrum obtained after treatment with succinic anhydride, in presence or absence of inhibitor, and after enzymatic digestion, allowed to identify the lysine residues not exposed. According to this analysis, **SCH53870** and **SCH54292** bind Ras close to **Lys101**, localized next to the region of Switch 2: the inhibitor binding site is therefore

---

[51] Taveras A. G., Remiszewski S. W., Doll R. J., Cesarz D., Huang E. C., Kirschmeier P., Pramanik B. N., Snow M. E., Wang Y.-S., Del Rosario J. D., Vibulbhan B., Bauer B. B., Brown J. E., Carr D., Catino J., Evans C. A., Girijavallabhan V., Heimark L., James L., Liberles S., Nash C., Perkins L., Senior M. M., Tsarbopoulos A., Ganguly A. K., Aust R., Brown J. E., Delisle D., Fuhrman S., Hendrickson T., Kissinger C., Love R., Sisson W., Villafranca E. and Webber S. E., "Ras Oncoprotein Inhibitors: The Discovery of Potent, Ras Nucleotide Exchange Inhibitors and the Structural Determination of a Drug-Protein Complex", _Bioorganic & Medicinal Chemistry_, **1997**, 5, 1, 125-133.

distinguished from the nucleotide binding site.[52,53] **SCH54292** interaction with Ras-GDP has been further investigated by NMR spectroscopy. It has been possible to verify that Ras protein can exist in two alternative conformations and in slow exchange, respect to NMR time scale, when Mg^{2+} ion concentration is low. These conformational changes concern residues present in GDP-binding pocket, near Switch I and Switch II regions. The protein conversion to an open conformation seems to facilitate GDP release, and inhibitor binding. NOESY analysis of **SCH54292**-Ras-GDP complex furnished the data reported in Table 2-1. Such data were then submitted to a computational analysis, using the Monte Carlo method. All these information therefore were employed in order to elaborate a model of the interaction. According to this model, **SCH54292** binds Ras-GDP in the critical Switch 2 region, which is flexible and, like Switch I region, has the property to change its conformation depending on the nature of the bound nucleotide. The glucose is not involved in the interaction and is exposed outside. The naphthyl group is located in a hydrophobic pocket, formed by Met72, Gln99, Ile100 and Val103. The hydroxylamine extends into a pocket near the Mg^{2+}, probably coordinating the ion, and the phosphate group of GDP.

A graphical representation of this model is reported in Fig. 2-6.[54]

---

[52] Pramanik B. N., Bartner P. L., Mirza U. A., Liu Y.-H. and Ganguly A. K., "Electrospray Ionization Mass Spectrometry for the Study of Non-covalent Complexes: an Emerging Technology", *Journal of Mass Spectrometry*, **1998**, 33, 911-920.

[53] Ganguly A. K., Pramanik B. N., Huang E. C., Liberles S., Heimark L., Liu Y.-H., Tsarbopoulos A., Doll R. J., Taveras A. G., Remiszewski S. W., Snow M. E., Wang Y. S., Vibulbhan B., Cesarz D., Brown J. E., Del Rosario J. D., James L., Kirschmeier P. and Girijavallabhan V., "Detection and Structural Characterization of Ras Oncoprotein-Inhibitors Complexes by Electrospray Mass Spectrometry", *Bioorganic & Medicinal Chemistry*, **1997**, 5, 5, 817-820.

[54] Ganguly A. K., Wang Y. S., Pramanik B. N., Doll R. J., Snow M. E., Taveras A. G., Remiszewski S. W., Cesarz D., Del Rosario J. D., Vibulbhan B., Brown J. E., Kirschmeier P., Huang E. C., Heimark L., Tsarbopoulos A. and Girijavallabhan V., "Interaction of a novel GDP Exchange Inhibitor with the Ras Protein", *Biochemistry*, **1998**, 37, 15631-15637.

assignment	distance restraint	distance in model[a]
Hc1−Hd	2.5	2.5 (reference)
Hc1−Hf	2.5	2.5
Hc2−He	2.5	2.5
Hc3−Hg	2.5	2.5
Hz−Hh	2.5	2.5
Hz−Hf	VW[b]	5.8
Hz−H1	3.2	3.2
Hc1−Hjc	4.4	4.8
Hz−Hja	2.9	2.7
Hz−Hjb	3.4	3.3
Hz−H5	3.5	3.8
Hz−H6	3.9	4.2
Hf−Hja	3.9	4.1
Hf−Hjb	2.9	2.6
Hf−Hjc	2.4	2.5
Hf−H2	VW[b]	5.2
Hd−He	2.5	2.5
Hjd−Hjb	2.9	3.0
Hjd−H2	2.8	2.4
Hjd−H6′	4.4	4.9
Hja−Hjb	2.2	1.8
Hja−H6	3.9	4.3
H1−H2	3.4	3.1
H1−H3	2.6	2.5
H1−H5	2.4	2.4
H6−H4	2.2	2.7
H6−H6′	2.1	1.8
H3−H5	2.4	2.7
H6′−H5	2.3	2.6

[a] From the model of SCH-54292 in complex with the Ras protein.
[b] VW denotes very weak.
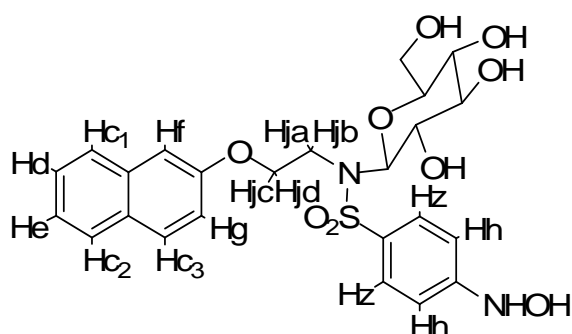
Table 2-1. Intramulecular distances for SCH54292-Ras-GDP complex obtained from NOESY analysis [from ref. 54].
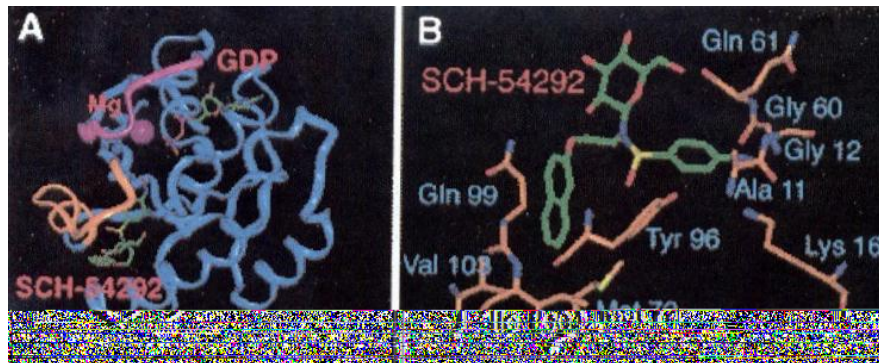
Figure 2-6. Interaction of SCH54292 with the complex Ras-GDP. (A) Structure of the ternary complex constituted by Ras (blue), GDP (green and purple), SCH54292 (green) and magnesium (purple). Switch I is represented in magenta, Switch II in orange. (B) Detail of the interaction between SCH54292 (green) and Ras protein (brown).

3. Protein-ligand interaction studies

It is a general assumption that the biological function of a macromolecule depends on its interaction with ligand molecules; as a consequence, binding events of ligands to receptors are crucial key in order to understand biological processes. In particular, for a protein, a ligand can be represented by another macromolecule, for example activator and effector proteins, DNA, RNA, or by a small molecule, for example a second messenger, a coenzyme, an inhibitor.

There have been many attempts in order to accurately characterize protein binding processes with a variety of biophysical methods. Among these methods, **Nuclear Magnetic Resonance** (**NMR**) and **Surface Plasmon Resonance** (**SPR**) have found wide application.

Aim of this chapter is not to make a complete discussion on the most important existing techniques employable for protein interaction studies, but to give to the reader enough tools for the understanding of the applications described in the present thesis.

3.1. NMR-based protein-ligand interaction studies

The study of protein–protein and protein–ligand interactions in solution has recently become possible on an atomic level by new NMR spectroscopy experiments able to identify binding events either by looking at the resonance signals of the ligand or the protein. Ideally, a combination of these two techniques allow obtaining a complete picture of ligand binding to a receptor. These methodologies can be applied to the **lead generation** in drug discovery, that is the identification of compounds that demonstrate specific activity against a therapeutic target, as well as to dynamic

structure–activity relationships (**SAR**). Among the most important approaches, we can distinguish: (1) the use of the *transferred NOE effect* for detecting and characterizing ligand binding, as in Saturation Transfer Difference (STD) spectroscopy, Water-LOGSY, transferred-NOESY (trNOESY), NOE pumping experiments, (2) the use of *chemical-shift changes* to identify ligand binding and the binding pocket of the receptor, as in ^{1}H/^{15}N-HSQC experiments and ^{1}H/^{13}C-HSQC experiments, (3) the use of *relaxation times* to identify ligand binding though transverse relaxation rates and longitudinal relaxation rates measurements, (4) the use of *diffusion* to identify ligand binding with DOSY spectroscopy. Some of the most important features of these techniques are summarized in Table 3-1. An exhaustive discussion on the topic can be found in recent reviews and books,[55, 56, 57] while, in the following sections, only the NMR experiments employed in order to study our inhibitor-Ras interaction will be described.

3.1.1. The fast-exchange approximation

The process underlying most NMR-based ligand binding screening experiments can be described by the following equation:

$$[E] + [L] \underset{K_{off}}{\overset{K_{on}}{\rightleftharpoons}} [EL] \quad \text{[Equation 1]}$$
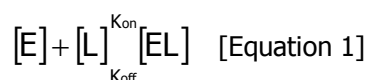
It represents a dynamic equilibrium involving three species: the free receptor E, the free ligand L, and the receptor-ligand complex, EL.

[55] Meyer B. and Peters T., "NMR Spectroscopy Techniques for Screening and Identifying Ligand Binding to Protein Receptors", *Angew. Chem. Int. Ed.*, **2003**, 42, 864–890.

[56] Peng J. W., Moore J., Abdul-Manan N., "NMR experiments for lead generation in drug discovery, *Progress in Nuclear Magnetic Resonance Spectroscopy*, **2004**, 44, 225–256.

[57] Zerbe O., "BioNMR in Drug Research", **2002**, Wiley-VCH.

	SAR by NMR	STD NMR	Spin labeling	Diffusion editing	Inverse NOE Pumping	Water-LOGSY
Large protein (>30 kDa)	limited[a]	yes	yes	no	yes	yes
small protein (<10 kDa)	yes	no	yes	yes	no	no
Isotope-labeled protein required	yes	no	no	no	no	no
Binding epitope on protein	yes[c]	no	no	no	no	no
Binding epitope on ligand	no	yes	no	no	yes[d]	yes[e]
Amount of protein [nmol] at 500 MHz	25	0.1	~1	~100	~25	~25
K_D tight binding K_D weak binding	no limit ~1 mM	100 pM ~10 mM	100 pM ~10 mM	~100 nM ~1 mM	1 nM ~1 mM	100 pM ~10 mM
Identification of ligand	no	yes	yes	yes	yes	yes
Comments	robust method	robust method	sensitive method, but results ambiguous if lysine positions unknown	relatively insensitive method	stable method, but ligand excess and mixing time need to be optimized	good for very hydrophilic targets and/or ligands

[a] TROSY necessary. [b] But chemical modification. [c] If protein is assigned. [d] Not realized. [e] But water contact surface.

Table 3-1. NMR spectroscopy techniques for the identification and characterization of binding of ligands to proteins [from ref. 55]

Protein-ligand interaction studies

The unimolecular rate constant K_{off} is inversely proportional to the mean lifetime τ_B of the receptor-ligand complex. The bimolecular rate constant, K_{on}, measures the probability of a productive encounter between the free receptor and the ligand and is often assumed to be controlled by diffusion. K_{on} can vary between 10^7 and $10^9 M^{-1}s^{-1}$. The binding affinity can be described by the temperature-dependent equilibrium dissociation constant, K_D:

$$K_D = \frac{[E][L]}{[EL]} = \frac{K_{off}}{K_{on}} \quad \text{[Equation 2]}$$

The bound receptor fraction is defined by:

$$P_B^E = \frac{[EL]}{[E]+[EL]} \quad \text{[Equation 3]}$$

These two equations can be combined giving the following:

$$P_B^E = \frac{[L]}{[L]+K_D} \quad \text{[Equation 4]}$$

where P_B^E is the fractional occupation of the receptor binding site by ligand L. When $[L] \ll K_D$, P_B^E is proportional to $[L]$. When $[L] = K_D$, the receptor is half-saturated, that is, half of the receptor molecules exist in a one-to one complex with the ligand. When $[L] \gg K_D$, the receptor is completely saturated and $P_B^E = 1.0$; in this limit, every receptor binding site is occupied by one ligand, which on average exchanges with a second distinct ligand every $\approx 1/ K_{off}$ seconds. According to these points, ligands with weak affinity have large K_D and thus require the addition of more ligand to saturate the receptor binding site.

In the two-state equilibrium given by Eq. 1, ligand and receptor molecules

_____

will exist in either the free (L, E) or the complexed (EL) state. In the free state, both receptor and ligand retain their intrinsic NMR parameters (e.g. chemical shifts, relaxation rates, translational diffusion coefficients). When ligand and receptor interact, the mutual binding affinity drives an exchange process that toggles both sets of molecules between the free and complexed states. At the equilibrium, they adopt free and bound state populations ([E], [L], [EL]) consistent with Eq. 1. Under these conditions, the ligand transiently adopts the NMR parameters characteristic of the typically much larger receptor. Alternatively, from the receptor's perspective, the ligand transiently perturbs the binding site microenvironment(s), which may alter the distribution of conformations sampled by the ensemble of receptor molecules. In either case, *the exchange modulates the NMR parameters of both molecules*. It is the ability to experimentally distinguish these exchange-modulated parameters from those of the free state what enables NMR detection of the receptor-ligand interaction and hence NMR-based screening.

The solutions to the HMM equations (Bloch equation formalism by Hahn, Maxwell and McConnell)[58, 59] describe the behaviour of a system magnetization on arbitrary exchange time scales. In NMR-based screening, however, these equations are almost never solved, and **fast exchange is simply assumed**. This assumption is made for two reasons. First, the experimental conditions for ligand-based NMR screening are often well suited to fast exchange. These experiments are typically carried out with $L_T/E_T > 10$ (where L_T and E_T are total ligand and total receptor concentration respectively) and the binding compounds have $K_D \geq 100\mu M$. If K_{on} is well approximated by a diffusion-limited value (10^7-10^9 $M^{-1}s^{-1}$), then the slowest exchange rate K_{ex} values lie in the range $1000 < K_{ex} < 100\ 000\ s^{-1}$. Ligand-

_____

[58] Hahn E. L. and Maxwell D. E. (1952) "Spin Echo Measurements of Nuclear Spin Coupling in Molecules" *Phys Rev*, **1952**, 88, 5, 1070-1084.
[59] McConnell H. M. "Reaction Rates by Nuclear Magnetic Resonance", *J Chem Phys*, **1958**, 28, 3, 430-431.

based NMR screening methods are primarily ^{1}H based and consequently, K_{ex} exceeds most differences in intrinsic ^{1}H relaxation rates and rotating frame precession frequencies, thus ensuring that the fast exchange assumption is valid. A second motivation for assuming fast exchange is the resulting algebraic simplicity. Generally, the NMR parameters Q become the simple averages:

$$Q_{avg} = P_B Q_B + P_F Q_F \quad \text{[Equation 5]}$$

Here, Q_{avg} is the observed exchange-averaged parameter for the ligand (or the receptor) in the presence of the receptor (or the ligand). Observed differences between Q_{avg} and Q_F provide a signature of receptor binding and indicate a hit in a NMR screening based on that parameter. Q_{avg} is a simple population-weighted average and it can be applied to those parameters Q for which chemical shift modulations are not relevant. These parameters include longitudinal auto relaxation and cross-relaxation rates, rotating-frame spin-locking auto relaxation and cross-relaxation rates, and translational diffusion coefficients. The bound state contribution is $P_B Q_B$. The ability to detect binding with adequate sensitivity depends critically on $P_B Q_B$, being significant relative to $P_F Q_F$. However, typical screening conditions where $L_T \gg E_T$ make $P_B \ll P_F$. For this reason, it is much preferred to measure NMR parameters Q that become amplified in the bound state (i.e. $Q_B \gg Q_F$).

3.1.2. Ligand-based vs Receptor-based screening

Screening may proceed by ligand- or receptor-based methods. Receptor-based methods observe and compare the NMR parameters of the receptor molecule resonances in the presence and absence of compound mixtures. On the contrary, the receptor-based methods have focused mostly on

_____

proteins. Such methods incorporate site-specific characterization afforded by assigned protein NMR spectra along with *a priori* knowledge of the protein three-dimensional structure (either from X-ray or NMR) to drive lead generation. By identifying perturbations of assigned protein resonances, not only ligands are identified, but also their binding sites are localized. Localization of binding sites also enables one to immediately distinguish specific from non-specific binding. Finally, unlike ligand-based methods, receptor-based methods do not rely on fast exchange to obtain bound state information. Observation of receptor resonances permits the characterization of both higher and lower affinity hits. But these NMR methods demand physicochemical properties of the protein target that present progressively more difficult challenges. First, milligram quantities of soluble, non-aggregated protein must be over-expressed and purified. Then, suitable expression hosts must be found that permit isotope enrichment (e.g. ^{13}C, ^{15}N, ^{2}H) critical for the resonance assignment of typically large (> 30 kDa) therapeutic targets. After sufficient quantities of labelled protein are available, it must be ensured that the sample is stable for the time required for sequential resonance assignment. Although new data acquisition approaches promise to accelerate resonance assignment, it can still be a relatively lengthy process (weeks) for the large monomeric proteins. Unfortunately, the time required for NMR assignment of such targets inevitably favours other approaches, such as X-ray crystallography, that can provide high-resolution structural information to medicinal chemistry on a faster time scale (if crystals are available). Alternatively, the typical implementation of ligand-based methods compares the NMR parameters of a single compound or of a mixture of compounds in the presence and absence of the receptor molecules. This approach renders the molecular weight of the receptor molecule irrelevant. In fact, the most powerful ligand-based approaches become more sensitive when dealing with larger receptors. Additionally, ligand observation bypasses the need to produce milligram quantities of isotope labelled receptor. Depending on the

approach, less than 1 mg of unlabeled protein is required for these experiments (receptor concentration is often $\leq$ 1µM, and no assignments are necessary). This allows to evaluate new targets more rapidly and to work on a time scale useful for chemistry and high-throughput screens. An obvious disadvantage of ligand-based approaches is the inability to localize the binding site of the small molecule hits on the receptor. Also, ligand-based approaches rely on the exchange-mediated transfer of bound state information to the free state. This requirement biases ligand-based methods towards the identification of weakly binding ligands (rapid exchange) and the use of large ligand molar excesses ($L_T/E_T \gg 1$). The consequent risk is that, under these conditions, ligand may start to occupy non-specific binding sites. Both receptor- and ligand-based approaches have distinct advantages and disadvantages. Clearly, if receptor-based methods are possible, then the potentially higher information content that can be obtained makes these the methods of choice. However, due to the scarcity of low-molecular weight drug targets, ligand-based screening is, in general, of broader applicability and places less demands on other research disciplines and infrastructure.

3.1.3. The NMR techniques used in this thesis

The results presented this thesis refers both to ligand-based NMR methods, STD, trNOESY experiments and relaxation time measurements, and receptor-based methods, in particular $^1H/^{15}N$-HSQC titration experiment. The fundamental of these methodologies will be explained in the next sections.

3.1.3.1. Saturation Transfer Difference (STD)

STD results from the difference of two experiments. In a first experiment, the "on-resonance" experiment, various receptor proton magnetizations are

_____

selectively saturated via a train of frequency-selective rf pulses. The rf train is applied to a frequency window that contains receptor resonances, but not resonances from the compounds. The saturation propagates from the point of application to other receptor protons via the vast network of intramulecular ^1H–^1H cross-relaxation pathways; this process of spin-diffusion is quite efficient, due to the typically large molecular weight of the receptor. Bound compounds pick up this saturation via inter-molecular ^1H–^1H cross-relaxation at the ligand–receptor interface. They then dissociate back into free solution where the saturated state persists, due to the small free state R_1 values. At the same time, more "fresh" ligand exchanges on and off the receptor while saturation energy continues to enter the system through the sustained application of rf. Thus, saturated free ligands accrue during the saturation time and this allows the "amplification" of the signal. For the on-resonance irradiation frequency values around -1 ppm are practical because no ligand nuclei resonances are found in this spectral region, whereas the significant line width of protein signals still allows selective saturation. If the ligand(s) show no resonance signals in the aromatic proton spectral region, the saturation frequency may also be placed there (7 ppm) or even further downfield (δ=11– 12 ppm). In order to achieve the desired selectivity and to avoid side-band irradiation, shaped pulses are employed for the saturation of the protein signals.

A complementary reference experiment, the "off-resonance" experiment, that applies the identical rf train for off-resonance, was then recorded; the spectrum yields a normal NMR spectrum of the ligand-protein mixture.

The "on-resonance" and "off-resonance" experiments are recorded in an interleaved fashion and subtracted. A difference spectrum is produced in which only the signals of the ligand(s) that have felt the transfer of saturation from the protein do appear. The receptor resonances will not be visible, or will be scarcely visible, as consequence of their minimal concentration or because of R_2 relaxation-filtering (spin-lock) applied just prior to detection.

If binding is very tight, and consequentially off rates are in the range of 0.1–0.01 Hz, the saturation transfer to ligand molecules is not very efficient. This is usually the case for K_D values less than 1 nM. If the K_D values are 100 nM, or larger, fast exchange of free and bound ligands leads to a very efficient build up of saturation of the ligand molecules in solution. On the other hand, when binding is very weak, the probability of the ligand being in the receptor site becomes very low, which results in weak STD signals. Thus, STD can be used from tight binding up to a K_D of about 10 mM.

Concerning on the intensity of the STD signals, it depends, among other things, on the irradiation time / saturation time and on the excess of ligand molecules used.[55] The more ligand is used and the longer the irradiation time, the stronger the STD signal is. In general, the irradiation time is 2s and unti a 100-fold excess of ligand is used to give good results. In fact, upon dissociation, the saturation of the ligand is transported into solution, where it accumulates as a result of the slow decline of the saturation by relaxation processes in solution. Before ligands in solution have lost their saturation, the process of association (followed by dissociation) can occur many times and thus put many more saturated ligands into solution. The maximum net effect of saturation on ligand protons occurs if a large excess of ligand is used, because it is very unlikely that a ligand with saturation renters the binding site. From the high ligand:protein ratios it is clear that the amount of protein required for the measurements is very small.

The ligand saturation is higher for those protons that are in closer contact with the receptor. For those ligand protons that interact with protein protons through an intermolecular NOE, a decrease in intensity is observed in the "on-resonance" spectrum, while no intensity variations take place in the "off-resonance" spectrum. Subtraction of the "on-resonance" from the "off-resonance" spectra leads to a difference spectrum, in which only the signals of the protons that were attenuated by saturation transfer are visible (Fig. 3-1). In this way, STD spectroscopy not only furnishes an evidence of ligand-protein binding, but also allows to obtain the **ligand epitope mapping**,

_____

that is the identification of the ligand regions involved in the interaction with the receptor.

off resonance spectrum

on resonance spectrum
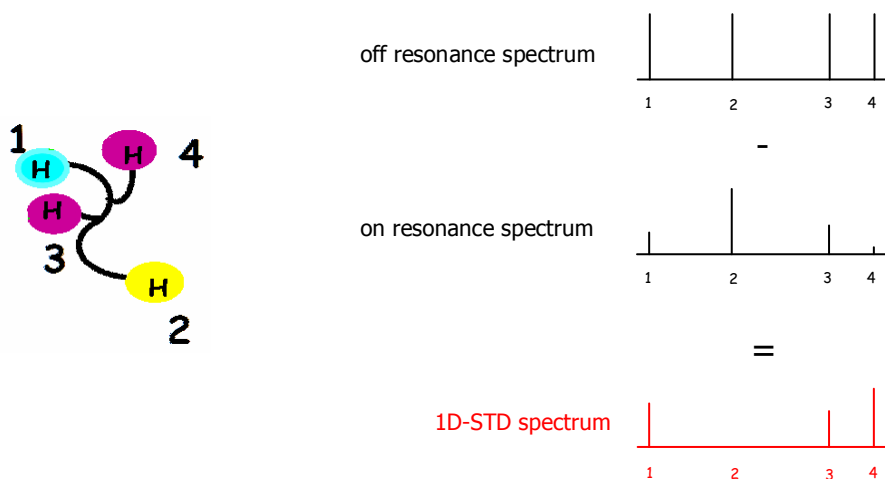
1D-STD spectrum

Figure 3-1. STD spectrum is generated by subtraction of "on-resonance" spectrum from "off-resonance" spectrum.

This kind of information is of primarily importance for pharmacophore group identification in the rational drug design process.

3.1.3.2. Transferred NOE

NOE effects (NOEs) have been broadly exploited in determining the 3D structure of molecules in solution,[60] recently they have found important applications also studying the field of ligand-protein interaction. When ligand molecules bind to receptor proteins, the NOEs undergo drastic changes leading to the observation of transferred NOEs (trNOEs). The observation of trNOEs relies on the existence of different tumbling times τ_c for the free and bound molecules. Low or medium molecular weight molecules (MW < 1000 Da) have short correlation times τ_c and, as a consequence, such molecules

_____

[60] Neuhaus, D. and Williamson M. P., "The nuclear Overhauser effect in structural and conformational analysis", **2000**, New York, J. Wiley.

exhibit positive NOEs. Large molecules, however, exhibit strongly negative NOEs. When a small molecule (ligand) is bound to a large molecular weight protein (the protein receptor molecule), it behaves as a part of the large molecule and adopts the corresponding NOE behaviour, that is, it shows strong negative NOEs, so-called trNOEs. These trNOEs reflect the bound conformation of the ligand. Binding of a ligand to a receptor protein can thus easily be distinguished by looking at the sign and size of the observed NOEs (Fig. 3-2).

free state   bound state
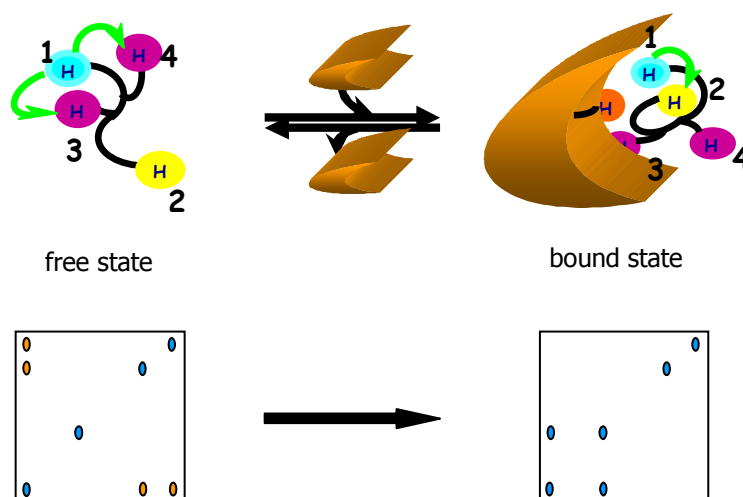
Figure 3-2. Left. Schematic representation of a NOESY spectrum for a free ligand. Cross peaks and diagonal peaks have different sign. Right. Schematic representation of a trNOESY spectrum recorded for an exchanging ligand–protein system. Cross peaks and diagonal peaks have the same sign, as expected for a large molecule, thus indicating binding to the protein.

However, one of the major drawbacks of this experiment is the possible existence of spin diffusion effects, which are typical for large molecules. In this case, apart from direct enhancements between protons close in space, other spins (including those of the receptor) may mediate the exchange of magnetization, thus producing negative cross peaks between protons far apart in the macromolecule. Thus, protein-mediated, indirect trNOE effects

_____

may lead to interpretation errors in the analysis of the ligand bound conformation. However, using trNOEs in the rotating frame (trROESY) experiments[61,62] it is possible to distinguish which cross peaks are dominated by an indirect effect, usually mediated by a protein proton, and hence distinguish direct from indirect enhancements.

The estimated range of binding affinities that can be probed by trNOESY is $100nM \leq K_D \leq 1mM$.[63]

Thus, the trNOE method allows fast screening of putative binders respect to a specific target receptor and, at the same time, permits the knowledge of the recognized conformation of the ligand bound to the receptor, with considerable implications for a rational structure-based drug design.

3.1.3.3. Relaxation time measurements

Free compounds presenting low molecular weight are characterized by small relaxation rates $R_1=1/T_1$ and $R_2=1/T_2$. On the contrary, compounds bound to a protein molecule with large molecular weight share the NMR relaxation properties of the receptor. Thus, bound compounds have large $R_1=1/T_1$ and $R_2=1/T_2$ values.

When considering $R_1=1/T_1$ measurements as a binding assay, inter-proton cross-relaxation (NOE) makes it important to distinguish between selective and non-selective R_1 measurements. Selective R_1 values are sensitive probes of binding while non-selective R_1 values are not. To achieve selective R_1 values (for detecting binding) we must differentially perturb the salient

[61] Arepalli, S. R., Glaudemans C. P. J., Daves G. D., Kovac P. and Bax A., "Identification of protein-mediated indirect NOE effects in a disaccharide-Fab' complex by transferred ROESY", *J. Magn. Reson. Ser. B*, **1995**, 106, 195-198.

[62] Asensio J. L., Canada F. J., Bruix M., Rodriguez-Romero A. and Jimenez-Barbero J., "The interaction of hevein with N-acetylglucosamine-containing oligosaccharides. Solution structure of hevein complexed to chitobiose", *Eur. J. Biochem.*, **1995**, 230, 2, 621-33.

[63] Mayer M. and Meyer B., "Mapping the active site of angiotensin-converting enzyme by transferred NOE spectroscopy", *J. Med. Chem.*, **2000**, 43, 11, 2093-2099.

magnetizations, either by selective inversions (as in 1D-NOE experiments) or at different times (as in 2D-NOESY experiments). On the other hand, popular experiments actually monitor R_2 relaxation using a spin-lock such as the Carr-Purcell-Meiboom-Gill (CPMG) pulse train or continuous wave irradiation as in a $R_{1\rho} = 1/T_{1\rho}$ experiment.[64, 65]

Basic steps for identifying binders using R_1- and R_2-edited experiments are the following: (1) the R_1 or R_2 experiment for the lone compound(s) for a set transverse relaxation delay, is recorded; (2) a second R_1 or R_2 experiment on the compound(s) is recorded in the presence of the receptor. If there is interaction between compound(s) and receptor, T_1 and T_2 values for the ligand(s) decrease.

3.1.3.4. $^1H/^{15}N$-HSQC experiments

One typical experimental setup to detect binding of ligands to receptor proteins and to identify at the same time the protein binding pocket amino acids involves the acquisition of $^1H/^{15}N$ HSQC (Heteronuclear Single-Quantum Correlation) spectra of probes with and without ligands present. This technique requires that the ^{15}N-labeled protein is available.

In general, the $^{15}N/^1H$ HSQC spectrum of a protein shows one signal for every amino acid residue, that is the backbone N-H signal, except for proline residue, of course, to which no peak correspond, and basic amino acids that can present additional side chain signals, depending on the spectral window selected. The detection of ligand binding works as follows: (1) the $^{15}N/^1H$ HSQC spectrum of the ^{15}N-labeled protein is acquired as a reference spectrum; (2) samples are prepared, that contain different concentrations of the potential ligand(s), in order to perform a titration; (3) the $^{15}N/^1H$ HSQC spectrum of each sample is recorder and compared with the reference spectrum. If the resonance position of a cross-peak is significantly shifted

---

[64] H.Y. Carr, E.M. Purcell, *Phys. Rev.*, **1954**, 94, 630.
[65] S. Meiboom, D. Gill, *Rev. Sci. Instr.*, **1958**, 29, 688.

_____

compared to the reference spectrum this is an indication of binding. If the sample contained only one potential ligand molecule, the binding ligand is identified. If a mixture had been used, the active component has to be identified by separation.
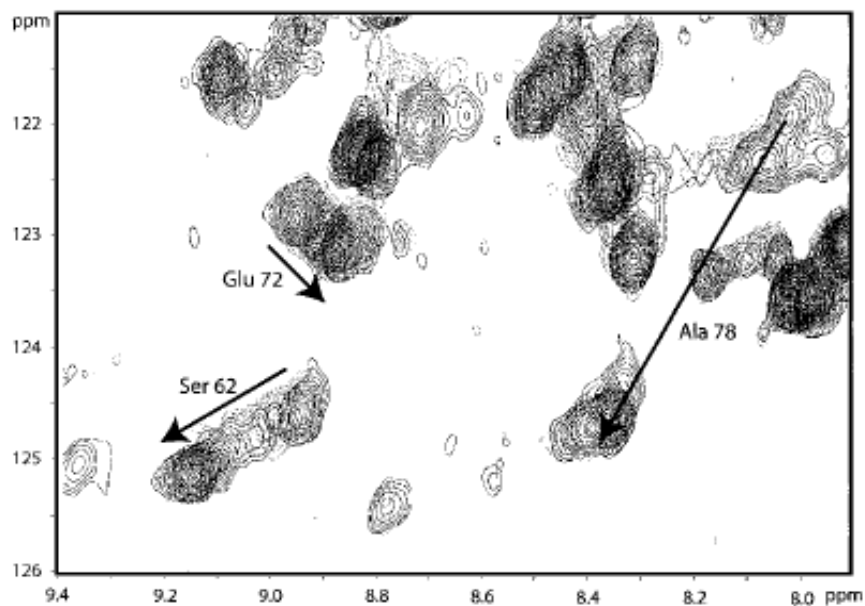
Figure 3-3. Expanded region of the overlaid ^{1}H-^{15}N HSQC spectra from a titration of ^{15}N-labeled S100B with CapZ peptide. The protein concentration was 1 mM, and the spectra shown are for peptide concentrations of 0, 0.25, 0.5, 0.75, 1.0, 1.5, 2.5 and 3.0 mM. Chemical shift changes for the cross peaks of Ser62, Glu72 and Ala78 are indicated [from ref. 66].

In principle, ^{1}H/^{15}N-HSQC NMR experiments have been known for a while to be useful to study the binding of ligands to proteins. For instance, ^{1}H/^{15}N-HSQC experiments were known to provide also an effective method to investigate interactions of the guanidinium groups of arginine units with charged groups on the ligand.

Today, this is the most used NMR technique in order to obtain a **map of the receptor binding site**.

_____

[66] Kilbi P. M., Van Eldik L. J., and Roberts G. C. K., *Protein Sci.*, **1997**, 6, 2494-2503.

3.2. SPR protein-ligand interaction studies[67]

3.2.1. SPR principles

Surface Plasmon Resonance (SPR) is a physical process that can occur when plane-polarized light hits a metal film under **total internal reflection conditions**. In particular, when a light beam hits a half circular prism, the light is bend towards the plane of interface, when it is passing form a denser medium to a less dense one. Changing the incidence angle changes the out coming light until a critical angle is reached. At this point all the incoming light is reflected within the circular prism. This is called total internal reflection (**TIR**) (Fig. 3-4). Although no light is coming out of the prism in TIR, the electrical field of the photons extends about a quarter of a wave length beyond the reflecting surface.
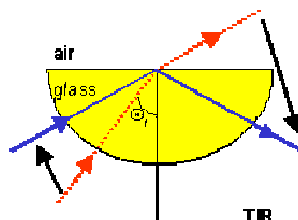
Figure 3-4. Schematic representation of total internal reflection phenomenon.

Generally the prism is coated with a thin film of a noble metal on the reflection site. In most cases gold is used because it gives a SPR signal at convenient combinations of reflectance angle and wavelength. In addition,

---

[67] For a detailed account of the application of SPR to the study of protein-protein interaction: a) Nieba L., _Analytical Biochemistry_, **1997**, 252, 217-228; b) Gershon P. D., _Journal of Immunological Methods_, **1995**, 183, 65-67; c) Ferguson A. L., _FEBS Letter_, **2000**, 481, 281-284.

_____

gold is chemical inert to solutions and solutes typically used in biochemical contexts. When the energy of the photon electrical field is just right it can interact with the free electron constellations in the gold surface. The incident light photons are absorbed and converted into surface plasmons. In accordance with the quantum theory, a **plasmon** is the particle name of the electron density waves. Therefore, when in a TIR situation the quantum energy of the photons is right, the photons are converted to plasmons leaving a 'gap' in the reflected light intensity (Fig. 3-5).
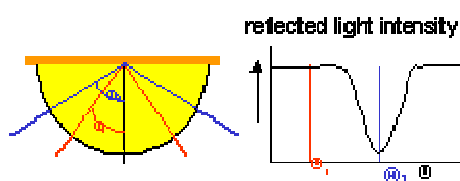
Figure 3-5. Conversion of photons to plasmons create a gap in the reflected light intensity.

Like all conversions, the photon to plasmon transformation must conserve both momentum and energy in the process. Plasmons have a characteristic momentum defined by factors that include the nature of the conducting film and the properties of the medium on either side of the film. Resonance occurs when the momentum of incoming light is equal to the momentum of the plasmons (momentum resonance). The momentum of the photons and plasmons can be described by a vector function with both magnitude and direction. The relative magnitude of the components changes when the angle or wavelength of the incident light changes. However, plasmons are confined to the plane of the gold film, so, for SPR, it is only the vector component parallel to the surface that matters. Thus, the energy and the angle of incident light must be right to form surface plasmon resonance.

In TIR, the reflected photons create an electric field on the opposite site of the interface. The plasmons create a comparable field that extends into the medium on either side of the film. This field is called the evanescent wave because the amplitude of the wave decreases exponentially with increasing

distance from the interface surface, decaying over a distance of about one light wavelength. The dept of the evanescent wave which is useful for measurements is within ~ 300 nm of the sensor surface. The wavelength of the evanescent field wave is the same as that of the incident light. The energy of the evanescent wave is dissipated by heat. Equations, which describe how electric fields travel through a medium, include a term for the properties of the medium. For light, this term is the **refractive index**. The light is seen as refracted because the photons have a different velocity in different media. In the same way, _the velocity (and therefore the momentum) of the plasmons is changed when the composition of the medium changes_. Because of the change in momentum, the angle of incident light at which the resonance occurs changes. This can be measured very precise. This type of SPR is known as resonant angle or **angular SPR** and is commonly used. On the other hand, at a fixed angle of incident light, the wavelength can be varied until resonance occurs. This is known as resonant wavelength SPR or **spectral SPR** and is not used widely.

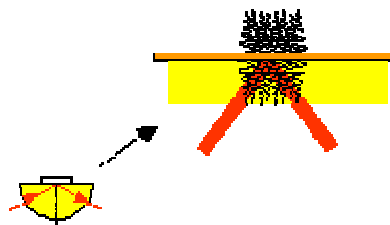**Figure 3-6**. Resonance angle SPR. The velocity (and therefore the momentum) of the plasmons is changed when the composition of the medium changes.

However, the best angular accuracy of the goniometer in angular SPR is 0.001°, which corresponds to an optical wavelength shift of 0.6 nm. A full wavelength spectrophotometer can simultaneously observe the wavelength from 400 - 800 nm and is more accurate than angle measurements.

_____

3.2.2. SPR application to ligand-protein binding studies

The phenomenon of *SPR is completely non-specific*. It cannot distinguish between different chemical changes. While this may appear to be a limitation, it is really a powerful advantage. Specificity depends upon selection of pairs of molecules which react only with each other. One member of the pair is the detector and the other is the target analyte (i.e. the substance we wish to detect/quantitate). Any pair of molecules which exhibit specific binding can be adapted to SPR measurement. These may be an antigen and antibody, a DNA probe and complementary DNA strand, an enzyme and its substrate, an oil and a gas or liquid which is soluble in the oil, or a chelating agent and metal ion.

SPR can be used as the basis for a sensor which is capable of sensitive and quantitative measurement of a broad spectrum of chemical and biological entities. It offers a number of important practical advantages over current analytical techniques. The time from sample application to reported result varies with the specific chemistry but can be as short as 5 minutes. In most cases there is no need to pre-treat the sample before its presentation to the sensor. A single sensor format (i.e. size, storage and usage protocol, reader, etc.) may be used for a variety of assay chemistries including immunological, nucleic acid binding, enzymatic, chemical, and gas adsorption. Some of the potential areas of application include medical diagnostics, environmental monitoring, agriculture pesticide and antibiotic monitoring, food additive testing, military and civilian airborne biological and chemical agent testing, and real time chemical and biological production process monitoring.

During a binding analysis SPR changes occur as a solution is passed over the surface of a sensor chip. To perform an analysis, one interactant is captured on a sensor surface. The sensor surface forms one wall of a flow cell. Sample containing the other interactant(s) is injected over this surface in a

_____

precisely controlled flow. Fixed wavelength light, in a fan-shaped form, is directed at the sensor surface and biomolecular binding events are detected as changes in the particular angle where SPR creates extinction of light. This change is measured continuously to form a sensorgram (Fig. 3-7), which provides a complete record of the progress of association or dissociation of the interactants.
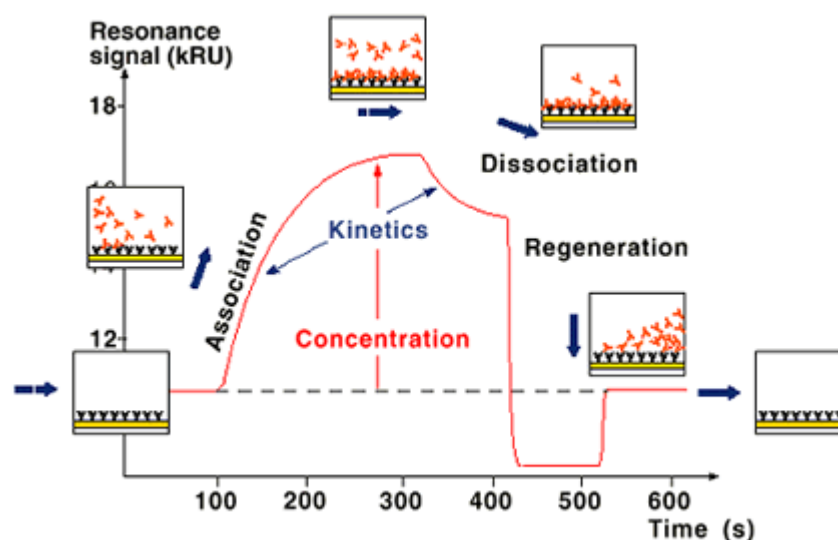
Figure 3-7. The progress of an interaction is monitored as a sensorgram. Analyte binds to the surface-attached ligand during sample injection, resulting in an increase in signal. At the end of the injection, the sample is replaced by a continuous flow of buffer and the decrease in signal now reflects dissociation of interactant from the surface-bound complex. A response of 1000 RU (resonance units) corresponds to a change in surface concentration of 1 ng mm^{-2}.

Setting up an assay for any particular protein is very fast, and the data provided are highly informative. However, this technique presents some limitations. The fact that in an SPR experiment only one sample can be analysed at a time, with each analysis taking 5-15 min, means that it is neither practical nor efficient for high throughput assays. Automation does not solve this problem because the sensor surface deteriorates over time and with re-use. In addition, because the SPR measures the mass of material binding to the sensor surface, very small ligand (MW < 1000) give very small responses. As a consequence, SPR is not suitable for small ligand-

_____

protein binding studies, but it can only be used in order to characterize protein-protein interactions.

Coimbra, summer holydays 2006

EXPERIMENTAL SECTION

4. Results and Discussion

4.1. Objective and strategy

Because of their role in oncogenesis [1.2.], inhibition of Ras proteins, particularly of their tumorigenic variants, represents today one of the principal strategies finalized to the obtainment of new antitumoral therapies [2.1.]. Among the different possible approaches, one of the most innovative and less explored is represented by the *inhibition* of this protein activation, key event for the explication of their biological activity, but also for the Ras-induced tumoral cell transformation [2.2.].

Objective of this thesis has been the development of new small molecules able to inhibit, at least partially (total inhibition in fact would result lethal for cell), Ras protein activation, in particular the GEFs-promoted GDP/GTP nucleotide exchange.

Inhibitors able of inactivating Ras have been previously described by Schering-Plough [2.2.].[51-54] All these molecules contain a *phenyl-hydroxylamino group* that binds Ras in a region close to the nucleotide binding site and one aromatic group (Fig. 4-1). Nevertheless, they present some negative characteristics that prevent their employment as potential drugs: (1) they are chemically unstable and (2) they are insoluble in water and in the most commonly used organic solvents.

In order to obtain new more efficient inhibitors, we adopted the *rational drug design strategy*.
Firstly, we studied the structure-activity relationship (SAR) of Schering-

Plough compounds and of new molecules containing variants of their functional groups that we designed and synthesized. The data collected demonstrated that the phenylhydroxylamino group is an essential pharmacophore, while other positions are not so critical for the biological activity.
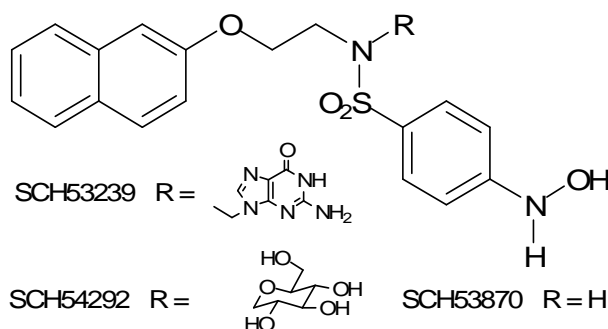
Figure 4-1. Schering–Plough inhibitor structures.

Keeping in mind this, we prepared new compounds in which the phenyl-hydroxylamino moiety is supported on glycidic templates, in an attempt to try to take advantage of carbohydrate capability of orienting substituents in space, in this case in a suitable manner for the interaction with Ras proteins. In addition, the sugar portion can improve compound pharmacokinetic properties and decrease their toxicity.

In this way, a new class of Ras inhibitors was obtained, their biological activity and the nature of their interaction with the molecular target were characterized.

With the aim to allow a correct evaluation of my job, it is necessary to underline that all the results here presented derive from the research activity of our group, except for the docking studies, performed by Anterio Consult & Research GmbH, Augustaanlage, Mannheim, Germany.

_____

4.2. Structure-activity relationship in Ras inhibitors[68]

Starting from Schering–Plough inhibitor structures, we developed mini-library of compounds have been generated by small variations in the structure of compound **1** (**SCH-53870**) (Fig. 4-2).
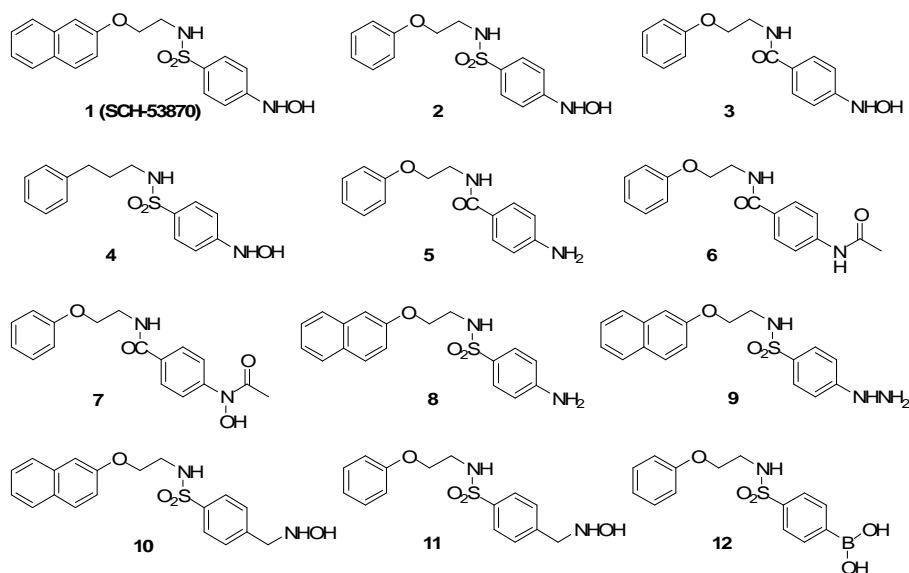
Figure 4-2. Chemical structures of compounds **1**-**12**.

We investigated the structure-activity relationship in this panel of compounds by analyzing their capacity to inhibit the guanine nucleotide exchange and dissociation on purified p21 h-Ras and to inhibit the growth of normal mammalian cells and of k-Ras transformed cells. Moreover, we

[68] Colombo S., Peri F., Airoldi C., Tisi R., Fantinato S., Palmioli A., Martegani E., and Nicotra F., "Structure-activity relationship in Ras inhibitors", _Bioorg. Med. Chem._, submitted

present a further characterization of the interaction between **1** and Ras-GDP using the two-hybrid system.

4.2.1. Chemical synthesis

Molecules **1**-**12** were synthetically derived from the amine precursors **13**, **14** and **15** as showed in Scheme 4-1.

Scheme 4-1. Reagents and conditions: a) 4-carboxybenzaldehyde, HOBt, DIC, DIPEA, DMF, r.t., 20 h and 95% for **21**; b) p-nitrobenzenesulfonyl chloride, Et₃N, DMF, r.t., 3 h and 80% for **16**, 3 h and 82% for **17**; c) 4-nitrobenzoic acid, HOBt, DIC, DIPEA, DMF; d) 4-carboxyphenylboronic acid, HOBt, DIC, DIPEA, DMF, r.t., 2 h, 40%; e) NH₂OH, pyridine, 5 h and 85% for **23*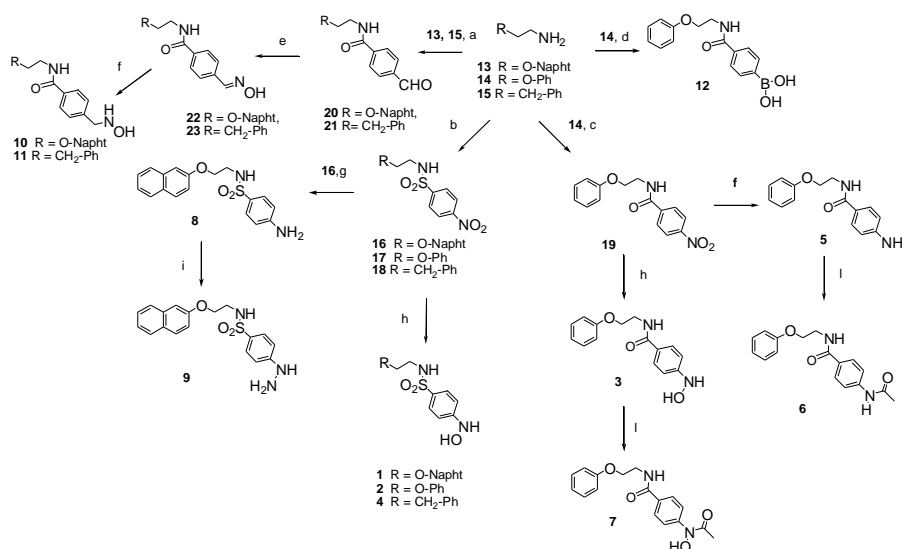*; f) NaCNBH₃ in AcOH, r.t., 1.5 h and 61% for **10**, 2 h and 56% for **11**; g) H₂, Pd-C, MeOH-THF, r.t., 30 min and 87% for **5**; h) NH₂-NH₂, Pd-C, MeOH-THF, 0° C, 1 h and 80% for **2**, 45 min and 90% for **3**, 1 h and 80% for **4**; i) NaNO₂, HCl, SnCl₂, 4°C, 2 h 30 min, 82%; l) Ac₂O/pyridine, r.t., 1 h and 93% for **6**, 1 h and 95% for **7**. DIC = *N,N*-diisopropylcarbodiimide; DIPEA = diisopropylamine; Et₃N = triethylamine; DMAP = 4-(dimethylamino)-pyridine; HOBt = *N*-hydroxybenzotriazole.

Condensation of 2-(2-naphtoxy)-ethylamine **13** and 3-phenyl-propylamine **15** with 4-carboxybenzaldehyde in the presence of N-hydroxybenzotriazole

_____

(HOBt), diisopropylcarbodiimide (DIC) and diisopropylethylamine (DIPEA) in DMF afforded aldehydes **20** and **21** that, after treatment with hydroxylamine in pyridine, gave the corresponding oximes **22** and **23**. Reduction with sodium cyanoborohydride in glacial acetic acid converted oximes **22** and **23** into hydroxylamines **10** and **11**, respectively. Condensation of 2-phenyloxy-ethylamine **14** with 4-carboxy-phenylboronic acid with HOBt, DIC and DIPEA afforded compound **12**. Amines **13**-**15** were condensed with p-nitrobenzenesulfonyl chloride in the presence of triethylamine providing p-nitrophenyl-sulfonamides **16**-**18**, whose aromatic nitro groups were reduced to hydroxylamines by treatment with hydrazine and Pd/C in methanol affording compounds **1** (**SCH-53870**), **2** and **4**. Compound **16** was converted into amine **8** by catalytic hydrogenation that was in turn transformed into hydrazide **9** by treatment with sodium nitrite and $SnCl_2$ in concentrated aqueous HCl. 2-phenyloxy-ethylamine **14** was condensed with *p*-nitrobenzoic acid using HOBt, DIC and DIPEA in DMF, affording **19** whose nitro group was partially reduced to hydroxylamine (hydrazine, Pd/C) to give **3** or completely reduced to amine (H_2-Pd/C) giving **5**. Acetylation of **3** and **5** (acetic anhydride in pyridine) afforded respectively compounds **7** and **6**.

4.2.2. Biological evaluation

4.2.2.1. Characterization of 1 (SCH-53870)/Ras interaction

Despite the previous characterisation by NMR of the complex **1**-Ras-GDP,[54] the mechanism of action of this compound is still poorly understood. We have found that this compound inhibits the nucleotide exchange on human Ras protein (p21 h-Ras) stimulated by C-Cdc25^{Mm} exchange factor with an ID_{50} of about 50 μM. Higher concentration of **1** (100 μM) completely inhibits

the exchange *in vitro*, but the C-Cdc25^{Mm} stimulated dissociation of the nucleotide (mant-GDP) occurs, although at a reduced rate (Figure 4-3).
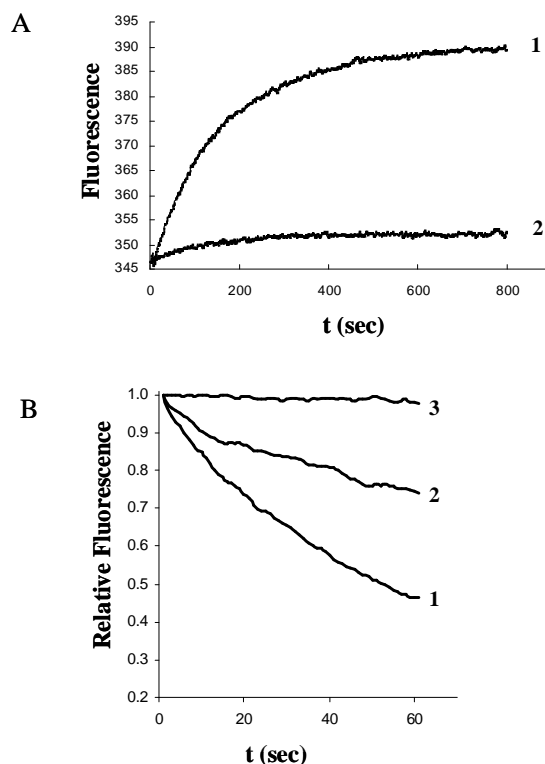
Figure 4-3. (A) C-Cdc25^{Mm}-stimulated nucleotide exchange on p21-hRas. (B) C-Cdc25^{Mm}-stimulated dissociation of p21 h-Ras·MANT-GDP complexes. Trace 1, control (no inhibitor added); trace 2, 100 μM **SCH-53870**; trace 3, nucleotide dissociation due to Ras intrinsic activity in the absence of C-Cdc25^{Mm}.

Compound **1** was also able to inhibit the EDTA-stimulated nucleotide exchange, suggesting that it primarily interacts with the Ras protein and not with the GEF (Figure 4-4). In fact, the removal of Mg^{2+} by EDTA partially unfolds the protein and induces an open conformation,[69] thereby enhancing the spontaneous nucleotide exchange on the Ras protein. The effect of this inhibitor on Ras-GEF interaction was studied using a yeast two-hybrid system, where a lacZ reporter was expressed under the control of a hybrid Gal4BD-Ras2^{N24}/ CDC25-Gal4 AD.[69]

---

[69] Hall A., Self A. J., *J. Biol. Chem.*, **1986**, 261, 10963-10965.

_____

Figure 4-4. EDTA-stimulated nucleotide exchange on p21-hRas. The values are expressed as a percentage of the control exchange rate. The inhibitors **1**, **2**, **3** and **4** were added at a concentration of 100 μM.
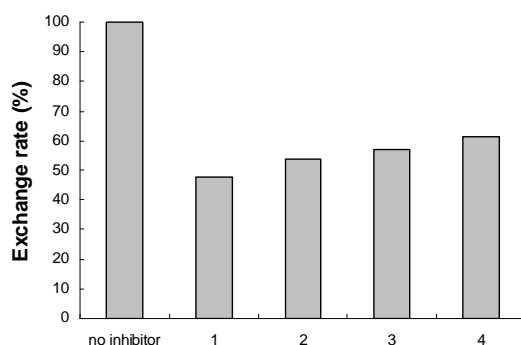
Compound **1** reduced the interaction between Ras2^{N24} and CDC25, but the inhibition is not complete even at higher concentration (Figure 4-5). This suggests that the strong inhibition of the nucleotide exchange is not only a consequence of an impairment of the GEF interaction with Ras, but probably is mainly due to a lack of or a reduced flexibility of Ras protein, in agreement with the results observed in the presence of EDTA.
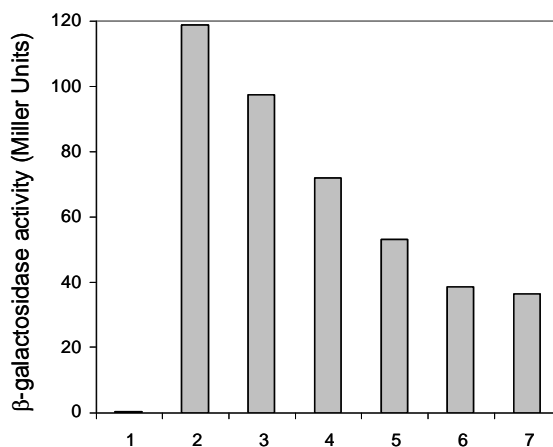
Figure 4-5. Two-hybrid system: inhibition test of the interaction Ras/GEF. Yeast cells were grown in the presence of sub-lethal concentration of **1** and β-galactosidase activity was assayed. (1), Y190 strain carrying the pGBT9-RAS2^{N24} plasmid and the pGADGH plasmid (negative control); Y190 strain carrying the pGBT9-RAS2^{N24} plasmid and the pGADGH-CDC25y plasmid, grown in the presence of: (2), 0.5%(v/v) DMSO (positive control); concentrations of compound **1**: (3), 1 μM; (4) 10 μM; (5) 20 μM; (6) 50 μM; (7) 100 μM.

4.2.2.2. *In vitro* experiments on human Ras protein

Inhibitors **1-12** were first tested *in vitro* for their ability to inhibit the C-Cdc25[Mm]-stimulated nucleotide exchange on purified p21 h-Ras (Figure 4-6). For this purpose a modified version of Lenzen's method was used.[70] The C-Cdc25[Mm]-stimulated guanine nucleotide exchange was monitored using the fluorescent 2'(3')-*O*-(*N*-methylantraniloyl)-GTP (mant-GTP). p21-hRas was incubated with mant-GTP in the absence and in the presence of 100 μM of the putative inhibitors **1-12**. Molecule **1** was used as a positive control. The exchange reaction was started by the addition of C-Cdc25[Mm]. Phenylhydroxylamine containing compounds **1**-**4** were the most potent inhibitors, since the nucleotide exchange was almost completely inhibited. All the other compounds that do not contain a hydroxylamine group were practically inactive. Surprisingly enough, compounds **8** and **9** were still able to inhibit the exchange although at a lower extent (about 50%).

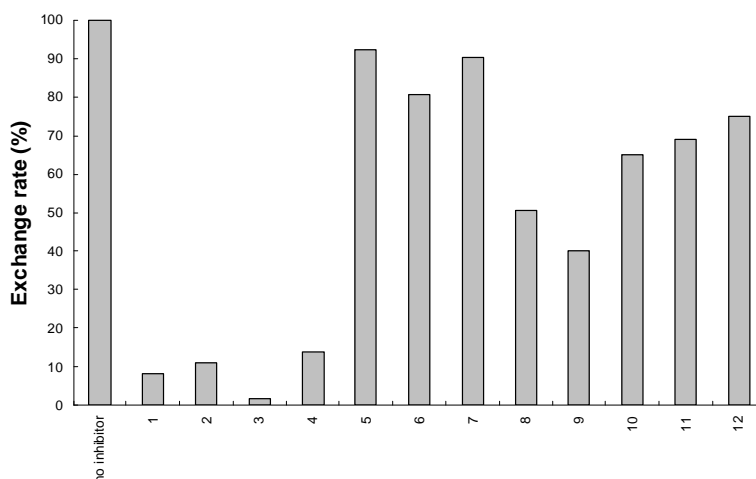**Figure 4-6**. C-Cdc25[Mm]-stimulated nucleotide exchange on p21-hRas.
Compounds **1**-**4** were also able to inhibit the EDTA-stimulated nucleotide

---

[70] Lenzen C., Cool R. H., Wittinghofer A., *Methods in Enzymology,* **1995**, 255, 95-109.

_____

exchange, suggesting that they primarily interact with the Ras protein and not with the GEF (Figure 4-4). The mechanism of action of the most potent inhibitors, molecules **1**-**4,** was also investigated in a nucleotide-dissociation assay by measuring the release of fluorescent nucleotide by the p21-hRas·MANT-GDP complex in the presence of GDP and exchange factor C-Cdc25^{Mm}. Compounds **1-4** partially reduced the dissociation rate of p21-hRas in complex with MANT-GDP (Figure 4-7).
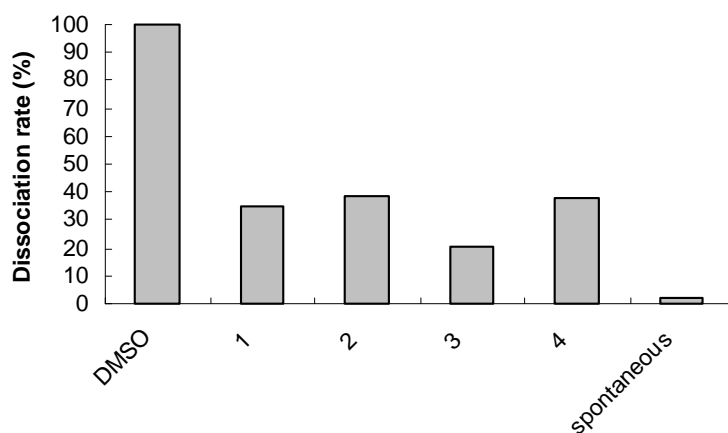
Figure 4-7. C-Cdc25^{Mm}-stimulated dissociation of p21- hRas•MANT-GDP complexes. The last column represents spontaneous nucleotide dissociation due to Ras intrinsic activity. The values are expressed as a percentage of the control dissociation rate. The inhibitors were added at a concentration of 100 µM.

4.2.2.3. Effect of compounds 1-4 on mammalian cell growth

We previously tested the capacity of compounds **1**-**7** of inhibiting *Saccharomyces cerevisiae* cell growth. Based on the assumption that the activity of Ras is essential for cellular growth and proliferation, we have found that compound **1** severely inhibits growth of the wild type strain W303-1A in liquid medium (data not shown).

Encouraged by these preliminary results on yeast, we evaluated the action of compounds **1**-**4** on NIH3T3 mammalian cells. We used both normal and

k-Ras-transformed[71] cells. Compounds **1-4** inhibited only slightly the growth of k-Ras-transformed cells when added at a concentration of 200 µM, while growth was completely blocked in normal cells using these compounds at a same concentration (Figure 4-8). In sharp contrast with other molecules, compound **3** inhibited completely the growth of both normal and k-Ras-transformed mammalian cells.
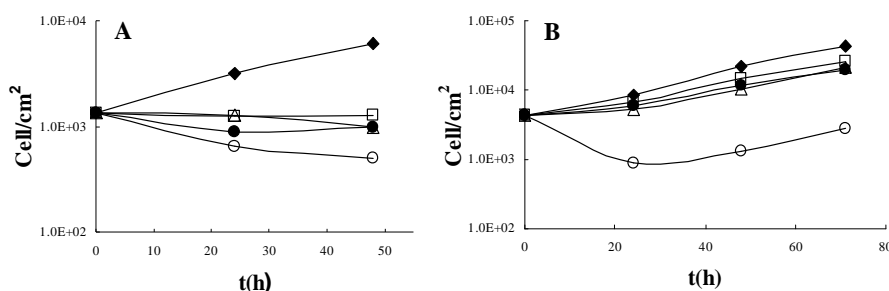
Figure 4-8. Inhibition test in mammalian cells. NIH3T3 (A) and NIH3T3 k-Ras (B) mouse fibroblasts were seeded into 60 mm dishes and grown for one day: three dishes were allowed to continue growing without addition of the inhibitor (♦), while molecules **SCH-53870** (●), **2** (Δ), **3** (o) and **4** (□) were added at the other dishes at a final concentration of 200 µM. At different time points sample cells were collected for determination of cell number.

4.2.3. Discussion

Compounds **1**-**4**, containing the phenylhydroxylamine moiety were the most active in inhibiting guanine nucleotide exchange on p21 h-Ras, as shown in Figure 4-6. This finding confirms the major role of the aromatic hydroxylamine in the binding and inactivation of Ras. Interestingly, if the hydroxylamino group is linked to phenyl through a methylene group, as in the case of compounds **10** and **11**, the biological activity is totally lost. A possible explication is that the electronic properties of aromatic hydroxylamines (in terms of pK_a) are quite different from aliphatic, moreover

---

[71] Milburn M. V., Tong L., de Vos A.M., Brunger A., Yamaizumi Z., Nishimura S., Kim S.H., *Science*, **1990**, 247, 939-945.

_____

the introduction of the CH_2 group increases the steric bulk of the pharmacophore, probably disfavouring the interaction with Ras binding pocket. Compounds **5** and **8** with an amino group instead of a hydroxylamine behave quite differently: while **5** is totally inactive, **8** presents some residual biological activity. This difference could be explained by the fact that the decrease of binding due to the amine-hydroxylamine substitution is partially compensated in **8** by the presence of a larger aromatic moiety (naphtyl instead of benzyl) that favours binding with Ras. Compound **9**, in which the phenyl hydroxylamine has been replaced by phenyl hydrazine, still maintain a partial biological activity in inhibiting nucleotide exchange *in vitro*. This indicates that the hydrazino group could be more suitable than the amino, the acetylamino, the acetylhydroxylamino and the boronic acid groups in replacing the hydroxylamino pharmacophore. Anyway, these results confirm the importance of the phenylhydroxylamino group as essential pharmacophore for Ras protein inhibition.

4.3. Development of a new glycidic scaffold for Ras inhibition[72]

In the second step of our work, molecular modelling and virtual ligand docking were used in order to develop a new class of Ras inhibitors, structurally related to the Schering-Plough inhibitors, that could constitute similar ligand-Ras-GDP complexes. In particular, these compounds present the phenylhydroxylamino moiety, together with two additional aromatic entities (benzyl groups), attached to a bicyclic scaffold derived from the

---

[72] Peri F., Airoldi C., Colombo S., Martegani E., Van Neuren A. S., Stein M., Marinzi C., Nicotra F., "Design, Synthesis and Biological Evaluation of Sugar-Derived Ras Inhibitors", *ChemBioChem*, **2005**, 6, 1839-1848.

natural sugar D-arabinose. The structures of these molecules are reported in Fig. 4-9.
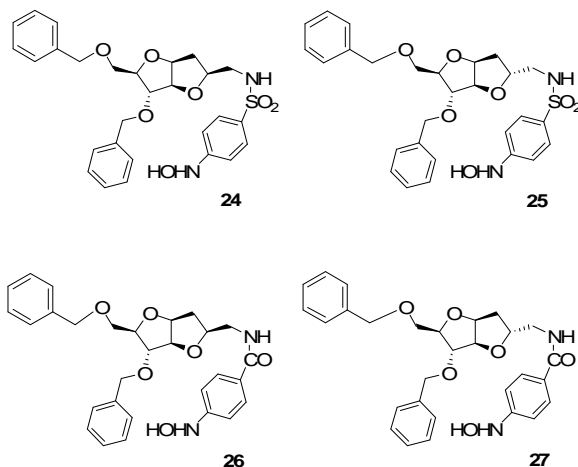
Figure 4-9. Structures of the first generation of bicyclic Ras inhibitors.

4.3.1. Molecular Modelling

4.3.1.1. Proof-of-concept: Docking of known binders

In order to validate the computational (docking) methodology, we initially investigated the interaction of the Schering-Plough inhibitors with Ras using the GLIDE program.[73] All of the known compounds docked well into the binding site in close proximity of the Switch II region. **SCH54292**, **SCH53239** and **SCH53870** (**1**), bearing a naphthyl group, were oriented in the binding site in accordance with the experimental derived NOE distances. The orientation of the inhibitors within the binding site was found to be similar to that described by Schering-Plough,[54] with the hydroxylamine group coordinating both the bivalent Mg^{2+} ion and the β-phosphate of GDP,

---

[73] GLIDE 2.7, Schrodinger LLC, **2003**.

_____

whereby an aromatic-charged interaction between the phenyl group and Lys-16 is induced. The sugar moiety of **SCH-54292** and the guanine moiety of **SCH-53239** point outwards of the binding pocket and are not involved in significant interactions with the protein. However, we found important hydrogen bond interactions not mentioned by the Schering-Plough research institute; namely between the sulfonamide group of the inhibitor and Gly-10/Gly-60, and between the hydroxylamine group of the ligand and Thr-58 (Fig. 4-10).
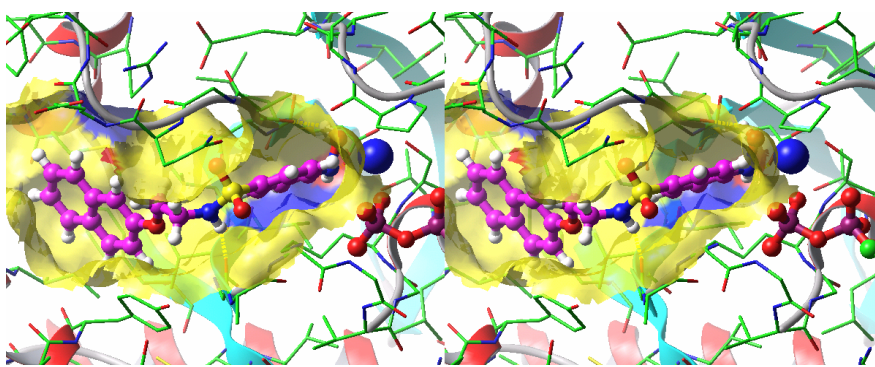
Figure 4-10. Stereo view of compound **SCH-53870** (**1**) docked into the binding site of human p21-Ras-GDP; the molecular surface of the protein in close proximity of the ligand is coloured as follows: yellow for neutral residues, blue for positive charged residues and red for negative charged residues. The Mg^{2+} ion is depicted as a blue CPK-model and part of the GDP molecules as atom type coloured ball&stick-model.

The interactions of the inhibitors hydroxylamine group with the magnesium ion and the β-phosphate of GDP are the main constituents of the binding enthalpy and these interactions are therefore the major contributors to the GlideScore, which is an indication for the binding affinity for Ras. A good agreement between GlideScore ranking and experimental IC$_{50}$ values was observed.

4.3.1.2. Docking of Novel Structures

In the light of these encouraging results, the GLIDE program was applied for

the *in silico* screening of novel inhibitors. Since the saccharidic moiety was shown not to interact with the protein, a series of structures lacking that residue were designed as potential new inhibitors. Compounds **24**-**27** present the putative pharmacophore groups covalently bound to a bicyclic core derived from the natural sugar D-arabinose (Fig. 4-9). The bicyclic moiety is a conformationally rigid scaffold, able to orient the pharmacophores (the hydroxylamino- and the two aromatic groups) in a spatial arrangement potentially suitable for binding with the Ras-GDP complex.

All representative conformations of the compounds using the protocol described above were docked into the model of the Ras-GDP complex.

Compound	IC$_{50}$ [µM][a]	Glidescore	Percentage of Top40[b]
24	76.0±1.4	-10.2	17%
25	57.3±5.8	-9.9	25%
26	35.5±0.7	-10.0	42%
27	62.3±5.7	-10.1	15%
1 (SCH-53870)	56.0±5.2	-8.9	

Table 4-1. IC$_{50}$ values and binding affinities for compounds **24**–**27** and **SCH-53870**. a) Data represent the mean ± SD (n=3). b) For each of the four compounds the 20 best scoring poses were selected and from these 80 poses the 40 best scoring poses were and the recovery rate for each compound was calculated.

Compounds **24**-**27** fit well into the binding pocket as observed by docking the molecules into the model of the Ras-GDP complex (Fig. 4-11) and have very similar docking scores (Table 4-1). The two aromatic rings of the benzyl ethers on the bicyclic scaffold were expected to fill the hydrophobic pocket in analogy with the naphthalene group behaviour of the Schering inhibitors. This is the case for only one of the aromatic rings, the second aromatic ring pointing outwards of the binding cavity (Fig. 4-11). As expected, the phenyl group bearing the hydroxylamine is accommodated in the narrow pocket in

_____

close proximity of the Mg^{2+} ion, probably interacting with Lys-16 through an aromatic-charge interaction. The hydroxylamino group of all four compounds is able to coordinate both the bivalent Mg^{2+} ion and the β-phosphate of GDP thus providing a strong polar interaction. Furthermore, in analogy with the binding model of the Schering-Plough compounds, the backbone carbonyl group of Thr-58 is also an important potential hydrogen bond interaction partner for all four new compounds. In the modelled Ras-GDP-inhibitor complexes, the different configurations (S in **24** and **26**, R in **25** and **27**) of C-2 in the bicyclic cores and the different nature of the hydrogen bond-forming groups (amide or sulfonamide) do not significantly influence the ligands orientations within the binding pocket of Ras, neither are the ligands predicted binding affinities (Glidescores) for Ras significantly different.
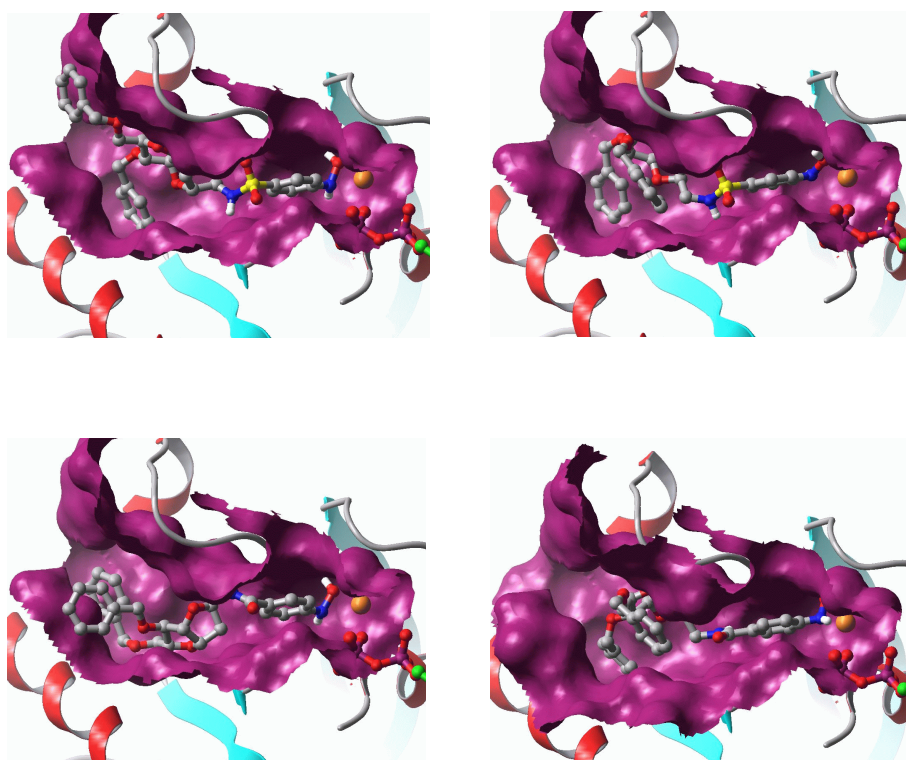

Figure 4-11. Docking of compounds **24**-**27** into the binding cavity of Ras.

_____

4.3.2. Chemical synthesis

The commercially available **2,3,5-tri-*O*-benzyl-D-arabinofuranose** (**28**) was converted into the anomeric acetate **29** (mixture of anomers), which was allylated by treatment with allyltrimethylsilane (ATMS) in the presence of the Lewis acid promoter $BF_3 \cdot Et_2O$. The reaction, made at rt in dry acetonitrile, afforded **30** as a 1 : 1 mixture of α and β diastereomers (75% yield). Iodocyclization was then carried out with NIS in dry THF at rt affording bicyclic iodo ether **31** as a mixture of diastereomers (80% yield based on the β-anomer), the major isomer having the 2*R* configuration. This reaction is the crucial step for the synthesis of the bicycle and its mechanism is based on the opening of the intermediate iodonium ion by attack of the γ-benzyloxy groups in the 5-*exo*-mode with formation of a cyclic iodo ether with concomitant debenzylation. Only the β-anomer of **30** reacted and this allowed its easy separation from the α-anomer. Pure α-anomer of **30** was then isolated and characterized. The reaction of the iodo derivative **31** with tetrabutylammonium azide in toluene gave azido derivative **32** (60 °C, 60% yield). The two diastereomers were separated at this point of the synthesis by flash chromatography on silica gel. Compounds **24**-**27** were prepared in parallel syntheses from diastereoisomers **32-R** and **32-S** with, respectively, R and S configuration at C-2. Bicyclic azides **32-S** and **32-R** were treated with triphenylphosphine in THF in the presence of 1% water generating the corresponding amines **33** and **34** that were further reacted with *p*-nitrobenzensulfonyl chloride and triethylamine in dichloromethane to yield sulfonamides **35** and **37** respectively. **33** and **34** were also condensed with *p*-nitrobenzoic acid in the presence of *N*-hydroxybenzotriazole (HOBt), diisopropylcarbodiimide (DIC) and diisopropylethylamine (DIPEA) thus obtaining *p*-nitrobenzencarboxyamides **36** and **38**. Final reduction of the nitro groups with zinc and ammonium chloride in methanol generated the

_____

target compounds **24**, **25**, **26**, **27** (Scheme 4-2).
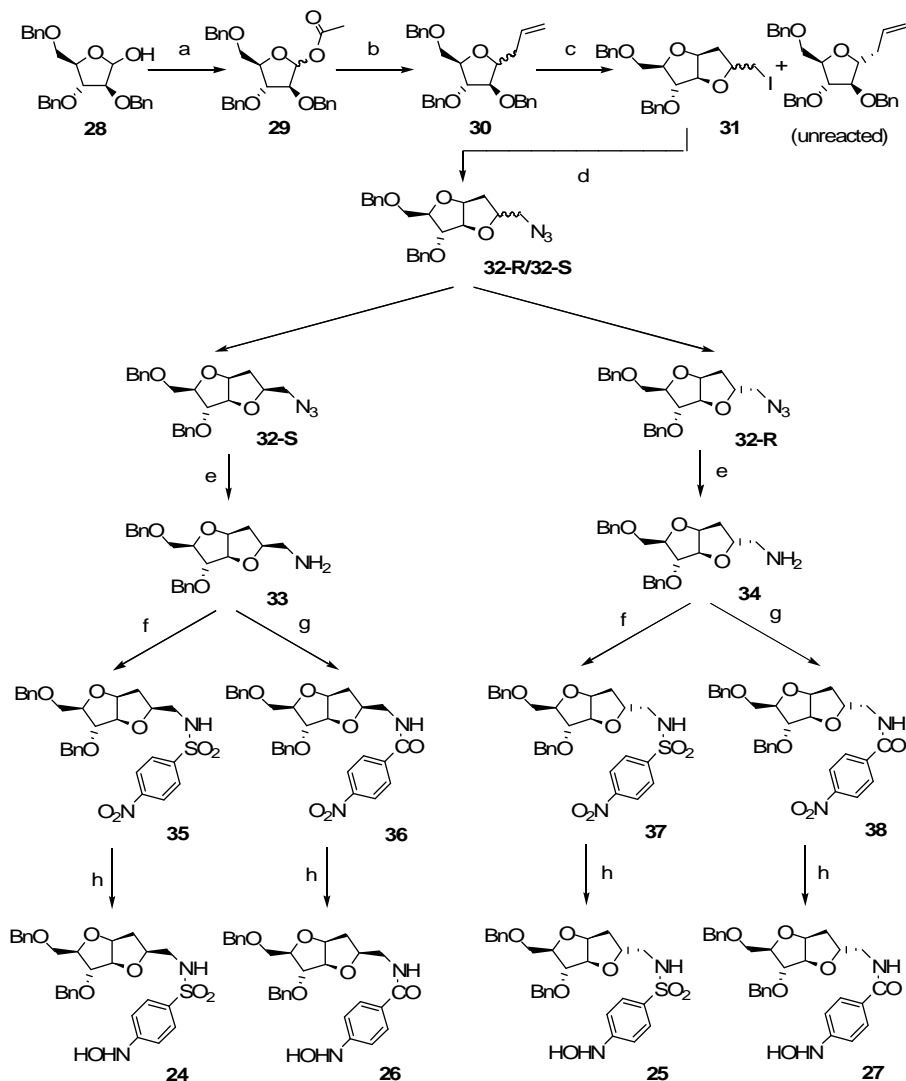
Scheme 4-2. Reagents and conditions a) Ac2O, dry CH$_2$Cl$_2$, rt, quant. yield; b) ATMS, BF$_3$·Et$_2$O, dry CH$_3$CN, rt, 75%; c) NIS, dry CH$_2$Cl$_2$ 80% on the β-anomer; d) Bu$_4$NN$_3$, dry toluene, 70 °C 60%, separation of diastereomers by column chromatography; e) PPh$_3$,THF, H$_2$O, 70 °C, 75% for **32-R**, 96% for **32-S**; f) _p_-nitrobenzenesulfonyl chloride, Et$_3$N, CH$_2$Cl$_2$, rt, 96% for **35**, 87% for **37**; g) _p_-nitrobenzoic acid, HOBt, DIC, DIPEA, DMF, rt, 98% for **36**, 87% for **38**,; h) Zn, NH$_4$Cl, MeOH, rt, (89% for **24**, 93% for **25**, 87% for **26**, 54% for **27**). ATMS = allyltrimethylsilane; DIC = _N,N_-diisopropylcarbodiimide; DIPEA = diisopropylamine; HBTU = 2-(1_H_-benzotriazol-1-yl)-1,1,3,3-tetramethyluronium hexafluorophosphate; NIS = _N_-iodosuccinimide; DMAP = 4-(dimethylamino)-pyridine; HOBt = _N_-hydroxybenzotriazole.

_____

4.3.2. Biological evaluation

4.3.2.1. *In Vitro* characterization of Ras inhibitors

Compounds **24-27** were initially tested *in vitro* to investigate their ability to inhibit the C-Cdc25^{Mm}-stimulated nucleotide exchange on purified human Ras protein (p21 h-Ras) as previously described [4.2.2.2.]. p21-hRas was incubated with mant-GTP in the absence and in the presence of increasing concentrations of the putative inhibitors **24**-**27**. Compound **SCH-53870** was used as a positive control in the same experimental conditions. The Cdc25-stimulated nucleotide exchange on p21 h-Ras in the presence of increasing concentrations (20 to 100 μM) of **25** is significantly inhibited in a dose-dependent manner *in vitro* (Figure 4-12) .
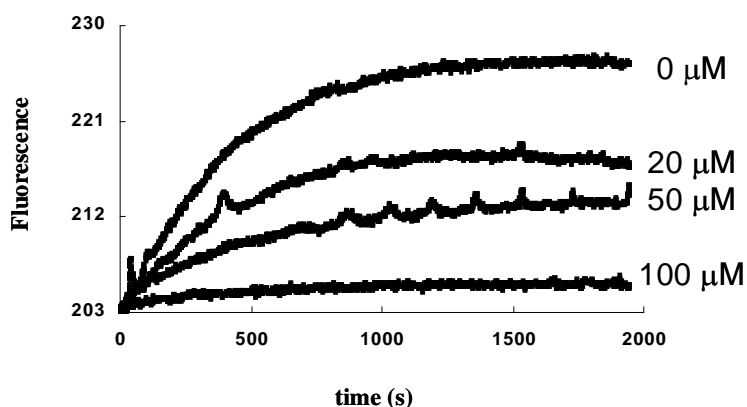

Figure 4-12. Cdc25^{Mm}-stimulated nucleotide exchange on p21 h-Ras in the presence of increasing concentrations of **25**.

IC$_{50}$ values for compounds **24**-**27** and for **SCH-53870** (Table 4-1) are of the same order of magnitude, being **26** slightly more potent than all the others. *In vitro* activities and docking scores of the bicyclic ligands suggest

_____

that they find analogous accommodation into the Ras cavity and thus very similar binding orientation and affinity. For these reasons, further biological characterisation was performed only on compounds **25** and **27**, for advantages in their preparation.[74]

On the other hand, a very significant difference between the behaviour of **25** and **27** in comparison with **SCH-53870** results from the analysis of kinetics of exchange, whereby an interesting inhibition of the fluorescent nucleotide binding is observed.

The mechanism of action of the inhibitors was also investigated in a nucleotide-dissociation assay measuring the release of fluorescent nucleotide by the Ras-mant-GDP complex in the presence of GDP and of the exchange factor, where a strong inhibition of guanine nucleotide release from Ras, and therefore a blocking of the exchange, was observed in the presence of **25** and **27** (Figure 4-13).
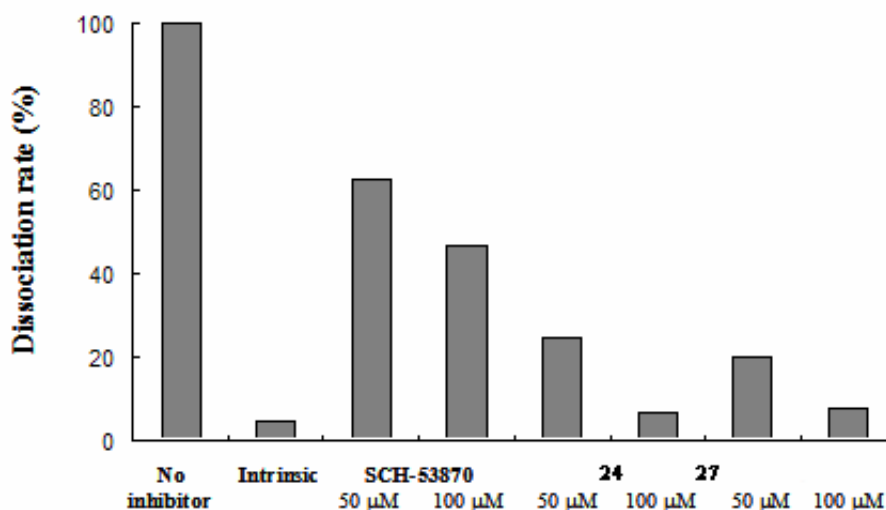
Figure 4-13. C-Cdc25[Mm]-stimulated dissociation of p21-hRas.mant-GDP complexes. The second column represents nucleotide dissociation due to Ras intrinsic GTPase activity. The values are expressed as a percentage of the control dissociation rate $(54 \times 10^{-4} \, s^{-1})$.

_____

[74] Diastereomers **32-R** and **32-S** were obtained by nucleophilic displacement on iodo-bicyclic precursors in a 4:1 ratio. Therefore compounds **25** and **27** were obtained in higher overall synthetic yields.

4.3.2.2. *In Vivo* characterisation of Ras inhibitors: Inhibition of yeast growth

It is very well known that yeast cells have signal transduction pathways similar to mammalian cells and many genes structurally and functionally homologous to human genes. On the other hand yeast cells grow faster and present a simpler cellular organisation. The functional conservation between mammalian p21 Ras and yeast Ras proteins and the deep knowledge of the Ras-dependent processes in yeast offer the possibility to use *S. cerevisiae* as a model organism for studying Ras function and interactions with its modulators and/or inhibitors. Two homologs of mammalian p21 Ras, Ras1 and Ras2, have been identified in *S. cerevisiae* and it was demonstrated that these proteins are normally required for cell growth and proliferation.[75, 76] Yeast Ras proteins are in fact key elements of a signal transduction pathway involved in nutrient sensing and growth control. The main component of this pathway is adenylate cyclase, which catalyses the synthesis of cAMP. This molecule activates the cAMP-dependent protein kinase (PKA), an enzyme composed of catalytic subunits encoded by the *TPK1*, *TPK2* and *TPK3* genes, along with regulatory subunits encoded by the *BCY1* gene. The catalytic subunits phosphorylate substrate proteins involved in many important cellular processes such as cell growth. In *S. cerevisiae* adenylate cyclase activity is controlled by the Ras proteins. Since these proteins are normally required for cell growth and proliferation, it is possible to test the *in vivo* activity of Ras inhibitors by monitoring their ability to inhibit or to reduce cell growth. Consequently, compounds **SCH-53870** and **24**-**27** were used to perform an inhibition test in a liquid medium using two different strains: a wild type W303-1A strain and a *ras1Δ, ras2Δ, bcy1* strain. In this latter

---

[75] D. Broek, N. Samily, O. Fasano, A. Fujiyama, F. Tamanoi, J. Northup, M. Wigler, *Cell*, **1985,** 41, 763-769.
[76] J. M. Thevelein and J. H. de Winde, *Molecular Microbiology*, **1999**, 33**,** 904-918.

_____

strain, *bcy1* mutation bypasses the need of Ras for the cells to grow.[17] In such a strain we expect a normal growth phenotype (as in a wild type without addition of inhibitors) if the inhibitor interacts selectively with the Ras proteins, while we expect inhibition or retardation of growth if the inhibitor interacts with other components involved in Ras-independent pathways. Therefore this strain allows testing the specificity of the inhibitors for the Ras/cAMP /PKA pathway. W303-1A and *ras1Δ, ras2Δ , bcy1* strains were grown till early exponential phase. The cultures were then divided into aliquots: one aliquot was allowed to continue growing without addition of the inhibitor, while compounds **SCH-53870** and **24**-**27** were added to the other aliquots at a final concentration of 200 µM (Fig. 4-14a, 4-14c).
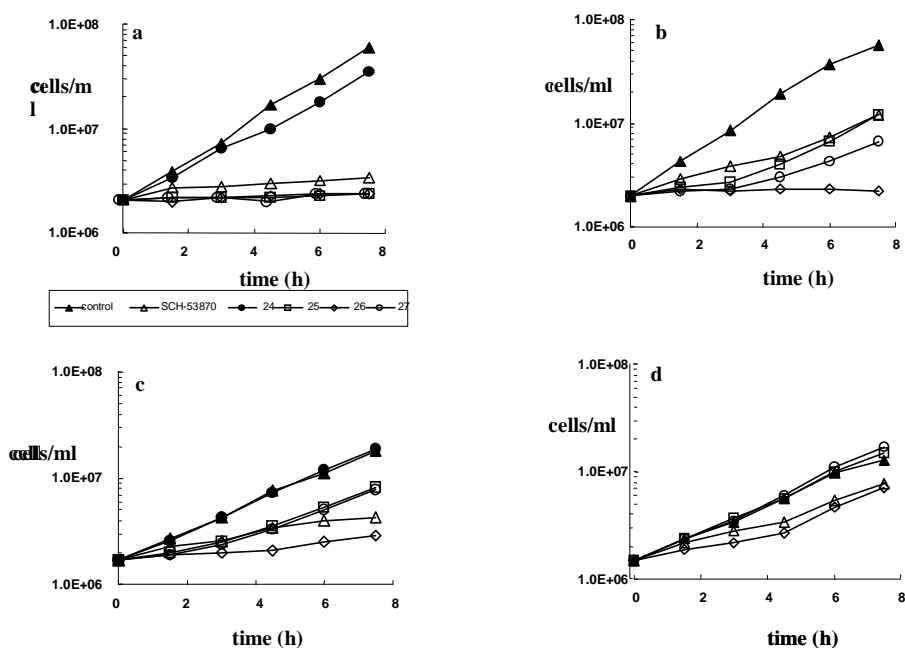
Figure 4-14. Inhibition test in liquid medium. W303-1A (**a, b**) and *ras1Δ, ras2Δ, bcy1* (**c, d**) cells were grown till early exponential phase and then divided into aliquots: one aliquot was allowed to continue growing without addition of the inhibitor (σ), while molecule **SCH-53870** (Δ), molecule **24** (•), molecule **25** (□), molecule **26** (◊) and molecule **27** (○) were added at the other aliquots at a final concentration of either 200µM (**a, c**) or 50 µM (**b, d**). At different time points a sample of culture was collected for determination of cell number.

_____

At different time points a sample of culture was collected for cell number determination. Addition of compounds **25**, **26** and **27** to a wild type W303-1A strain completely inhibited cell growth, an almost complete inhibition was observed after addition of **SCH-53870**, while **24** was inactive (Fig. 4-14a). On the contrary, only a small decrease of the cell growth was observed in strains *ras1Δ, ras2Δ, bcy1*, after addition of **25** and **27**, while **26** and **SCH-53870** did not show to be very specific at this concentration. As expected, **24** was inactive (Fig. 4-14c). Since all the arabinose-derived inhibitors (with the exception of **24**) completely inhibited cell growth at a concentration of 200 µM, the same inhibition tests were performed at a final inhibitors concentration of 50 µM (Fig. 4-14b, 4-14d). In these conditions, a reduction in cell growth was observed in strain W303-1A in the presence of **25**, **27** and **SCH-53870**, while a complete inhibition of cell growth was observed with **26**. These results are in agreement with the *in vitro* analysis, in which **25**, **27** and **SCH-53870** were observed to have a lower inhibition capacity than **26**. When added to strain *ras1Δ, ras2Δ, bcy1*, **25** and **27** are inactive, while a small reduction in cell growth was observed after addition of **26** and **SCH-53870**.

These experiments on yeast cells suggest that our inhibitors specifically inhibit Ras-dependent growth, with compounds **25** and **27** giving the most significant results.

4.3.2.3. Effect of Ras inhibitor on mammalian cells.

In order to investigate *in vivo* a specific effect on Ras-mediated signalling, inhibition of mammalian cell growth by compounds **25** and **27** were evaluated both in normal cells and in cells that had been transformed by k-Ras Arg12. Compounds **25** and **27** inhibit the growth of normal mouse fibroblasts NIH3T3 at concentration of 100 µM, and this effect was even more pronounced in k-Ras transformed NIH3T3 where a complete arrest of growth is observed (Figure 4-15).
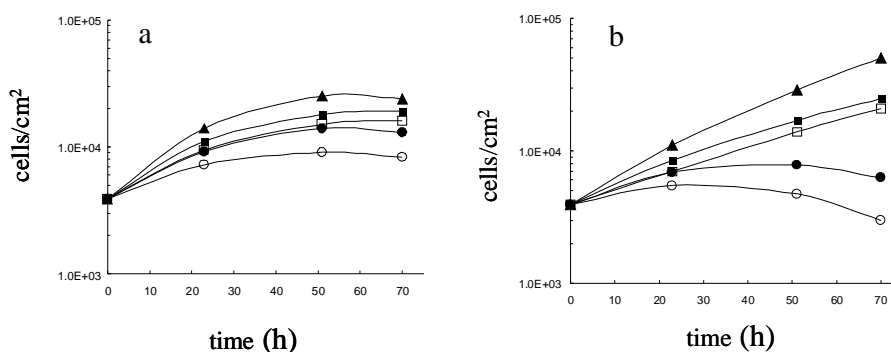
Figure 4-15. Inhibition test in mammalian cells. NIH3T3 (**a**) and NIH3T3 k-Ras (**b**) mouse fibroblasts were seeded into 60 mm dishes and grown for one day: 3 dishes were allowed to continue growing without addition of inhibitor (σ), while **25** (□, ■) and molecule **27** (○, ●) were added to the other dishes at a final concentration of either 50μM (□, ○) or 100 μM (■, ●). At different time points a sample cells were collected for determination of cell number.

In order to verify that compounds **25** and **27** cause the *in vivo* inhibition of the Ras-mediated signalling, preliminary experiments were performed measuring the level of activation of MAPK after addition of the inhibitors to normal 3T3 fibroblast growing in 10% serum. A pronounced decrease of phospho-MAPK expression was observed after 5 hours at a final concentration of 50 μM and at 100 μM, where a stronger inhibition was obtained (Figure 4-16).

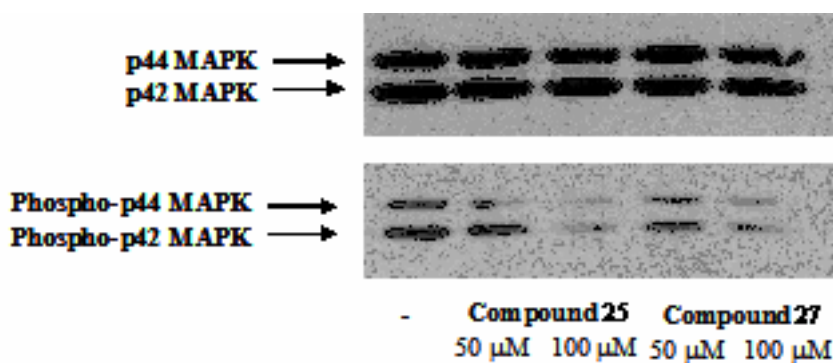
Figure 4-16. Assay of MAPK activation. Lysates (14 μg of total proteins) were separated by SDS-PAGE, transferred to nitrocellulose, and immunodecorated with anti-p42/44 MAPK antibody and anti-phospho- p42/44 MAPK antibody.

_____

4.3.2.3. Discussion

Arabinose-derived bicyclic compounds **25** and **27** inhibit GTP association to Ras and GDP dissociation, as observed *in vitro*. Furthermore, compounds **25** and **27** are active in inhibiting cell growth in transformed mouse fibroblasts NIH3T3 with mutated Ras, and showed a specificity of action, having a negligible effect on Ras-independent *ras1Δ, ras2Δ, bcy1* yeast cell strains. Compound **24**, the less potent inhibitor *in vitro*, is completely inactive in inhibiting yeast cell growth *in vivo*. Compound **26** showed good activity *in vitro*, but low specificity and toxic effects *in vivo*. Inhibitors **25** and **27** have similar activity both *in vitro* and *in vivo*, suggesting that for C-2' R isomers the nature of the hydrogen bond-forming groups (amide or sulfonamide) does not influence the binding affinity with Ras protein. On the contrary, quite a different behaviour is detected both *in vitro* and *in vivo* for **24** and **26** that have C-2' S configuration, but have respectively sulphonamide and amide functionalities. In this case the nature of hydrogen bond-forming groups seems to dramatically influence the bioactivity.

The reported data show that this new class of compounds is able to selectively inhibit the activation of oncogenic Ras in mammalian cells, therefore representing a very promising target for development of novel anti-cancer drugs.

4.4. The "second generation" of Ras bicyclic inhibitors[77]

We prepared a second generation of Ras bicyclic inhibitors, namely molecules **39**-**44** (Fig. 4-17), structurally very similar to the previously tested compounds **24**-**27**.
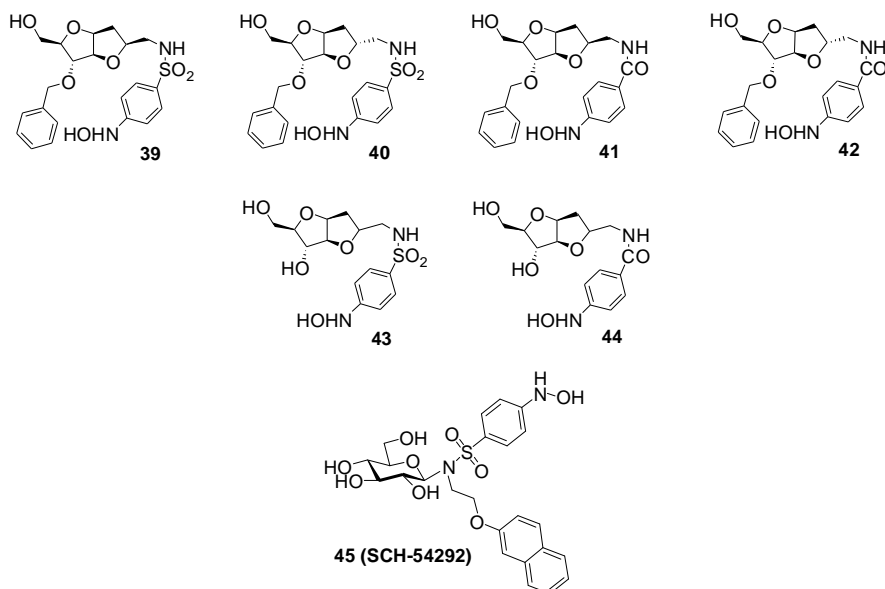
Figure 4-17. Chemical structures of compounds **39-44** and **45** (**SCH-54292**).

Compounds **39** to **42** have a free hydroxyl on C-2' instead of the benzyl group, **43** and **44** have free hydroxyls both on C-4 and C-2'. These molecules have been designed for two main reasons: to investigate the importance of the aromatic (benzyl) rings for the interaction with Ras, and

_____

[77] Peri F., Airoldi C., Colombo S., Mari S., Jimenez-Barbero J., Martegani M., Nicotra F., "Sugar-derived Ras inhibitors: Group Epitope Mapping by NMR Spectroscopy and Biological Evaluation", _Eur. J. Org. Chem._, **2006**, 3707–3720.

to have greater water-solubility compared to compounds **24**-**27**. The inhibitor **45** (**SCH-54292**) (Fig. 4-17) was also prepared by optimizing the synthetic procedure previously adopted by Schering. This compound was used as a reference in NMR binding studies and biological tests. The comparison of the binding properties and biological activities of compounds **24**-**27** and **39**-**44** provided further important information about the structure-activity relationship in this family of inhibitors.

4.4.1. Chemical synthesis

Compounds **39**-**44** were prepared according to the synthetic pathway of Scheme 4-3. The common bicyclic iodide intermediate **48** was obtained by the iodo-promoted cyclisation of the allyl-C-arabinofuranoside **47**. As previously illustrated, only the β-anomer reacted and α–anomer was recovered as reported elsewhere. Nucleophilic displacement of iodine with tetrabutylammonium azide afforded **49** that was converted into the corresponding amine **50** by treatment with triphenylphosphine. Reaction of **50** with *p*-nitrobenzenesulfonyl chloride followed by reduction of the aromatic nitro group with hydrazine and Pd/C yielded compound **43** as a mixture of diastereoisomers. Alternatively, the condensation of **50** with *p*-nitrobenzoic acid in the presence of *N,N*-diisopropylcarbodiimide (DIC) and *N*-hydroxybenzotriazole (HOBt) followed by reduction with hydrazine and Pd/C afforded the diastereomeric mixture **44**. Intermediate **49** was *O*-benzylated by using benzyl bromide and sodium hydride obtaining **51**. The C-2' benzyl ether of **51** was selectively converted into an *O*-acetate by treatment with Ac_2O/TFA and the acetyl group was then removed with sodium methoxide in methanol; the azide was reduced using triphenylphosphine in THF/water, affording amine **52**. Reaction of the amino group of **52** with *p*-nitrobenzenesulfonyl chloride allowed the introduction of

_____

the *p*-nitrophenylsulfonamide moiety (**55** and **56**).
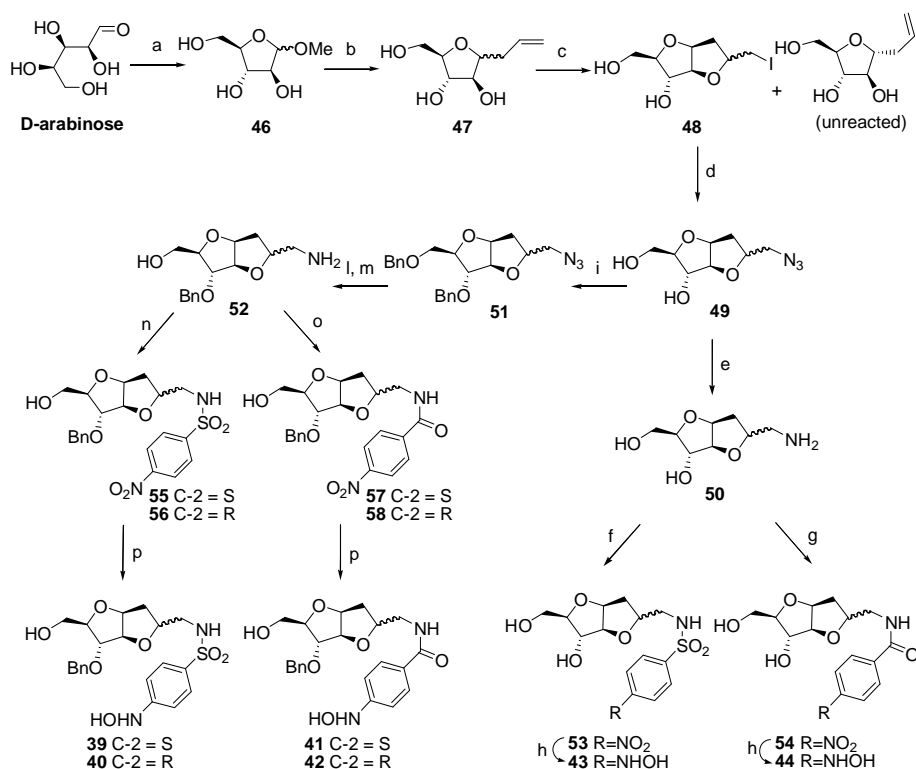
Scheme 4-3. Reagents and conditions: a) AcCl, MeOH, 18 h, 91%; b) BTSFA, CH$_3$CN, 100 °C, 3 h, then ATMS, TMSOTf, CH$_3$CN, room temperature, 1 h, then H2O, 97%; c) NIS, THF, 90 °C, 10 min, 58%; d) Bu$_4$NN$_3$, DMF, 70 °C, 72 h, 90%; e) PPh$_3$, THF/H$_2$O, 70 °C, 14 h, 85%; f) *p*-nitrobenzenesulfonyl chloride, pyridine, 0 °C, 6 h, 64%; g) DIC, HOBt, DIPEA, *p*-nitrobenzoic acid, DMF, room temperature, 24 h, 75.5%; h) NH$_2$NH$_2$, Pd/C, THF, 0 °C, 45 min, 98%; i) NaH, BnBr, DMF, room temperature, 15 min, 91%; l) Ac$_2$O/TFA (4:1, v/v), room temperature, 90 min, then MeONa, MeOH, room temperature, 30 min, 85%; m) PPh$_3$, THF/H$_2$O, 70 °C, 14 h, 94%; n) TEA, *p*-nitrobenzenesulfonyl chloride, CH$_2$Cl$_2$, 0 °C, 5 h, 82%; o) DIC, HOBt, DIPEA, *p*-nitrobenzoic acid, DMF, room temperature, 24 h, 70%; p) NH$_2$NH$_2$, Pd/C, THF, 0 °C, 45 min, 92%. BSTFA = *N,O*-bis(trimethylsilyl)trifluoroacetamide, ATMS = allyltrimethylsilane, TMSOTf = trimethylsilyl trifluoromethanesulfonate, NIS = *N*-iodosuccinimide, TEA = triethylamine, DIC = *N,N*-diisopropylcarbodiimide, HOBt = *N*-hydroxybenzotriazole, DIPEA = diisopropylethylamine.

Alternatively, condensation with *p*-nitrobenzoic acid yielded amides **57** and **58**. Amide and sulfonamide diastereomers were separated at this point of the synthesis by flash chromatography on silica gel. Finally, reduction of the

aromatic nitro group with hydrazine and Pd/C leaded to the final phenyl hydroxylamine compounds **39**-**42**.

For the synthesis of compound **45** (**SCH-54292**), the critical N-glycosylation step of tetraacetyl glucose with 4-Nitro-*N*-[2-(2-naphthyloxy)ethyl] benzensulfonamide **16** was achieved by a Mitsunobu-type glycosylation (Scheme 4-4)[78]. Unlike previously published methods based on the use of bromo tetracetylglucose as glycosyl donor, this glycosylation reaction was efficient and almost totally stereoselective in favour of the β-N-glycoside, yielding **59** with 84% yield. Removal of acetyl protecting groups was accomplished by mild basic hydrolysis (Na_2CO_3 in MeOH) in order to avoid base-promoted cleavage of N-glycoside bond. Final compound **45** was obtained after reduction of the nitro group with hydrazine and Pd/C.
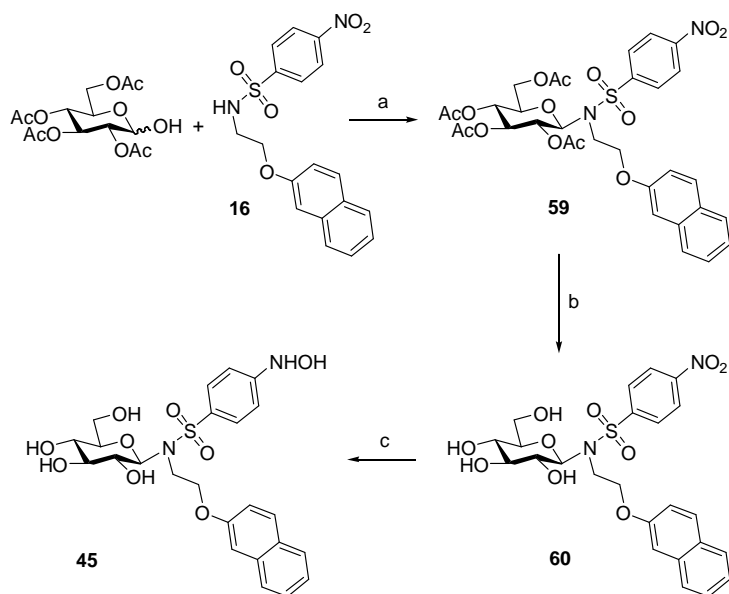
Scheme 4-4. Reagents and conditions: a) PPh_3, DIAD, −80 °C, 1 h, then room temperature, 18 h, 84%; b) K_2CO_3, dry CH_3OH, 24 h, 95%; c) NH_2NH_2, Pd/C, THF, 0 °C, 45 min, 93%. DIAD = diisopropyl azodicarboxylate.

[78] J. J. Turner, N. Wilschut, H. S. Overkleeft, W. Klaffke, G. A. van der Marel, J. H. van Boom, *Tetrahedron Lett.* **1999**, *40*, 7039-7042.

_____

4.4.2. NMR binding studies

For ligands that exchange between the free and bound states at a moderately fast rate, trNOESY experiments provide a helpful means to study their conformation at the receptor binding site. This is usually the case for carbohydrates (or glycomimetics) when they are bound to their receptors.[79] trNOESY experiments were performed to investigate the interaction in solution between compounds **39**-**44** and Ras-GDP complex. p21 h-Ras was incubated in a d_{11}-Tris buffer, containing 10% CD_3OD, 100 mM NaCl, 5 mM $MgCl_2$, an amount of GDP equimolar to the protein, and compounds **39**-**44**. An optimized ligand/protein molar ratio of 20 was used in all experiments. NOESY spectra of compounds **39**-**44** in the free state were obtained with mixing times of 800 ms. In trNOESY experiments, after different trials, an optimal value of 200 ms for mixing times was used. In contrast with what observed in the free state, negative NOEs (trNOEs) were observed for molecules **39**-**42**, as a consequence and proof of interaction with the protein (Figure 4-18). In the same experimental conditions, compounds **43** and **44** did not show any trNOE, probably indicating their lack of interaction with Ras-GDP.

_____

[79] a) For a detailed account of the application of NMR to the study of carbohydrates and their interactions see NMR Spectroscopy of glycoconjugates, J. Jiménez-Barbero, T. Peters, Eds., Wiley-VCH, Weinheim, **2002**. For applications of trNOESY experiments to the analysis of the bioactive conformation of carbohydrates, see, for instance, b) V. L. Bevilacqua, D. S. Thomson, J. H. Prestegard, *Biochemistry*, **1990**, 29, 5529-5537 (c) V. L. Bevilacqua, Y. Kim, J. H. Prestegard, *Biochemistry*, **1992**, 31, 9339-9349. d) H. Kogelberg, D. Solis, J. Jiménez-Barbero, J. *Curr Opin Struct Biol.*, **2003**, 13, 646-653. For applications of trNOESY experiments to the analysis of the bioactive conformation of glycomimetics, see, for instance, e) A. Bernardi, D. Arosio, L. Manzoni, D. Monti, H. Posteri, D. Potenza, S. Mari, J. Jimenez-Barbero, *Org. Biomol. Chem.*, **2003,** 1, 785 – 792; f) L. M. Mikkelsen, M. J. Hernáiz, M. Martín-Pastor, T. Skrydstrup, J. Jiménez-Barbero, *J. Am. Chem. Soc.*, **2002**, 124, 14940-14951.
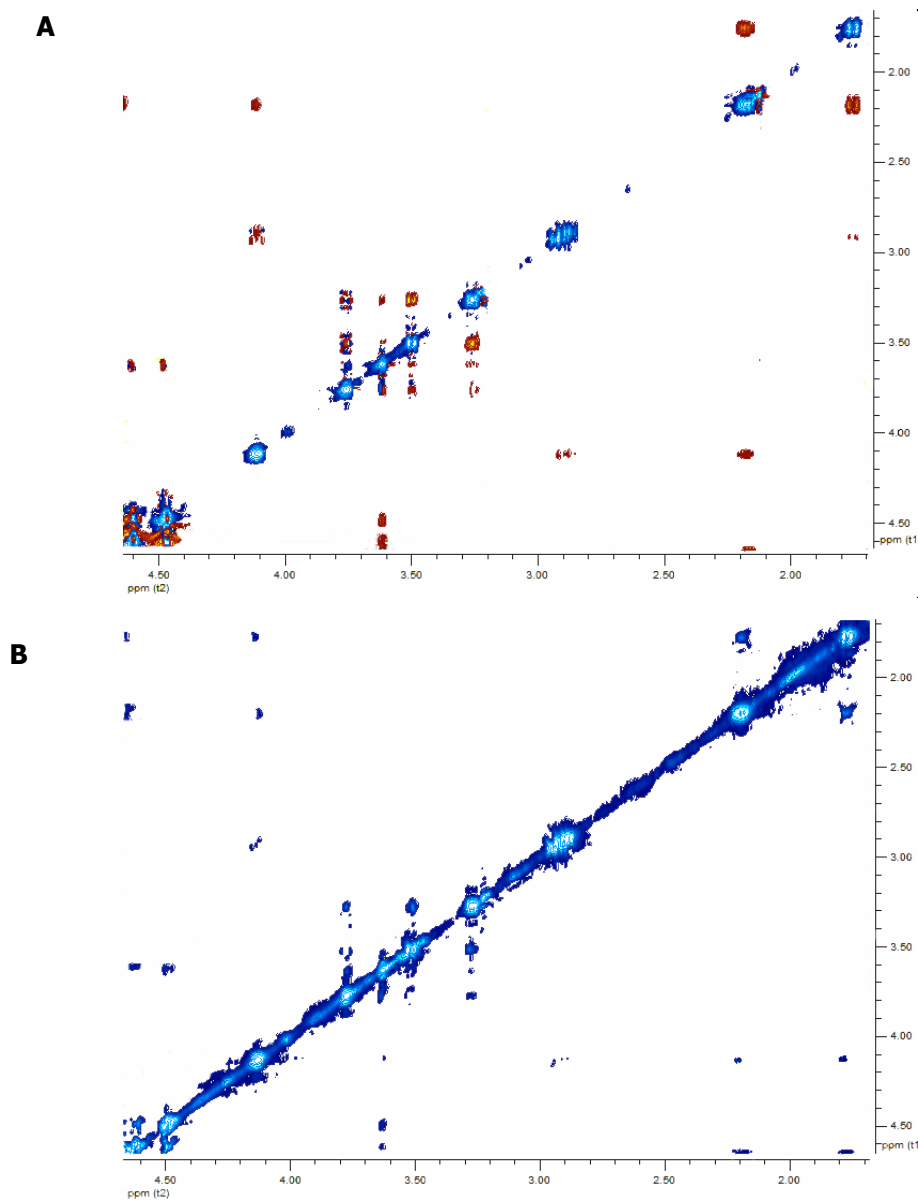
Figure 4-18. A) NOESY spectrum of compound **39**, mixing time=800 ms; B) trNOESY spectrum of compound **39**-Ras-GDP mixture, mixing time=200 ms. The spectral region between 1.7 and 4.7 ppm, containing all signals of protons on bicyclic scaffold, is shown. Both the samples were dissolved in a d_{11}-Tris buffer at pH=7.3, containing 10% CD_3OD, 100 mM NaCl, 5 mM $MgCl_2$. Total samples volume was 450 μL.

The specific binding of all new compounds to the Ras-GDP complex was also

_____

investigated by the analysis of the variations of the selective T_1 and $T_{1\rho}$ of several ligand protons measured in the free state and in the presence of the Ras-GDP complex. (Table 4-2).

Sample	Hx	Hbenz	Hm	H-2	H-1
			Selective T_1		
39	2.07±0.02	2.37±0.01	2.32±0.01	1.14±0.01	0.58±0.01
39+Ras-GDP	0.76±0.03	1.08±0.01	0.96±0.03	0.54±0.01	0.32±0.01
40	2.17±0.01	2.48±0.01	2.27±0.02	1.22±0.01	0.50±0.01
40+Ras-GDP	0.75±0.02	0.95±0.01	0.77±0.01	0.59±0.01	0.31±0.01
41	2.11±0.01	2.46±0.02	2.38±0.02	1.01±0.01	0.58±0.01
41+Ras-GDP	0.81±0.02	0.94±0.03	0.83±0.03	0.45±0.01	0.32±0.02
42	2.45±0.03	2.75±0.04	2.56±0.05	1.13±0.01	0.57±0.01
8+Ras-GDP	1.30±0.02	1.59±0.03	1.30±0.01	0.76±0.01	0.31±0.02
			$T_{1\rho}$		
39	0.95±0.01	1.16±0.01	1.06±0.02	0.82±0.03	0.26±0.01
39+Ras-GDP	0.51±0.02	0.49±0.01	0.42±0.02	0.31±0.01	0.14±0.01
40	1.11±0.01	1.63±0.01	1.35±0.01	0.78±0.02	0.26±0.01
40+Ras-GDP	0.55±0.01	0.39±0.01	0.41±0.01	0.25±0.01	0.19±0.02
41	1.20±0.00	1.72±0.01	1.37±0.01	0.72±0.01	0.27±0.00
41+Ras-GDP	0.47±0.01	0.42±0.01	0.46±0.02	0.26±0.01	0.16±0.02
42	1.13±0.02	2.09±0.03	1.55±0.02	0.53±0.03	-
42+Ras-GDP	0.72±0.02	0.75±0.01	0.79±0.04	0.43±0.02	-

Table 4-2. Selective T_1 and $T_{1\rho}$ values for compounds **39**–**42**.

As a consequence of the binding with Ras, selective T_1 and $T_{1\rho}$ of free compounds **39**-**42** are significantly larger than those determined in the presence of the protein. This effect was evident in all protons analyzed, and it was particularly strong for the aromatic ones. As also observed in the trNOESY experiments (see above), the measurements of the selective T_1 and $T_{1\rho}$ for compounds **43** and **44** provided values with no significant variations in the absence and presence of the Ras-GDP complex. For the reference compound, **SCH-54292** (**45**)**,** the aromatic protons showed a decrease in selective T_1 and $T_{1\rho}$ values when passing from free to bound state, while no change of T_1 values was observed for protons of the sugar moiety (Table 4-3).
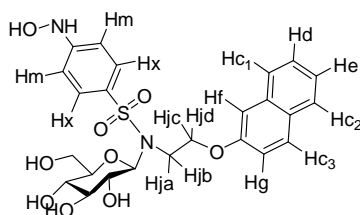
Sample	Hm	Hf	H-2
T_1			
SCH 54292	2.52±0.08	1.24±0.05	-
SCH 54292+Ras-GDP	1.97±0.05	0.96±0.03	-
$T_{1\rho}$			
SCH 54292	1.64±0.08	0.97±0.04	0.60±0.06
SCH 54292+Ras-GDP	1.33±0.04	0.62±0.07	0.60±0.06

Table 4-3. Selective T1 and T1ρ values for **SCH-54292**.

Interestingly, the magnitude of the variations of both selective T_1 and $T_{1\rho}$ values was always much larger for compounds **39**-**42** than for **SCH-54292**. Saturation-transfer difference (STD) experiments[80] are a very helpful means to detect ligand binding to receptors; therefore they were also performed on the same ligand-protein mixtures with the aim of confirming the interaction, and of studying which region of the ligand directly interacts with Ras (epitope mapping).[80] The comparison between the ^{1}H spectrum and STD spectrum of **39**-**42** (Figure 4-19) pointed out that the major interaction with Ras involved both the benzyl and the phenylhydroxylamine moieties of the ligands. In particular, the signals of Hm and Hx (phenylhydroxylamine) and of Ha and Hb protons (benzyl) were clearly observed in all STD experiments. In analogy with the previously described experiments, the STD experiments

---

[80] a) M. Mayer, B. Meyer, *Angew. Chem. Int. Ed.*, **1999**, *38*, 1784-1788. b) J. Klein, R. Meinecke, M. Meyer, B. Meyer, *J. Am. Chem. Soc.*, **1999**, *121*, 5336 −5337. c) M. Vogtherr, T. Peters, *J. Am. Chem. Soc.*, **2000**, *122*, 6093 −6099. d) A. Bernardi, D. Arosio, D. Potenza, I. Sanchez-Medina, S. Mari, F. J. Cañada, J. Jimenez-Barbero, *Chem. Eur. J.*, **2004**, *10*, 4395-4405. For new applications of STD experiments, employing living cells, see: e) S. Mari, D. Serrano-Gómez, F. J. Cañada, A. L. Corbi, J. Jiménez-Barbero, *Angew. Chem. Int. Ed.*, **2005**, *44*, 296. f) B. Claasen, M. Axmann, R. Meinecke, B. Meyer, *J Am Chem Soc.*, **2005**, *127*, 916-919.

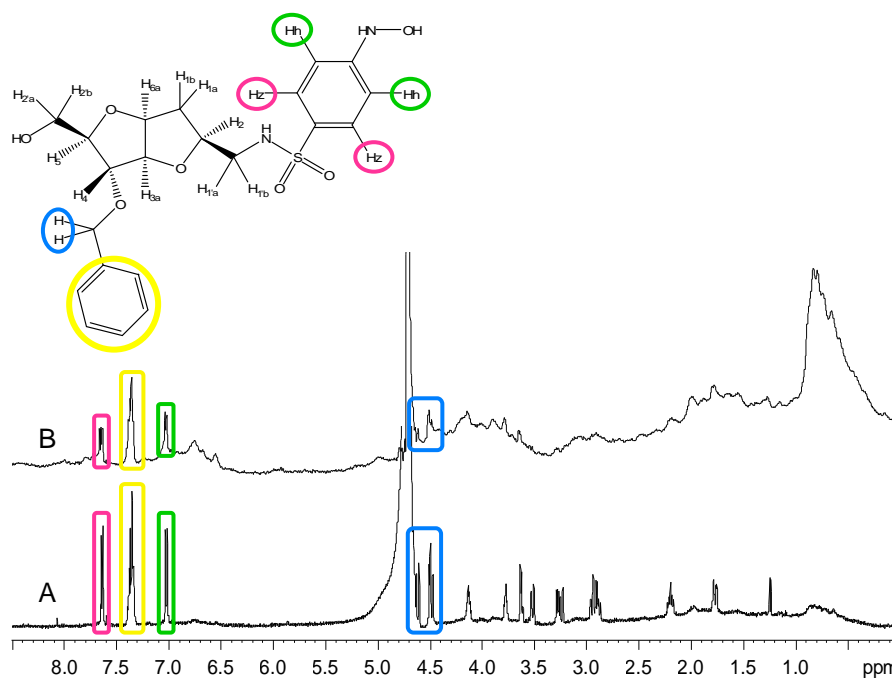_____

recorded for **43** and **44** did not show any signal.

Figure 4-19. A) ^{1}H-NMR of compound **39** with Ras-GDP complex; B) STD spectrum of compound **39** with Ras-GDP complex: ligand/protein ratio 20:1, number of scan (NS)=1360, on-resonance frequency=0.8 ppm, off-resonance frequency=40 ppm, total saturation time=2 s. Spectra were recorded on the same sample, dissolved in a d_{11}-Tris buffer at pH=7.3, containing 10% CD_3OD, 100 mM NaCl, 5 mM $MgCl_2$. Total sample volume was 450 µL.

Moreover, the STD spectrum of the reference compound **SCH-54292** indicated the interaction of both naphtyl and phenylhydroxylamine groups with the protein, while no interaction with the sugar moiety was detected. As outlined in previous studies,[54] in this case the glucose portion has the function to increase water-solubility and does not play any role in the binding with Ras.

Thus, all the NMR data for **39**-**42** and the parent compound seem to indicate a major interaction of the aromatic residues with Ras, while the bicyclic moiety is acting as scaffold providing the proper orientation of the interacting residues, along with the required solubility.

_____

4.4.3. Biological evaluation

4.4.3.1. *In vitro* experiments on p21 h-Ras

Compounds **39-44** were initially tested for their ability to inhibit the C-Cdc25^{Mm}-stimulated nucleotide exchange on purified human Ras protein (p21 h-Ras). Also in this case a modified version of Lenzen's method was used. p21 h-Ras was incubated with mant-GTP in the absence and in the presence of 100 µM of the putative inhibitors **39-44**. **SCH-54292** was used as a positive control in the same experimental conditions. The exchange reaction was started by the addition of C-Cdc25^{Mm}. **SCH-54292**, **39** and **40** are the most active compounds, inhibiting 90% (**40**) or totally (**39** and **SCH-54292**) the exchange. Lower activities were observed for **41** and **42**, (75% and 35% inhibition of nucleotide exchange), while compounds **43** and **44** were totally inactive (Figure 4-20).
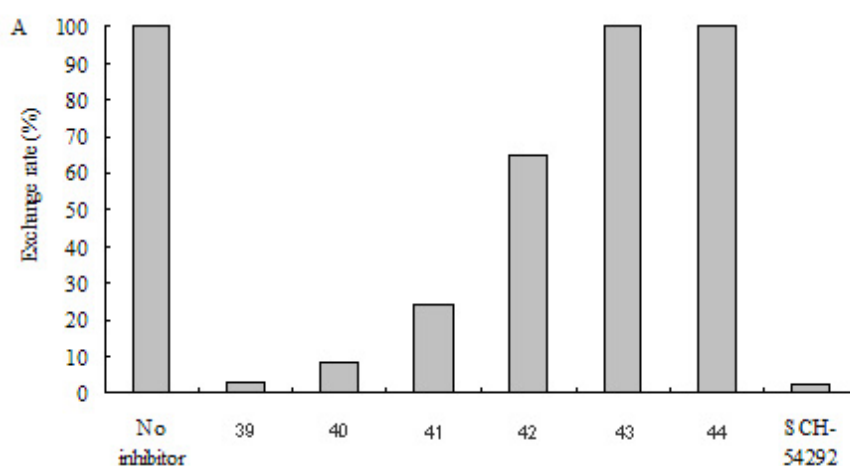

Figure 4-20. C-Cdc25^{Mm}-stimulated nucleotide exchange on p21-hRas**.** The values are expressed as a percentage of the control exchange rate.
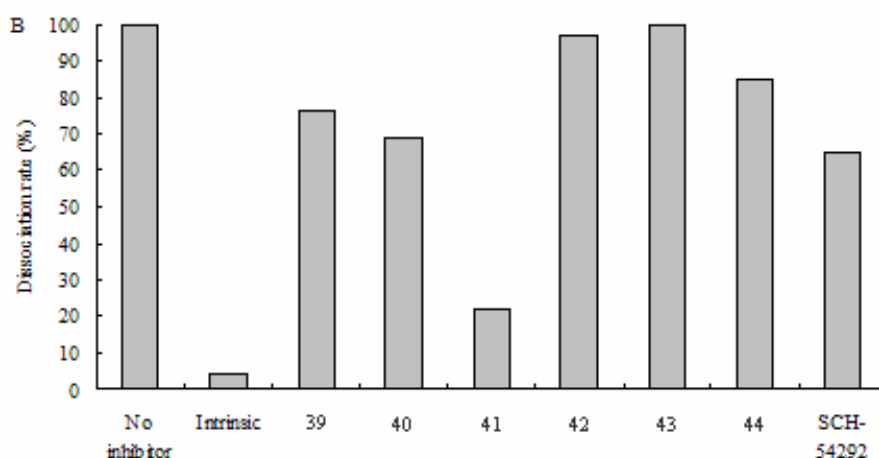
_____

Figure 4-21. C-Cdc25^{Mm}-stimulated dissociation of p21 h-Ras·mant-GDP complexes. The second column represents nucleotide dissociation due to Ras intrinsic activity. The values are expressed as a percentage of the control dissociation rate. The inhibitors (**39**-**44** and **SCH-54292**) were added at a final concentration of 100 μM.

The mechanism of action of these inhibitors was also investigated in a nucleotide-dissociation assay (Figure 4-21) by measuring the release of fluorescent nucleotide by the p21 h-Ras·mant-GDP complex in the presence of GDP and exchange factor C-Cdc25^{Mm}.

The dissociation rate of p21 h-Ras in complex with mant-GDP was partially reduced in the presence of compounds **SCH-54292, 39** and **40** and drastically reduced in the presence of compound **41**. Compounds **42, 43** and **44** inhibited only slightly the GDP dissociation. Both the nucleotide exchange and dissociation experiments strongly suggest the importance of inhibitor's benzyl group for the interaction with Ras: molecules **43** and **44**, lacking this group, do not show any interaction with the protein.

4.4.3.2. Effect of Ras inhibitors on mammalian cells

In order to investigate a specific effect of Ras-mediated signalling *in vivo*, inhibition of mammalian cell growth by compounds **39, 40, 41** and **42** was evaluated both in normal cells and in cells transformed by k-Ras (Arg12).

Compounds **5** and **6** inhibited only slightly the growth of both cell lines when added at a concentration of 100 µM, while growth was completely blocked in both cell lines using compounds **41** and **42** at a same concentration (Fig. 4-22).
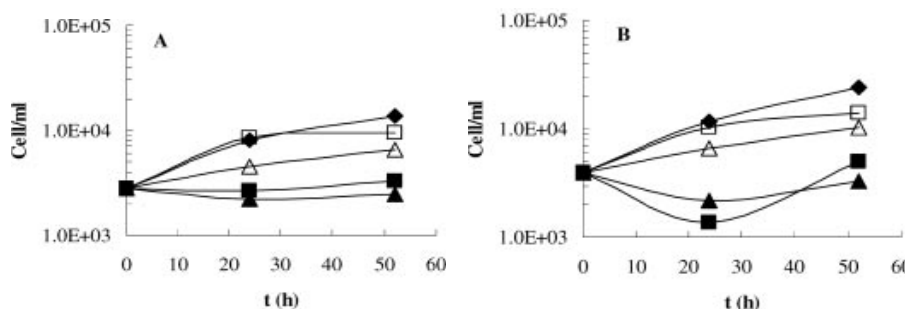

Figure 4-22. Inhibition test in mammalian cells. Normal NIH3T3 (**A**) and NIH3T3 k-Ras (**B**) mouse fibroblasts were seeded into 60 mm dishes and grown for one day: Three dishes were allowed to continue growing without addition of the inhibitor (◆), while molecule **39** (□), **40** (△), **41** (■) and **42** (▲) were added to the other dishes at a final concentration of 100 µM. At different time points sample cells were collected for determination of cell number.

In order to study the *in vivo* inhibition of the Ras-mediated signalling, preliminary experiments were performed to measure the level of activation of MAPK after addition of the inhibitors **39**, **40**, **41** and **42** to normal NIH3T3 fibroblasts growing in 10% serum.
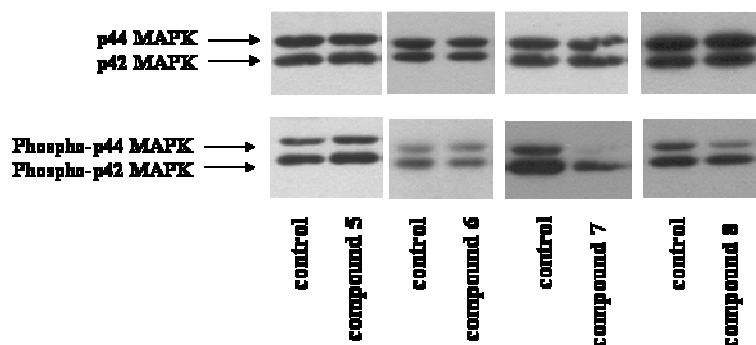

Figure 4-23. Assay of MAPK activation. Lysates (14 µg of total proteins) were separated by SDS-PAGE, transferred to nitrocellulose, and immunodecorated with anti-p42/44 MAPK antibody and anti-phospho- p42/44 MAPK antibody.

_____

As shown in Fig. 4-23 a pronounced decrease in phospho-MAPK expression was observed after 2 hrs at a final concentration of 100 μM for compounds **41**, a less pronounced decrease was observed for compound **42**, while no difference in phospho-MAPK expression was observed for compounds **39** and **40** compared with the control. Since compounds **39** and **40** were the most potent inhibitors *in vitro*, the fact that they are less active than **41** and **42** in cell growth inhibition and completely inactive in decreasing the phospho-MAPK expression suggests that the polar sulfonamide group can prevent the crossing of the cell membrane.

4.4.4. SPR analysis

As previously reported (see above), our Ras inhibitors present the capability of preventing the GDP/GTP nucleotide exchange required for Ras activation. As this process is promoted *in vivo* by GEFs proteins, we wondered if our compounds were able to interfere with Ras-GEF interaction. In order to verify this point, we performed a BIAcore[81] analysis of the p21 h-Ras–C-Cdc25^{Mm} interaction.

N-terminal His-tagged p21 h-Ras protein (GDP-bound) was immobilized on an NTA sensor chip, presenting high affinity for hystidine residues after activation with $NiCl_2$, by injection of a 100 nM solution of the protein. After 5 min, a 50 nM solution of C-Cdc25^{Mm} was passed on the chip and a change in the resonance signal (in RU) in time was recorded, as consequence and proof of the Ras-Cdc25 interaction. The same procedure was repeated treating preventively the chip with different concentration solution of compound **39**-**44** (0.5 μs M, 1 μM, 3 μM, 5 μM and 10 μM) before injection of C-Cdc25^{Mm}. Compounds **43** and **44** was used as negative controls. Molecule effect on the Ras-Cdc25 interaction was estimated as decrease in

_____

[81] www.biacore.com/lifesciences/index.html.
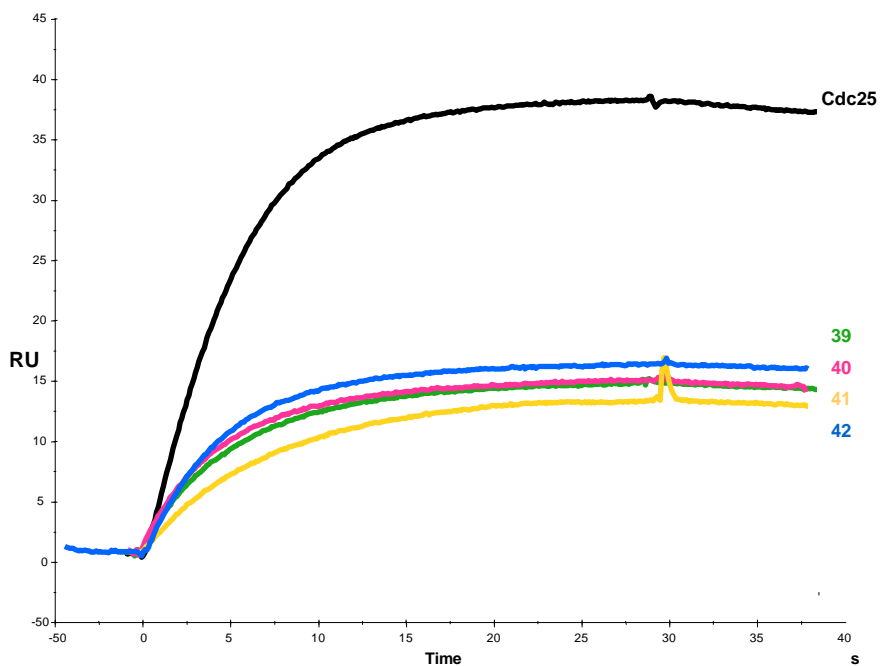
the resonance signal change (Fig. 4-24).

Figure 4-24. SPR sensograms of Ras-Cdc25 interaction in the absence (black) and in the presence of compounds **39**-**42** (coloured lines).

For every compound the inhibition percentage was calculated. Compounds **39**-**42** showed an inhibition of about 65% (the best is **41**, with 68% of inhibition), while compound **43** and **44**, as expected, did not show significant activity.

4.4.5. Discussion

The data that we have presented allow some general considerations on the structure-activity relationship of bicyclic Ras inhibitors. The epitope mapping through STD-NMR experiments for compounds **39**-**42** clearly points out that both the phenylhydroxylamino and the benzyl moieties of the ligands directly

interact with Ras. On the contrary, the protons on the bicyclic scaffold do not interact directly with the protein. Both the benzyl and the phenylhydroxylamine groups can therefore be considered pharmacophores. The observation that compounds **43** and **44**, lacking both benzyl groups, are totally inactive in inhibiting nucleotide exchange and dissociation and Ras-dependent cellular proliferation, strengths our hypothesis that the phenylhydroxylamino group must be accompanied by another aromatic moiety to have binding and biological activity.

The D-arabinose-derived bicyclic scaffold has the function of orienting the pharmacophore groups without directly interacting with the protein. STD-NMR experiments show that the inhibitor orientation in the binding pocket of Ras is not strongly affected by the C-2 configuration and the nature (amide or sulfonamide) of the C-2 linker. However, these molecules have a different behaviour in *in vitro* tests on p21 h-Ras: while **39** and **40** are more potent in blocking nucleotide exchange, compound **41** is the strongest inhibitor of the GDP dissociation. Moreover, only amide-containing molecules **41** and **42** are active in inhibiting cellular growth in both normal and k-Ras transformed mammalian cells, while sulfonamides **39** and **40** are inactive. These data suggest that, while interacting stronger with purified Ras, the sulfonamides can prevent uptake thus decreasing their potency in cells. We are presently investigating the molecular mechanism of action of these inhibitors, with particular attention to their interaction with effectors and exchange factors.

In addition, SPR studies demonstrated our inhibitor capability of preventing the Ras-Cdc25 interaction, suggesting that the GDP/GTP nucleotide exchange inhibition depends on their ability to interfere with Ras binding to GEFs.

4.5. Trying to increase Ras inhibitor water solubility

Bicyclic compounds previously presented show an interesting Ras inhibition activity both *in vitro* and *in vivo* and, some of them, also revealed a good selectivity for the molecular target. Nevertheless their water solubility is scarce.

In order to try to increase this property, important from a pharmacokinetic point of view, we thought to employ a new scaffold, represented by the natural sugar D-glucose. To this purpose, D-glucose was functionalized putting the two putative pharmacophore groups (the phenylhydroxylamino and the thiophenyl moieties) in position 1 and 6, leaving free the hydroxyl groups in position 2, 3, 5 (Fig. 4-25).
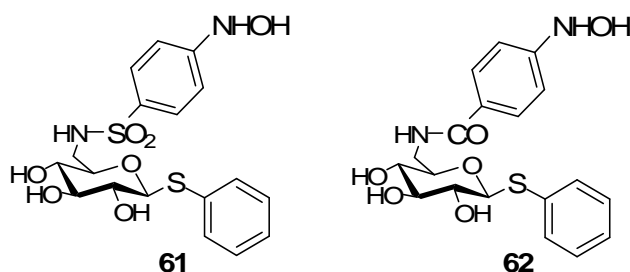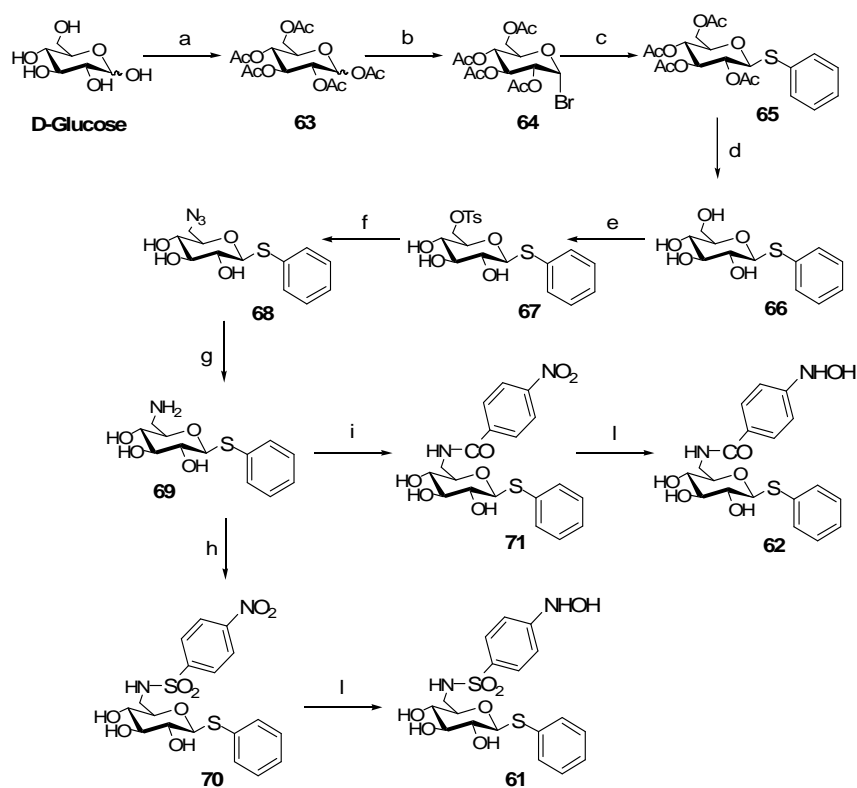

Figure 4-25. Chemical structures of compounds **61** and **62**.

4.5.1. Chemical synthesis

Compounds **61** and **62** were prepared staring from **D-glucose** according to the synthetic pathway reported in Scheme 4-5.

Scheme 4-5. a) Ac$_2$O, DMAP, dry Py, rt, 2 h, quant. yield; b) 33% HBr in AcOH, dry CH$_2$Cl$_2$, rt, 1 h 30 min; c) thiophenol, TEA, dry CH$_3$CN, rt, 30 min; d) NaOMe, dry MeOH, rt, 1 h; e) tosyl chloride, DMAP, dry Py, rt, 20 h, 74%; f) NaN$_3$, TBAI, dry DMF, 80 °C, 18 h, 93%; g) H$_2$, Pd/C, MeOH, rt, 2 h, 71%; h) *p*-nitrobenzenesulfonyl chloride, pyridine, 0 °C, then rt, 18 h, 86%; i) DIC, HOBt, DIPEA, *p*-nitrobenzoic acid, DMF, rt, 2 h, 50%; l) NH$_2$NH$_2$, Pd/C, THF-MeOH, 0 °C, 45 min and 79% for **61**, 1 h and 68% for **62**. DMAP = dimethylamino pyridine; TBAI = tetrabutylammonium iodide; TEA = triethylamine, DIC = *N,N*-diisopropylcarbodiimide, HOBt = *N*-hydroxybenzotriazole, DIPEA = diisopropylethylamine.

Selective bromuration of the anomeric position of **63**, followed by treatment with thiophenol in the presence of triethylamine, gave the thioglucoside **66**. Position 6 was activated to nucleophilic substitution by tosylation, yielding **67**. Nucleophilic displacement of tosyl group with ammonium azide afforded **68** that was converted into the corresponding amine **69** by catalytic hydrogenation. Reaction of **69** with *p*-nitrobenzenesulfonyl chloride followed by reduction of the aromatic nitro group with hydrazine and Pd/C yielded

compound **61**. Alternatively, the condensation of **69** with *p*-nitrobenzoic acid in the presence of *N,N*-diisopropylcarbodiimide (DIC) and *N*-hydroxybenzotriazole (HOBt) followed by reduction with hydrazine and Pd/C afforded compound **62**.

4.5.2. NMR binding studies

NMR binding studies were performed as previously described [4.4.2.]. p21 h-Ras was incubated in a d_{11}-Tris buffer, containing 10% CD_3OD, 100 mM NaCl, 5 mM $MgCl_2$, an amount of GDP equimolar to the protein, and compounds **61** or **62**. An optimized ligand/protein molar ratio of 20 was used in all experiments. NOESY spectra of compounds **39**-**44** in the free state were obtained with mixing times of 800 ms. In trNOESY experiments, an optimal value of 200 ms for mixing times was used. Also in this case we observed negative NOEs (trNOEs) for both **61** and **62**, indicating our compound ability to interact with the protein (Figure 4-26).
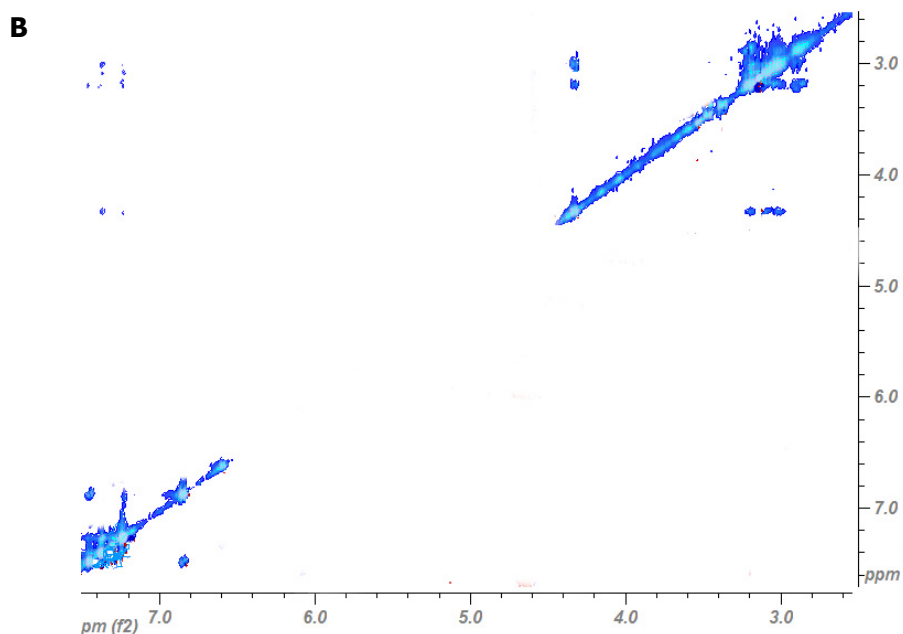
B
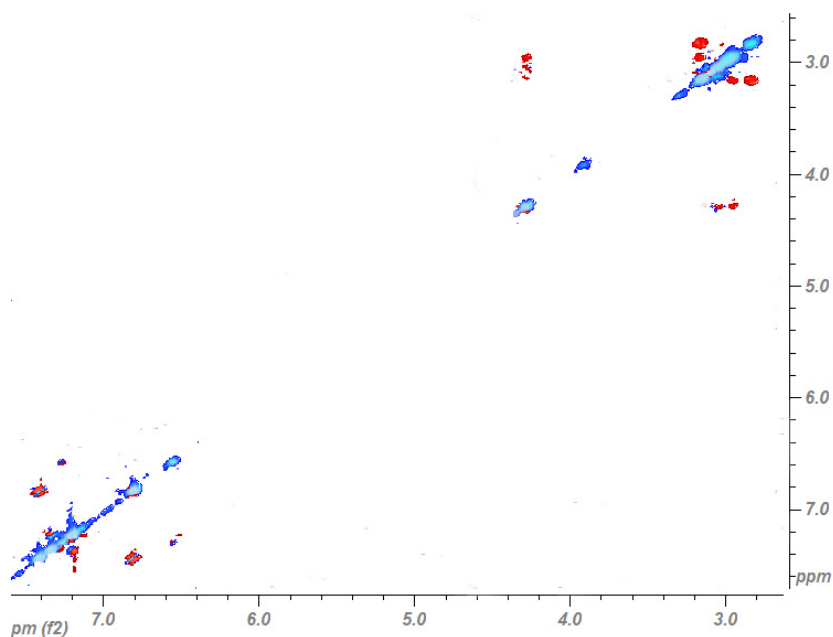
Figure 4-26. A) NOESY spectrum of compound **61**, mixing time=800 ms; B) trNOESY spectrum of compound **61**-Ras-GDP mixture, mixing time=200 ms. Both the samples were dissolved in a d_{11}-Tris buffer at pH=7.3, containing 10% CD_3OD, 100 mM NaCl, 5 mM $MgCl_2$. Total sample volume was 700 µL.

The comparison between the ^{1}H spectrum and STD spectrum of **61** and **62** (Figure 4-27) furnished a further indication of the binding to Ras.
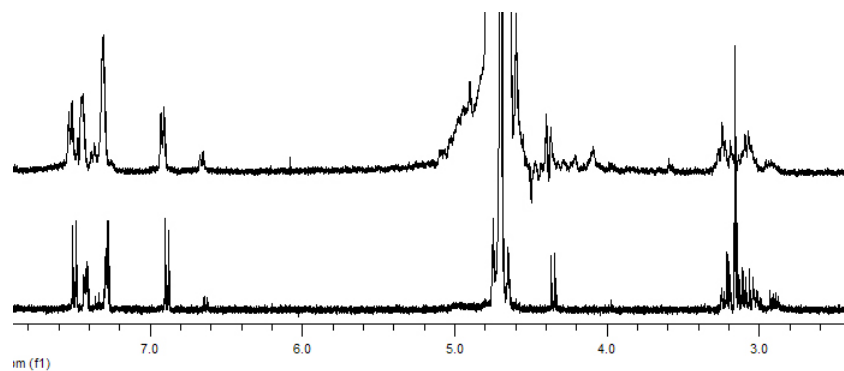

Figure 4-27. A) ^{1}H-NMR of compound **61** with Ras-GDP complex; B) STD spectrum of compound **61** with Ras-GDP complex: ligand/protein ratio 20:1, number of scan (NS)=1360, on-resonance frequency=0.8 ppm, off-resonance frequency=40 ppm, total saturation time=2 s. Spectra were recorded on the same sample, dissolved in a d_{11}-Tris buffer at pH=7.3, containing 10% CD_3OD, 100 mM NaCl, 5 mM $MgCl_2$. Total sample volume was 700 µL.

STD studies revealed that in this case the interaction with Ras involved not only the phenylhydroxylamine moiety and the second aromatic entity, but also the sugar ring. This suggests that probably the glucosidic scaffold takes part to our new ligand binding to Ras.

4.5.3. SPR analysis

These experiments were performed as described in [4.4.4.]. N-terminal His-tagged p21 h-Ras protein (GDP-bound) was immobilized on an NTA sensor chip, presenting high affinity for hystidine residues after activation with $NiCl_2$, by injection of a 100 nM solution of the protein. After 5 min, a 50 nM solution of C-Cdc25^{Mm} was passed on the chip and a change in the resonance signal (in RU) in time was recorded, as consequence and proof of the Ras-Cdc25 interaction. The same procedure was repeated treating preventively the chip with different concentration solution of compound **61** and **62** (0.5 µM, 1 µM, 3 µM, 5 µM and 10 µM) before injection of C-Cdc25^{Mm}. Molecule effect on the Ras-Cdc25 interaction was estimated as decrease in the resonance signal change (Fig. 4-28).
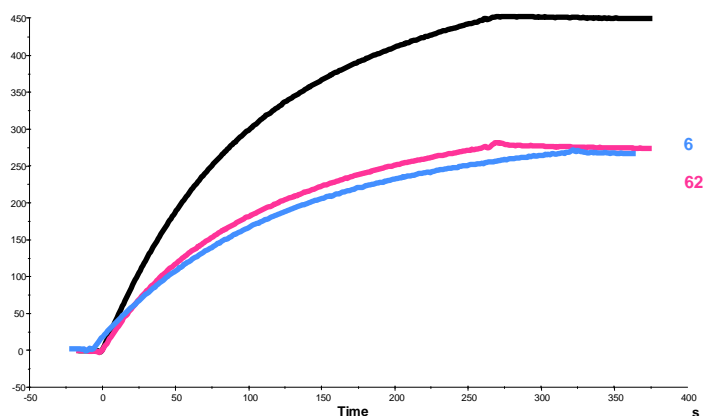

Figure 4-28. SPR sensograms of Ras-Cdc25 interaction in the absence (black) and in the presence of compounds **61** and **62** (coloured lines).

_____

For the two compound the inhibition percentage was calculated. Compounds **61** and **62** showed an inhibition of about 45% of the Ras-Cdc25 interaction.

4.5.4. Biological evaluation

Compounds **61** and **62** were tested for their ability to inhibit the C-Cdc25^{Mm}-stimulated nucleotide exchange on purified human Ras protein (p21 h-Ras) with the approach already described for the other molecules. p21 h-Ras was incubated with mant-GTP in the absence and in the presence of 100 µM of the putative inhibitors **61** and **62**. Both the molecules showed the capability of inhibiting the GDP/GTP nucleotide exchange. Nevertheless, further characterizations of their biological activity were as, during preliminary experiments, they revealed to be chemically instable.

4.6. Preliminary studies for the identification of our inhibitor Ras binding site

Until now, the interaction between our inhibitors and Ras was characterized only by ligand-based NMR binding studies, that is only from the ligand point of view. This allowed the identification of our ligand epitopes important for the interaction with the receptor, but it did not give information concerning on the Ras binding site [3.1.2.].

In order to achieve this kind of analysis, we decided to perform an ^{1}H/^{15}N HSQC titration of Ras with compound **41**, being which presenting the best biological activity and enough water solubility for the experimental conditions.

Figure 4-29. ^{15}N-p21h-Ras(1-166) ^{1}H/^{15}N-HSQC spectrum assignments.

_____

To this purpose, first of all we needed to express and purify the ^{15}N-labelled Ras truncated form p21 h-Ras(1-166), as the complete assignment of ^{15}N and ^{1}H chemical shifts was available.[82] The protein was expressed in an *Escherichia coli* strain transformed with the expression vector pTACCrasC'[83] and purified from inclusion bodies. Uniformly enriched ^{15}N samples were obtained by growing bacteria on a minimum medium with ^{15}NH$_4$Cl as the sole nitrogen source. An yield of 22 mg of protein/L of culture was afforded. ^{15}N-p21h-Ras(1-166) ^{1}H/^{15}N-HSQC spectrum assignments (Fig. 4-29) were compared with data present in literature; a perfect correspondence indicated that our protein was correctly folded. A further evidence was furnished by a functional test in which its capability of switch between the GDP-bound form and the GTP-bond form and binding mant-GTP in the presence of C-Cdc25^{Mm} was verified.

To perform the titration, ^{15}N-p21h-Ras(1-166) was dissolved in 500 µL of NMR buffer (95% H$_2$0/5% D$_2$O containing 20 mM d$_{11}$-Tris-HCl, pH (or pD) 6.7, 40 mM NaCl, 5 mM MgCl$_2$, 0.01% sodium azide, and 30 µM GDP). Compound **41** was dissolved in CD$_3$OD and added in portions to the protein solution. ^{1}H and ^{1}H/^{15}N-HSQC spectra were recorder for different protein-ligand ratios (1:0.25, 1:0.5, 1:0,75, 1:1, 1:1.25, 1:2) and they were then compared, looking for changes in protein signal chemical shifts of both ^{1}H and ^{15}N. The overlap of protein:ligand 1:0 and 1:2 spectra revealed a high number of differences (Fig. 4-30). ^{1}H/^{15}N-HSQC spectra of Ras sample added of different CD$_3$OD volumes were preventively acquired to evaluate possible CD$_3$OD effects, but a more detailed analysis of these data is required in order to discriminate between changes due to ligand addition and changes due to CD$_3$OD addition.

---

[82] Kraulis P. J., Domaille P. J., Campbell-Burk S. L., Van Aken T., and Laue E. D., "Solution Structure and Dynamics of Ras p2 bGDP Determined by Heteronuclear Three- and Four-Dimensional NMR Spectroscopy", *Biochemistry*, **1994**, 33, 3515-3531.
[83] John J., Schlichting I., Schiltz E., Rosch P., and Wittinghofer, A., *J. Biol. Chem.*, **1989**, 264, 13086-13092.
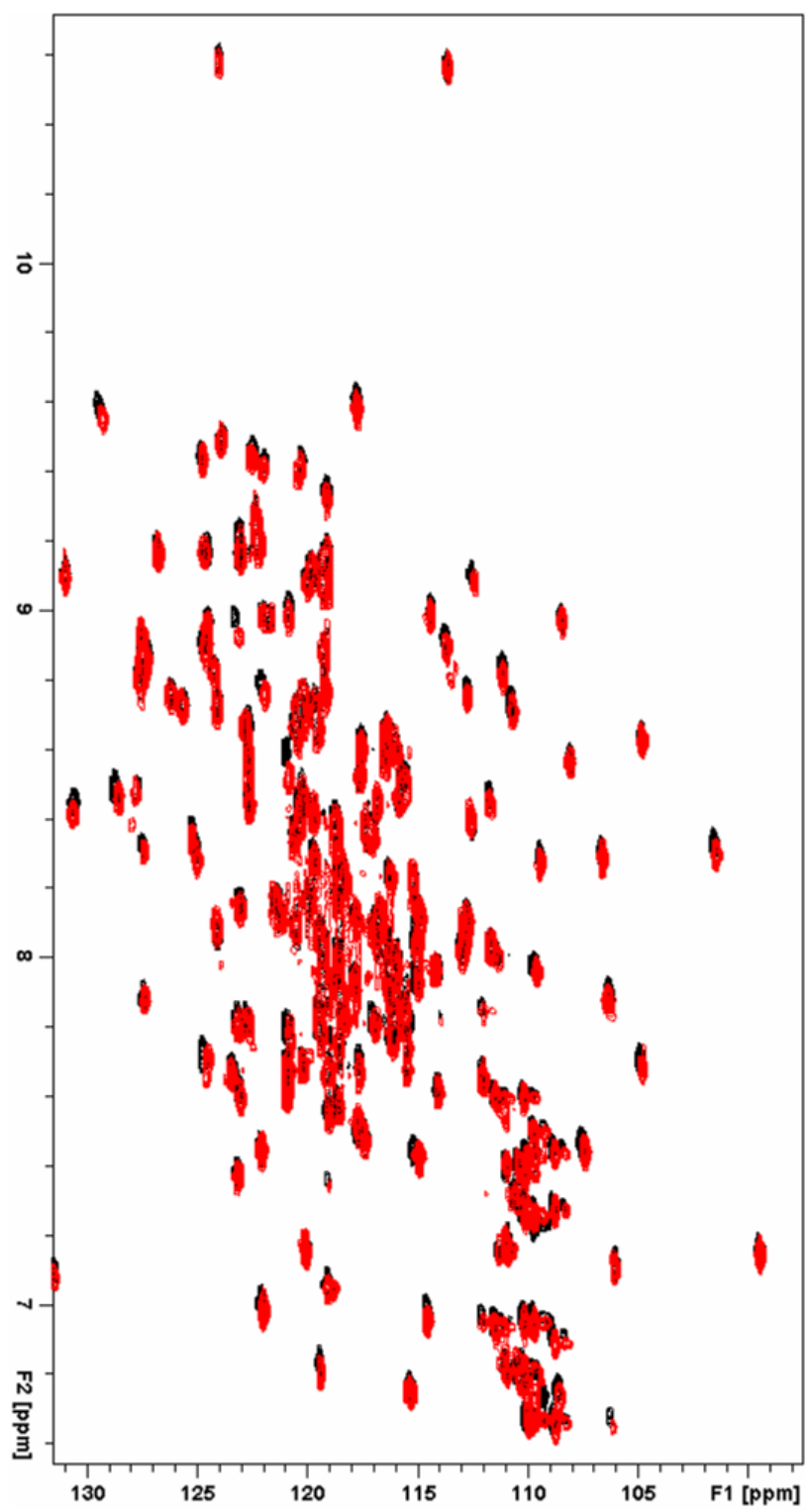
_____

Figure 4- 30. Overlapping of 1:0 and 1.2 P:L ^{1}H/^{15}N-HSQC spectra.

4.7. Conclusions and remarks

This work allowed the development of a new class of Ras protein inhibitors.

These compounds were demonstrated to be able to prevent the *in vitro* GDP/GTP nucleotide exchange, and thus Ras protein activation, and to block the k-Ras-dependent tumoral cell proliferation. In addition, our molecules, in which the pharmacophore groups (a phenylhydroxylamine and one or two benzyl moieties) have been supported on a bicyclic scaffold, show a great chemical stability and better solubility properties if compared with Schering Plough compounds that represent the only other known example of Ras nucleotide exchange inhibitors.

Several data have been collected, concerning their biological activity, their mechanism of action and the nature of their interaction with the molecular target. That required the application of different and complementary techniques, among which biological assay screening, molecular modelling, SPR protein-protein interaction measurements, NMR ligand-receptor binding studies, which gave us the possibility to realize a quite complete structure-activity relationship study on our compounds. Thus, this work also promoted the development of a general strategy for design, synthesis and evaluation of molecules of biological interest, based on the rational-drug design approach.

The most important future developments of this project will regard the completion of the Ras binding site characterization, through which structural information crucial for the design of new inhibitors will be acquired, and the investigation of our compound antiproliferative and antitumoral effect *in vivo* on animal models.

Experimental section
_____

5. Materials and Methods

5.1. Organic synthesis

5.1.1. General procedures

5.1.1.1. Dry solvents and reactions

All solvents were dried over molecular sieves (4 Å, Fluka) for at least 24 h prior to use. When dry conditions were required, the reactions were performed under argon atmosphere.

5.1.1.2. Thin-layer chromatography (TLC)

Thin-layer chromatography (TLC) was performed on Silica Gel 60 F254 plates (Merck) with UV detection, or using a developing solution of conc. H_2SO_4/EtOH/H_2O (5:45:45), followed by heating at 180 °C.

5.1.1.3. Flash column chromatography

Flash column chromatography was performed on silica gel 230–400 mesh (Merck), according with the procedure described in literature.[84]

---

[84] *J.Org. Chem.*, **1979**, 93, 14.

5.1.1.4. Mass spectroscopy

Mass spectra were recorded on a MALDI2 Kompakt Kratos instrument, using gentisic acid (DHB) as matrix and or a Fourier Transform Ion Cyclotrone Resonance (FT-ICR) instrument (model APEXII, Bruker Daltonics), equipped with a 4.7 T cryomagnet (Magnex).

5.1.1.5. NMR spectroscopy

^{1}H and ^{13}C NMR spectra were recorded on a Varian 400 MHz MERCURY instrument at 300 K unless otherwise stated. Chemical shifts are reported in ppm downfield from TMS as internal standard.

5.1.1.6. Optical rotation

Optical rotations were measured at ambient temperature, using the sodium D line, on a P3002 electronic polarimeter (A. Krüss, Germany).

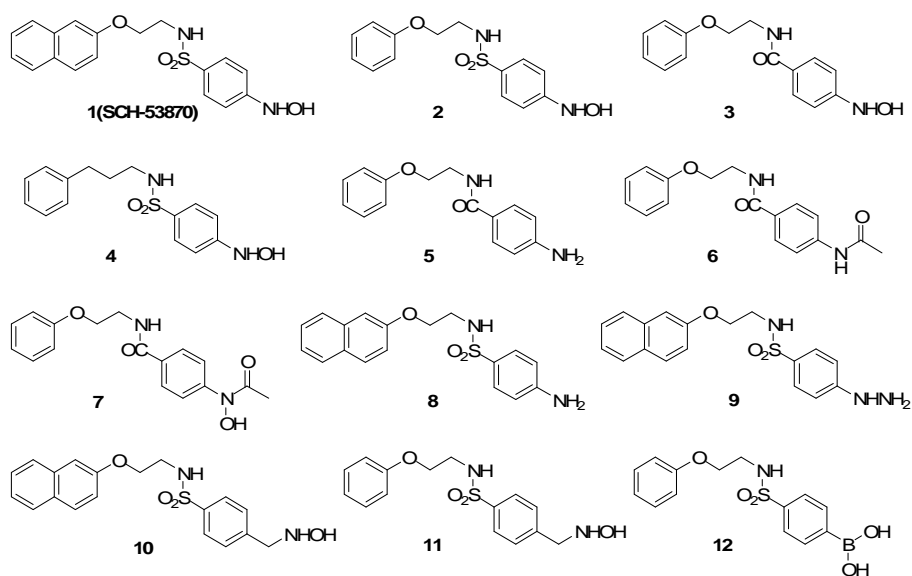## 5.1.2. Synthesis of compounds 1-12
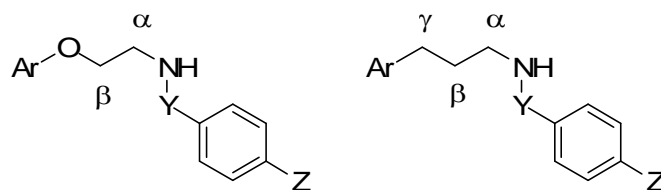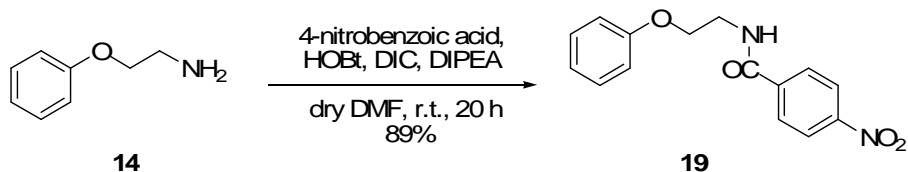

Figure 5-1. Structures of compounds **1**-**12**.

Figure 5-2. Carbon and hydrogen numbering in compounds **1-12**.

Compound 19

To a solution of 2-Phenoxy-ethylamine **14**[51] (580 mg, 4.23 mmol) in dry DMF (12 mL), 4-nitrobenzoic acid (850 mg, 5.1 mmol), N-hydroxybenzotriazole (HOBt, 860 mg, 6.35 mmol), diisopropylcabodiimide (DIC, 980 μL, 6.35 mmol) and diisopropylethylamine (DIPEA, 2.2 mL, 12.7 mmol) were added under argon atmosphere at 0℃, then the reaction mixture was allowed to warm to room temperature and stirred for 20 h. Solvent was evaporated *in vacuo* and the residue was purified by flash column chromatography (6:4 petroleum ether/AcOEt) affording **19** as a yellow powder (1.08 g, 89%).

^{1}H-NMR (CDCl$_3$): δ (ppm) 8.27, 7.93 (AA'XX', 4H, J = 7.0 Hz, benzamide), 7.29 (t, 2H, J = 8.0 Hz, aromatics), 6.98 (t, 1H, J = 6.7 Hz, aromatic), 6.91 (d, 2H, J = 8.5 Hz, aromatics), 6.77 (bs, 1H, NHCO), 4.17 (t, 2H, J = 5.1 Hz, H-β), 3.90 (q, 2H, J = 5.1 Hz, H-α). ^{13}C-NMR (CDCl$_3$): δ (ppm) 165.7, 158.4, 140.0, 129.9, 128.4, 124.1, 121.7, 114.7, 66.7 (C-β), 40.3 (C-α).
HRMS (FT-ICR): calcd for C$_{15}$H$_{14}$N$_2$O$_4$: 286.0954, found: 309.0853 [M+Na]$^+$.

_____

Compound 3
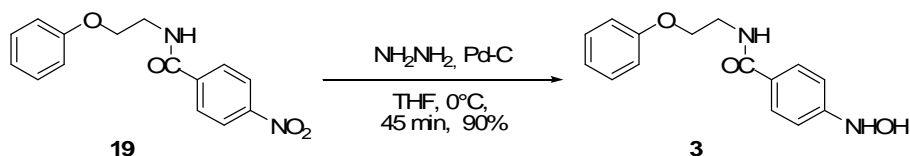
To a solution of **19** (200 mg, 0.7 mmol) in dry THF (10 mL), Pd/C (3.7 mg) was added at 0°C under argon atmosphere. After 15 m in, the suspension was treated with hydrazine hydrate (70 µL, 1.4 mmol) and stirred at 0°C for 45 min. The reaction was quenched by adding acetone. Then Pd/C was removed by filtering and the solvent was evaporated *in vacuo.* The crude residue was purified by flash column chromatography (6:4 petroleum ether/THF) affording **3** as a white powder (180 mg, 90%).
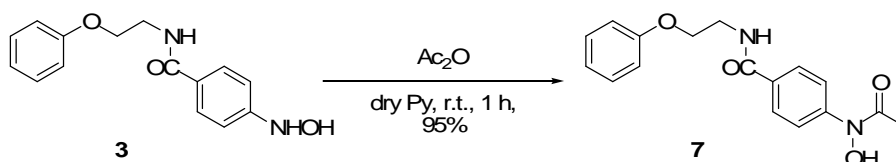
^{1}H-NMR (d[6]-DMSO): δ (ppm) 7.70, 7.30 (AA'XX', 4H, benzamide), 7.30-6.90 (m, 5H, phenyl), 4.13 (bt, 2H, J = 5.8 Hz, H-β), 3.73 (bt, 2H, J = 5.8 Hz, H-α). ^{13}C-NMR (d-MeOH): δ (ppm) 164.7, 155.0, 140.7, 129.2, 128.1, 125.2, 120.6, 112.2, 66.3, 39.6.
HRMS (FT-ICR): calcd for $C_{15}H_{16}N_2O_3$: 272,1161, found: 295.1032 [M+Na]$^+$.

_____

Compound 7

To a solution of **3** (100 mg, 0.37 mmol) in Ac_2O-pyridine (1:2, 3 mL), dimethylamino pyridine was added (catalytic) and the solution was stirred 1h at r.t. Then methanol (3 mL) was added and the solvents were evaporated *in vacuo*. The residue was purified by flash column chromatography (7:3 petroleum ether/AcOEt) affording **7** as a white powder (110 mg, 95%).

^{1}H-NMR (CDCl$_3$): δ (ppm) 7.81, 7.52 (AA'XX', 4H, J = 8.4 Hz, benzamide), 7.29 (t, 2H, J = 7.9 Hz, phenyl), 6.97 (t, 1H, J = 7.3 Hz, phenyl), 6.91 (d, 2H, J = 8.0 Hz, phenyl), 6.64 (bt, 1H, NHCO), 4.15 (t, 2H, J = 5.0 Hz, H-β), 3.87 (q, 2H, J=5.2 Hz, H-α), 2.24 (s, 3H, CH$_3$). ^{13}C-NMR (CDCl$_3$): δ (ppm) 167.9, 166.6, 158.5, 147.5, 142.0, 129.8, 128.2, 121.5, 114.7, 66.9, 40.0 , 22.1. HRMS (FT-ICR): calcd for $C_{17}H_{18}N_2O_4$: 314.1267, found: 337.1176 [M+Na]+.

_____

Compound 5
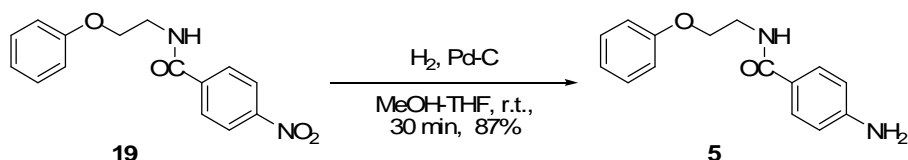


To a solution of **19** (100 mg, 0.35 mmol) in MeOH/THF (5:1, 6 mL), palladium on charcoal (catalytic) was added under H_2 atmosphere (vacuum/H_2 cycles). After 30 min, crude was filtered and solvents evaporated *in vacuo*. The residue was purified by flash column chromatography (4:6 petroleum ether/AcOEt) affording **5** as a white powder (78 mg, 87%).

^{1}H-NMR (d$_6$-DMSO): δ (ppm) 7.70, 6.70 (AA'XX', 4H, J = 7.0 Hz, benzamide), 7.20-6.70 (m, 5 H, phenyl), 7.22 (bs, 1H, NH-CO), 4.24 (t, 2H, J = 5.1 Hz, H-β), 3.65 (q, 2H, J = 5.1 Hz, H-α), 4.01 (bs, 2H, NH$_2$). ^{13}C-NMR (d$_6$-DMSO): δ (ppm) 166.7, 158.4, 150.0, 129.9, 128.4, 115.1, 123.5, 121.7, 114.7, 68.2, 43.3.
HRMS (FT-ICR): calcd for $C_{15}H_{16}N_2O_2$: 256,1212, found: 279.1089 [M+Na]$^+$.

_____

Compound 6
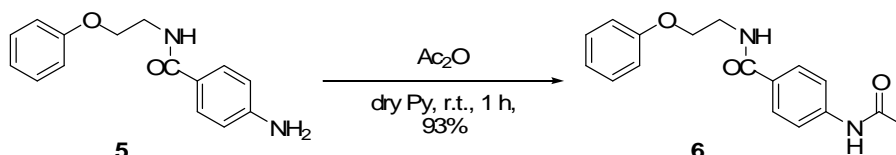
A solution of **5** (100 mg, 0.39 mmol) in Ac$_2$O pyridine (1:2, 3 mL) was stirred 1h at r.t. Then methanol (3 mL) was added and the solvents were evaporated *in vacuo*. The residue was purified by flash column chromatography (6:4 petroleum ether/AcOEt) affording **6** as a white powder (108 mg, 93%).

^{1}H-NMR (CDCl$_3$): δ (ppm) 7.81, 7.52 (AA'XX', 4H, J = 8.4 Hz, benzamide), 7.29 (t, 2H, J = 7.9 Hz, phenyl), 6.97 (t, 1H, J = 7.3 Hz, phenyl), 6.91 (d, 2H, J = 8.0 Hz, phenyl), 6.64 (bt, 1H, NHCO), 4.15 (t, 2H, J = 5.1 Hz, H-β), 3.87 (q, 2H, J = 5.1 Hz, H-α), 2.24 (s, 3H, NCH$_3$). ^{13}C-NMR (CDCl$_3$): δ (ppm) 167.9, 166.6, 158.5, 147.5, 142.0, 129.8, 128.2, 121.5, 114.7, 66.9, 40.0, 22.1.

HRMS (FT-ICR): calcd for C$_{17}$H$_{18}$N$_2$O$_3$: 298,1317; found: 321.1198 [M+Na]$^+$.

_____

Compound 16
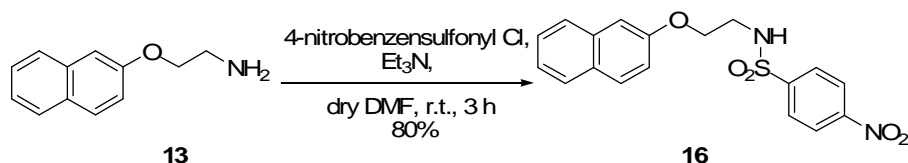
To a solution of amine **13** (1.7 g, 9.1 mmol) in dry CH_2Cl_2 (70 mL), triethylamine (1.9 mL, 13.62 mmol) and *p*-nitrobenzenesulfonyl chloride (3 g, 13.62 mmol) were added under argon atmosphere at 0°C. Then the stirred mixture was allowed to warm at r.t. and after 3 h reaction was stopped by evaporating the solvent *in vacuo*. The residue was purified by flash column chromatography (8:2 petroleum ether/AcOEt) affording **16** as a yellow powder (2.7 g, 80%).

^{1}H-NMR (CDCl₃): δ (ppm) 8.22, 7.98 (AA'XX', 4H, J = 8.8 Hz, benzenesulfonamide), 7.98 (d, 2H, J = 8.8 Hz, naphtyl), 7.65 (m, 2H, naphtyl), 7.38 (dt, 1H, J = 7.0, 11.0 Hz, naphtyl), 7.27 (dt, 1H, J = 6.9, 1.2 Hz, naphtyl), 6.92 (m, 1H, naphtyl), 5.13 (bt, 1H, NHSO₂), 4.06 (t, 2H, J = 5.1 Hz, H-β), 3.44 (q, 2H, J = 5.1 Hz, H-α). ^{13}C-NMR (CDCl₃): δ (ppm) 155.6, 150.0, 146.0, 134.3, 129.9, 129.3, 128.4, 127.8, 126.9, 126.8, 124.6 124.4, 118.32 107.7, 66.4, 43.1.
HRMS (FT-ICR): calcd for $C_{18}H_{16}N_2O_5S$: 372,0780, found: 395.0653 [M+Na]+.

_____

Compound 17
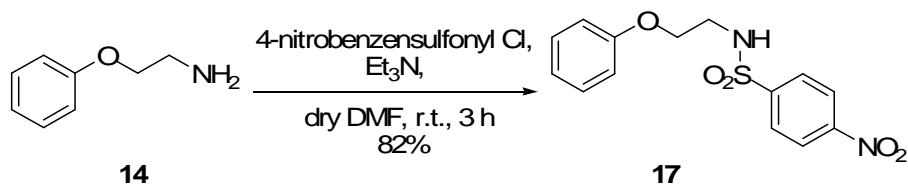
The same procedure used for the synthesis of **16** was employed starting from amine **14** (1.17 g, 8.53 mmol). The residue was purified by flash column chromatography (8:2 petroleum ether/AcOEt) affording **17** as a yellow powder (2.2 g, 82%).

^{1}H-NMR (CDCl$_3$): δ (ppm) 8.27, 7.93 (AA'XX', 4H, J = 7.0 Hz, benzensulfonamide), 7.29 (t, 2H, J = 8.0 Hz, phenyl), 6.98 (t, 1H, J = 6.7 Hz, phenyl), 6.91 (d, 2H, J = 8.5 Hz, phenyl), 6.77 (bs, 1H, NHCO), 4.17 (t, 2H, J = 5.1 Hz, H-β), 3.90 (q, 2H, J = 5.1 Hz, H-α). ^{13}C-NMR (CDCl$_3$): δ (ppm) 165.7, 158.4, 140.0, 129.9, 128.4, 124.1, 121.7, 114.7, 66.7, 40.3.
HRMS (FT-ICR): calcd for C$_{14}$H$_{14}$N$_2$O$_5$S: 322,0623, found: 345.0536 [M+Na]$^+$.
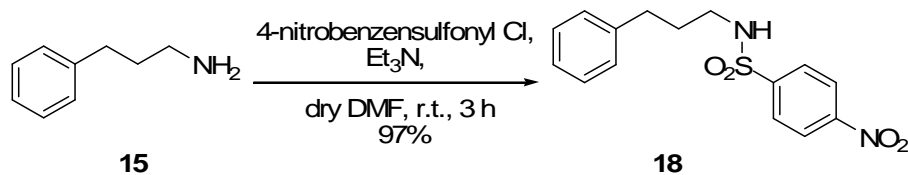
_____

Compound 18

The same procedure used for the synthesis of **16** was employed starting from amine **15** (528 μL, 3.7 mmol). The residue was purified by flash column chromatography (8:2 petroleum ether/AcOEt) affording **18** as a brownish powder (1.145 g, 97%).

^{1}H-NMR (CDCl$_3$): δ (ppm) 8.33, 8.01 (AA'XX', 4H, J = 8.8 Hz, benzensulfonamide), 7.27-7.07 (m, 5H, phenyl), 4.93 (t, 1H, J = 6.0 Hz, NH-SO$_2$), 3.03 (q, 2H, J = 6.8 Hz, H-α), 2.62 (t, 2H, J = 7.5 Hz, H-γ), 1.82 (quint, 2H, J = 7.0 Hz, H-β). ^{13}C-NMR (CDCl$_3$): δ (ppm) 150.1, 145.9, 140.6, 128.8, 128.5, 128.1, 126.5, 124.6, 43.1, 33.0, 31.5.
HRMS (FT-ICR): calcd for C$_{15}$H$_{16}$N$_2$O$_4$S: 320,0831, found: 343,0719 [M+Na]$^+$.

Compound 1
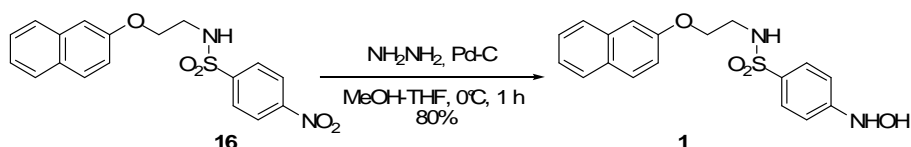
To a solution of **16** (100 mg, 0.26 mmol) in dry MeOH-THF (1:1, 4 mL), Pd/C (catalytic) was added at 0℃ under argon atmosphere. After 15 min, the suspension was treated with hydrazine hydrate (30 µL, 0.52 mmol) and stirred at 0℃ for 1 h. The reaction was quenched by adding acetone. Then Pd/C was removed by filtering and the solvent was evaporated *in vacuo*. The crude residue was purified by flash column chromatography (7:3 petroleum ether/THF) affording **1** as a white powder (74 mg, 80%).

^{1}H-NMR (d_6-DMSO): δ (ppm) 8.97 (s, 1H, NHO*H*), 8.68 (s, 1H, N*H*OH), 7.60, 6.90 (AA'XX', 4H, benzenesulfonamide), 7.70 (m, 2H, naphtyl), 7.65 (t, 1H, naphtyl), 7.45 (m, 1H, naphtyl), 7.32 (t, 1H, naphtyl), 7.22 (d, 1H, naphtyl), 7.09 (dd, 1H, J = 2.4, 8.0 Hz, naphtyl), 5.97 (s, 1H, J = 5.7 Hz, NHSO$_2$), 4.07 (t, 2H, J = 5.7 Hz, H-β), 3.11 (q, 2H, J = 5.7 Hz, H-α); ^{13}C-NMR (CDCl$_3$): δ (ppm) 156.6, 155.7, 134.8, 129.9, 129.5, 129.1, 128.5, 128.2, 127.3, 127.0, 124.3, 119.3, 112.1, 107.3, 67.3, 42.7.

HRMS (FT-ICR): calcd for C$_{18}$H$_{18}$N$_2$O$_4$S: 358.0987; found: 381.0867 [M+Na]+.
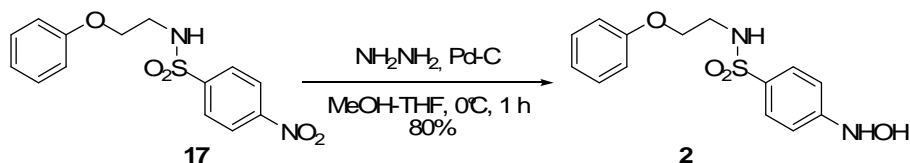
_____

Compound 2

To a solution of **17** (200 mg, 0.62 mmol) in dry MeOH-THF (1:1, 10 mL), Pd/C (catalytic) was added at 0°C under argon atmosphere. After 15 min, the suspension was treated with hydrazine hydrate (32 µL, 0.62 mmol) and stirred at 0°C for 1 h. The reaction was quenched b y adding acetone. Then Pd/C was removed by filtering and the solvent was evaporated *in vacuo*. The crude residue was purified by flash column chromatography (7:3 petroleum ether/THF), affording **2** as a white powder (147 mg, 80%).

^{1}H-NMR (d$_6$-DMSO): δ (ppm) 7.70, 7.30 (AA'XX', 4H, benzenesulfonamide), 6.90-7.30 (m, 5H, phenyl), 4.13 (bt, 2H, J = 5.8 Hz, H-β), 3.73 (bt, 2H, J = 5.8 Hz, H-α). ^{13}C-NMR (d-MeOH): δ (ppm) 164.7, 155.0, 140.7, 129.2, 128.1, 125.2, 120.6, 112.2, 66.3, 39.6.
HRMS (FT-ICR): calcd for $C_{14}H_{16}N_2O_4S$: 308.0831; found: 331.0701 [M+Na]$^+$.
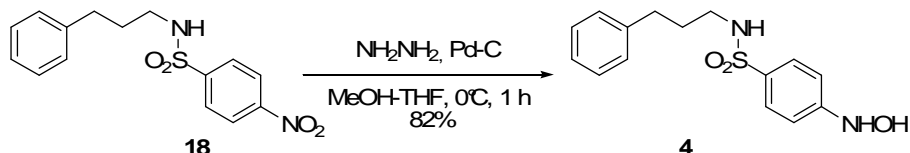

Compound 4

To a solution of **18** (200 mg, 0.62 mmol) in dry MeOH-THF (1:1, 10 mL), Pd/C (catalytic) was added at 0°C under argon atmos phere. After 15 min, the suspension was treated with hydrazine hydrate (60 μL, 1.2 mmol) and stirred at 0°C for 1 h. The reaction was quenched b y adding acetone. Then Pd/C was removed by filtering and the solvent was evaporated *in vacuo*. The crude residue was purified by flash column chromatography (7:3 petroleum ether/THF) affording **4** as a white powder (156 mg, 82%).

^{1}H-NMR (d$_6$-DMSO): δ (ppm) 8.91 (bs, 1H, NHO*H*) 8.64 (d, 1H, J = 1.7 Hz, N*H*OH), 7.52, 6.86 (AA'XX', 4H, J = 8.7 Hz, benzenesulfonamide), 7.27 (t, 1H, J =5.8 Hz, N*H*SO$_2$), 7.22 (bt, 2H, J = 7.3 Hz, phenyl), 7.14-7.07 (m, 3H, phenyl), 2.67 (q, 2H, J = 6.8 Hz, H-α), 2.51 (t, 2H, J = 8.0 Hz, H-γ), 1.82 (quintet, 2H, J = 7.4 Hz, H-β). ^{13}C-NMR (d$_6$-DMSO): δ (ppm) 155.6, 142.0, 129.9, 128.9, 128.8, 128.4, 126.4, 112.1, 42.8, 33.0, 31.6.
HRMS (FT-ICR): calcd for C$_{15}$H$_{18}$N$_2$O$_2$S: 290.1089; found: 314.1003 [M+Na]$^+$.

_____

Compound 8
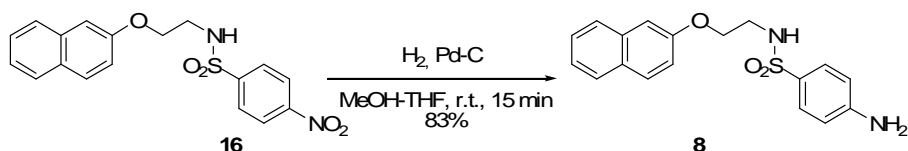
To a solution of **16** (80 mg, 0.21 mmol) in MeOH/THF (5:1, 6 mL), palladium on charcoal (catalytic) was added under H_2 atmosphere (vacuum/H2 cycles). After 15 min, crude was filtered and solvents evaporated *in vacuo*. The residue was purified by flash column chromatography (1:1 petroleum ether/AcOEt) affording **8** as a white powder (64 mg, 83%).

^{1}H-NMR (d_6-DMSO): δ (ppm) 7.81, 7.75 (m, 3H, naphtyl), 7.44, 6.60 (AA'XX', 4H, J = 8.8 Hz, benzenesulfonamide), 7.43 (m, 2H, NHSO$_2$, naphtyl), 7.32 (t, 1H, J = 8.1 Hz, naphtyl), 7.23 (d, 1H, J = 2.3 Hz, naphtyl), 7.09 (dd, 1H, J=8.9 Hz, 2.5 Hz, naphtyl), 5.94 (s, 2H, NH$_2$), 4.05 (t, 2H, J = 5.6 Hz, H-β), 3.08 (q, 2H, J = 5.6 Hz, H-α). ^{13}C-NMR (d_6-DMSO): δ (ppm) 156.7, 153.1, 134.8, 128.9, 129.15, 129.12, 128.1, 127.3, 127.0, 125.9, 124.3, 119.3, 113.3, 107.4, 67.3, 42.7.
HRMS (FT-ICR): calcd for $C_{18}H_{18}N_2O_3S$: 342,1038; found: 365,0912 [M+Na]$^+$.

Compound 9
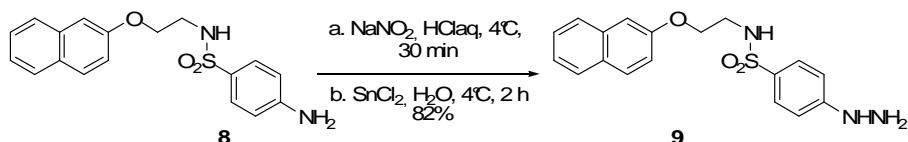
To a suspension of **8** (100 mg, 0.29 mmol) in concentrated HCl (37%, 1 mL), an aqueous solution of sodium nitrite (160 µL, 0.40 mmol) was added dropwise at 4°C. The suspension was stirred at this temperature for 30 min, then a soultion of $SnCl_2.H_2O$ (303 mg, 1.46 mmol) in concentrated HCl (37 %, 240 µL) was added. The suspension was further stirred at 4°C for 2 h. Then crude was filtered and the solid, containing the product, washed with water. The solid residue was dissolved in AcOEt (20 mL) and, after filtration on silica gel pad, pure compound **9** was recovered as a white solid (85 mg, 82%).

^{1}H-NMR (d6-DMSO): δ (ppm) 10.34 (bs, 2H, NHN*H*$_2$) 8.90 (bs, 1H, N*H*NH$_2$), 7.81-7.71 (m, 4H, N*H*SO$_2$, Harom), 7.72, 7.04 (AA'XX', 4H, J =7.9 Hz, Harom), 7.43 (m, 1H, J = 7.4 Hz, Harom), 7.32 (t, 1H, J=7.4 Hz, Harom), 7.24 (bs, 1H, Harom), 7.09 (d, 1H, J =8.9 Hz, Harom), 4.08 (t, 2H, J = 5.6 Hz, H-β), 3.13 (q, 2H, J = 5.3 Hz, H-α). ^{13}C-NMR (d6-DMSO): δ (ppm) 157.4, 145.3, 134.6, 129.7, 129.5, 129.3, 126.8, 126.4, 126.0, 123.7, 118.8, 112.3, 105.6, 71.9, 41.6.
HRMS (FT-ICR): calcd for $C_{18}H_{19}N_3O_3S$: 357.1147; found: 380.1067 [M+Na]$^+$.

_____

Compound 21
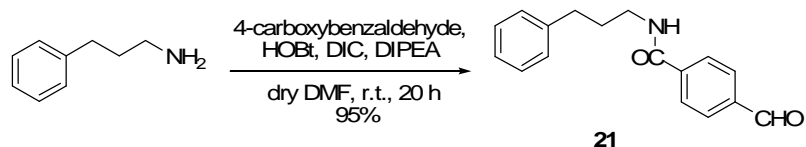
To a solution of 3-Phenyl-propylamine (422 µL, 2.96 mmol) in dry DMF (8 mL), 4-carboxybenzaldehyde (533 mg, 3.5 mmol), N-hydroxybenzotriazole (HOBt, 598 mg, 4.4 mmol), diisopropylcarbodiimide (DIC, 686 µL, 4.4 mmol) and diisopropylethylamine (DIPEA, 1.5 µL, 8.8 mmol) were added under argon atmosphere at 0 °C, then the reaction mixture was allowed to warm to room temperature and stirred for 20 h. The solvent was evaporated *in vacuo* and the residue was dissolved in CH_2Cl_2 (15 mL) and washed with aqueous saturated $NaHCO_3$, the organic layer was dried on sodium sulphate, filtered and evaporated. Flash column chromatography of the residue (6:4 petroleum ether/EtOAc) afforded **21** as a colourless oil (734 mg, 95%).

^{1}H-NMR ($CDCl_3$): δ (ppm) 10.03 (s, 1H, CHO), 7.88, 7.76 (AA'XX', 4H, J = 8.0 Hz, benzamide), 7.31-7.18 (m, 5H, phenyl), 6.27 (bt, 1H, NHCO), 3.52 (q, 2H, J = 6.6 Hz, H-α), 2.74 (t, 2H, J = 7.4 Hz, H-γ), 2.0 (quintet, 2H, J = 7.2 Hz, H-β). ^{13}C-NMR ($CDCl_3$): δ (ppm) 191.6 (aldehyde), 166.4 (amide), 141.5, 139.9, 138.2, 129.9, 128.8, 128.6, 127.7, 126.4, 40.5, 34.0, 31.3. HRMS (FT-ICR): calcd for $C_{17}H_{17}NO_2$: 267.1259; found: 290.1147 [M+Na]$^+$.

_____

Compound 23
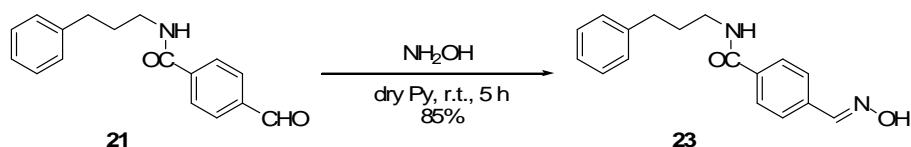
To a solution of 4-Formyl-N-(3-phenyl-propyl)-benzamide **21** (360 mg, 1.35 mmol) in dry pyridine (8 mL), hydroxylamine hydrochloride (142 mg, 2.03 mmol) was added under argon atmosphere and the solution was stirred for 5h at r.t. Solvent was then evaporated *in vacuo*, and the crude residue purified by flash column chromatography of the residue (6:4 petroleum ether/AcOEt) affording **23** as a colourless oil (322.6 mg, 85%).

^{1}H-NMR (CDCl$_3$): δ (ppm) 8.13 (s, 1H, CH=N), 7.65, 7.56 (AA'XX', 4H, J = 8.0 Hz, benzamide), 7.31-7.18 (m, 5H, phenyl), 6.27 (bt, 1H, NHCO), 3.52 (q, 2H, J = 6.6 Hz, H-α), 2.72 (t, 2H, J = 7.4 Hz, H-γ), 1.97 (quintet, 2H, J = 7.2 Hz, H-β). ^{13}C-NMR (CDCl$_3$): δ (ppm) 166.4 (amide), 152.0 (C=N), 141.5, 139.9, 138.2, 129.9, 128.8, 128.6, 127.7, 126.4, 40.5, 34.0, 31.3.
HRMS (FT-ICR): calcd for C$_{17}$H$_{18}$N$_2$O$_2$: 282.1368, found: 305.1267 [M+Na]$^+$.

_____

Compound 11
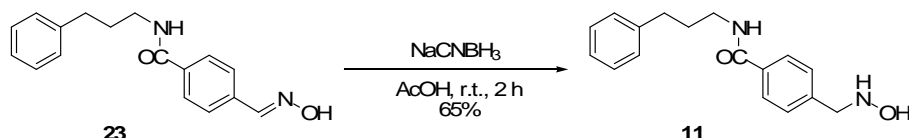
To a solution of 4-(Hydroxyiminomethyl)-*N*-(3-phenyl-propyl)-benzamide **23** (300 mg, 1.1 mmol) in glacial acetic acid (13 mL), sodium cianoborohydride (200 mg, 3.2 mmol) was added under argon atmosphere. After stirring the mixture for 2 h at r.t., solvent was evaporated *in vacuo*, the residue dissolved in CH_2Cl_2, washed with aqueous saturated $NaHCO_3$, the organic layer was dried on sodium sulfate, filtered and evaporated. Flash column chromatography of the residue (1:1 petroleum ether/AcOEt) afforded **11** (168 mg, 56%) as a white powder.

^{1}H-NMR (d_6-DMSO): δ (ppm) 8.40 (bt, 1H, J = 5.1 Hz, NH-CO), 7.76, 7.39 (AA'XX', 4H, J = 8.2 Hz, benzamide), 7.28-7.15 (m, 5H, phenyl), 6.16 (bs, 1H), 3.89 (s, 2H, CH_2NHOH), 3.26 (q, 2H, J = 6.6 Hz, H-α), 2.61 (t, 2H, J = 7.6 Hz, H-γ), 1.81 (quintet, 2H, J = 7.1 Hz, H-β). ^{13}C-NMR (d_6-DMSO): δ (ppm) 166.6, 143.1, 142.4, 133.6, 131.23, 128.94, 128.91, 128.88, 127.46, 126.36, 57.7, 33.5, 31.8.
HRMS (FT-ICR): calcd for $C_{17}H_{20}N_2O_2$: 284.1525, found: 307.1443 [M+Na]+.

Compound 10
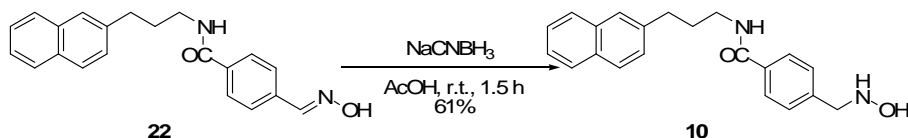
To a solution of 4-(Hydroxyimino-methyl)-N-[2-(naphthalen-2-yloxy)-ethyl]-benzamide**22**[85] (130 mg, 0.39 mmol) in glacial acetic acid (7 mL), sodium cyanoborohydride (73 mg, 1.2 mmol) was added under argon atmosphere. After stirring the mixture for 1.5 h at r.t., solvent was evaporated *in vacuo*, the residue dissolved in CH_2Cl_2, washed with aqueous saturated $NaHCO_3$, the organic layer was dried on sodium sulfate, filtered and evaporated. Flash column chromatography of the residue (1:1 petroleum ether/THF) afforded **10** (80 mg, 61%) as a white powder.

^{1}H-NMR (d_6-DMSO): δ (ppm) 8.69 (bt, 1H, J = 5.3 Hz, NH-CO), 7.80-7.20 (m, 11H, aromatics), 6.15 (bs, 1H), 4.23 (t, 2H, J = 5.7 Hz, H-β), 3.89 (s, 2H, CH_2NHOH), 3.69 (t, 2H, J = 5.7 Hz, H-α). ^{13}C-NMR (d_6-DMSO): δ (ppm) 167.0, 156.9, 143.4, 134.9, 133.2, 129.9, 129.1, 128.9, 128.1, 127.6, 127.3, 127.0, 124.2, 119.3, 107.5, 66.9, 57.7,
HRMS (FT-ICR): calcd for $C_{20}H_{20}N_2O_3$: 336.1474, found: 359.1359 [M+Na]$^+$.

---

[85] It was prepared with the same procedure described for **23**.

_____

Compound 12
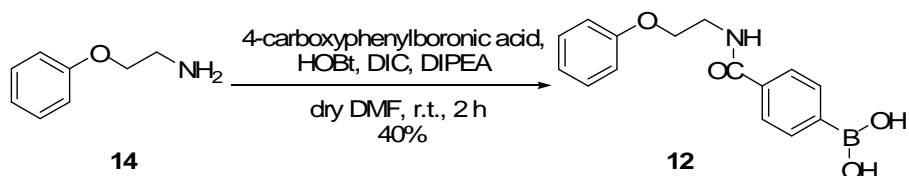
To a solution of 2-Phenoxy-ethylamine **14** (50 mg, 0.36 mmol) in dry DMF (1 mL), 4-carboxyphenylboronic acid (73 mg, 0.43 mmol), HBTU (190 mg, 0.5 mmol), N-hydroxybenzotriazole (HOBt, 73 mg, 0.54 mmol) and diisopropylethylamine (DIPEA, 185 µL, 1.1 mmol) were added under argon atmosphere at r.t., then the reaction mixture was stirred for 2 h. The solvent was evaportaed *in vacuo* and the crude residue purified by flash column chromatography (8:2 AcOEt/methanol), affording **12** as a white powder (41 mg, 40%).

^{1}H-NMR (d$_6$-DMSO): δ (ppm) 7.70, 6.80 (m, 9H, arom), 4.15 (t, 2H, J = 5.7 Hz, H-α), 3.76 (q, 2H, J = 5.7 Hz, H-β). ^{13}C-NMR (d$_6$-DMSO): δ (ppm) 166.9, 158.8, 134.8, 132.4, 129.6, 129.0, 127.3, 120.4, 114.2, 68.9, 57.7.
HRMS (FT-ICR): calcd for C$_{15}$H$_{16}$BNO$_4$: 285,1172, found: 308.1063 [M+Na]+.

_____

5.1.3. Synthesis of compounds 24-27
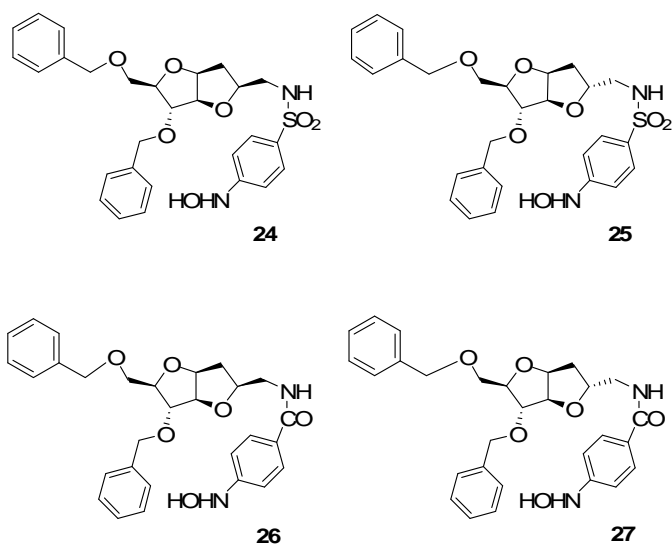
Figure 5-3. Structures of compounds **24-27**.
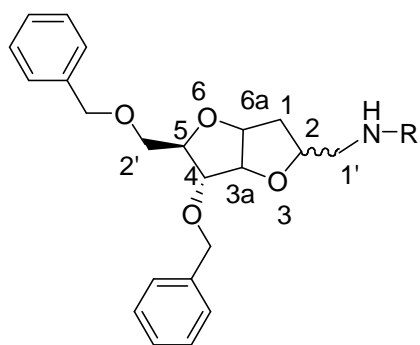
Figure 5-4. Carbon and hydrogen numbering in bicycles **24-27**.

Compound 30
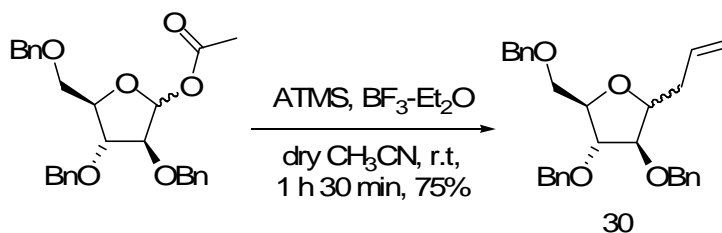
To a stirred solution of **1-*O*-acetyl-2,3,5-tri-*O*-benzyl-D-arabinofuranose** (10.0 g, 21.6 mmol) in dry CH_3CN (75 ml) were added allyltrimethylsilane (6.9 ml, 43.2 mmol) and BF_3Et_2O (2.7 ml, 21.6 mmol) at rt under argon atmosphere. After 1 h 30 min, solid Na_2CO_3 (5 g) was added to the solution to neutralize the acid, the solvent was partly evaporated, and the residue was diluted with CH_2Cl_2 (70 ml). The organic layer was submitted to usual work-up and purified by column flash column chromatography (9.5 : 0.5, petroleum ether–EtOAc) to afford **30** (7.2 g, 75%) as a colorless oil (mixture of α and β anomers; α : β = 1 : 1, as determined from the integration ratio of the ^{1}H-NMR signals). Anomers were not separable by chromatography.

MS(MALDI-TOF): *m/z* 468.7 [M+H+Na][+], 484.5 [M+H+K][+].
Elemental analysis Calc. (%) for $C_{29}H_{32}O_4$: C, 78.35; H, 7.26. Found: C, 77.95; H, 6.48.

Compound 31
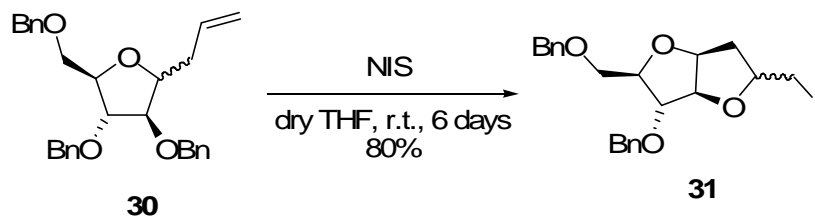
To a solution of **30** (mixture of anomers, 0.436 g, 0.98 mmol) in dry THF (25 ml) was added NIS (0.663 g, 2.95 mmol) at rt under argon atmosphere. The reaction mixture was stirred at this temperature for 6 days. After this time, TLC analysis of the crude product (eluent 9.5 : 0.5, petroleum ether–AcOEt) showed that a part of **30** did not react (α-anomer) and that two disteresomeric iodo derivatives were formed (two very close TLC spots with R_f = 0.3). The crude reaction product was then diluted with CH_2Cl_2 (25 ml), and the organic layer was subjected to usual work-up. The oily residue was purified by flash column chromatography (9.5 : 0.5, petroleum ether–AcOEt) to give **31** (mixture of diastereomers) as a pale yellow oil (0.185 g, 80% calculated on the β-anomer of **30**). The α-anomer of **30** was recovered unchanged.

_____

Compounds 32-R and 32-S

31   **32**
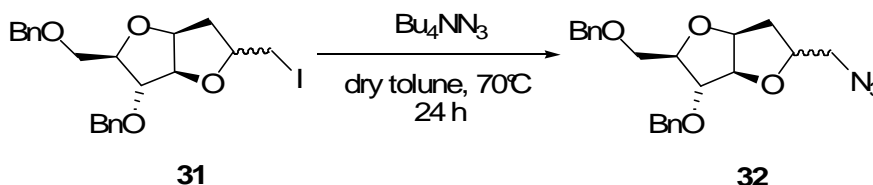
To a solution of **31** (mixture of diastereomers, 1.5 g, 3.15 mmol) was added tetrabutylammonium azide[86] (1.8 g, 6.3 mmol) under argon atmosphere and the mixture was stirred at 70 °C for 24 h. The solv ent was then evaporated *in vacuo*, the residue was diluted with AcOEt, and after usual work-up and flash column chromatography (8 : 2, petroleum ether–AcOEt) the two diastereomers **32-R** and **32-S** were separated and isolated as colorless oils (500 mg of **32-R**, 40%; 250 mg of **32-S**, 20%).

32-R. δ (ppm) (400 MHz; CDCl$_3$; 35°C) 7.4–7.2 (10 H, m, Harom), 4.79 (1 H, br t, J = 5.2, H-6a), 4.71 (1 H, m, H-3a), 4.7–4.5 (4 H, 2ABq, CH$_2$Ph), 4.29 (1 H, m, H-2), 4.03 (1 H, ddd, J = 6.2, J = 6.2, J = 3.8, H-5), 3.86 (1 H, dd, J = 6.2, J = 1.2, H-4), 3.61 (1 H, dd, J = 10.5, J = 3.8, H-2'a), 3.59 (1 H, dd, J = 10.5, J = 6.2, H-2'b), 3.52 (1 H, dd, J = 13.0, J = 3.5, H-1'a), 3.24 (1 H, dd, J = 13.0, J = 3.5, H-1'b), 2.19 (1 H, dd, J = 13.4, J = 5.2, H-1a), 1.78 (1 H, ddd, J = 13.4, J = 10.2, J = 6.3, H-1b); δ (ppm) (300 MHz, CDCl$_3$) 88.72, 85.60, 83.53, 83.35, 77.70, 73.41, 72.10, 70.18, 53.60, 35.82. [α]$_{20}^{D}$ +21.4 (c 1,

---

[86] Tetrabutylammonium azide was prepared from sodium azide according to the following procedure: to a stirred solution azide (228 mg, 3.5 mmol) in water (2 ml) was added Bu$_4$NOH (9.2 ml of a 20% aqueous solution) and the solution was stirred at rt for 30 min. After this time, the aqueous solution was extracted with CH$_2$Cl$_2$ (10 ml × 3), the organic layer was dried (Na$_2$SO$_4$), and the solvent removed *in vacuo* by adding toluene, until a solid powder is obtained. **CAUTION:** Bu$_4$NN$_3$ became explosive when solution was evaporated to dryness and the solid residue was heated.

CHCl$_3$).

MS (MALDI-TOF): m/z 419.2 [M+H+Na]$^+$, 435.0 [M+H+K]$^+$.

C$_{22}$H$_{25}$N$_3$O$_4$ requires C, 66.82; H, 6.37; N, 10.63. Found: C, 67.53; H, 7.01; N, 11.21%.

32-S. δ (ppm) (400 MHz; CDCl$_3$; 35℃) 7.4–7.2 (10 H, m, Ar H), 4.72 (1 H, br t, J 4.4, H-6a), 4.65–4.45 (5 H, m, 2 × CH_2Ph and H-3a), 4.24 (1 H, m, H-2), 4.03 (1 H, ddd, J = 6.0, J = 3.7, H-5), 3.94 (1 H, br d, J **=** 6.0, H-4), 3.65 (1 H, dd, J = 10.3, J = 3.0, H-2'a), 3.58 (1 H, dd, J = 10.3, J = 5.9, H-2_b), 3.48 (1 H, dd, J = 12.5, J = 8.1, H-1'a), 3.16 (1 H, dd, J = 12.5, J **=** 4.0, H-1'b), 2.20 (1 H, ddd, J **=** 14.1, J = 8.4, J = 5.6, H-1a), 1.91 (1 H, m, H-1b); δ (ppm) (300 MHz, CDCl$_3$) 90.00, 85.40, 85.03, 83.63, 80.23, 73.64, 72.57, 70.00, 55.28, 35.80.

[α]$_{20}$ ^{D} +29.3 (*c* 1, CHCl$_3$).

MS (MALDI-TOF): *m/z* 396.4 [M+H]$^+$, 419.6 [M+H+Na]$^+$, 435.3 [M+H+K]$^+$.

C$_{22}$H$_{25}$N$_3$O$_4$ requires C, 66.82; H, 6.37; N, 10.63. Found: C, 66.51; H, 6.81; N, 11.01%.

_____

Compounds 33 and 34
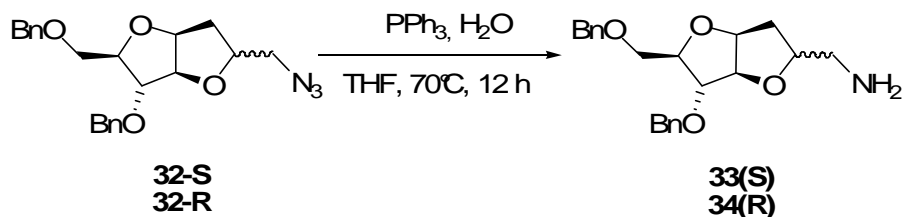
To a solution of azide **32-S** and **32-R** (400 mg, 1.01 mmol) in THF/water 10:1 (44 mL), triphenylphosphine (525 mg, 2.02 mmol) was added and the reaction mixture was stirred at 70 °C for 12 h. The solvents were evaporated and the residue was purified by flash column chromatography (gradient of polarity from AcOEt/MeOH 8:2 to 6:4) obtaining amines **33** and **34** as pale yellow oils (respectively, 354 mg of **33**, 96% yield and 277 mg of **34**, 75% yield).

33. ^{1}H-NMR (CDCl$_3$): δ (ppm) 7.40-7.20 (m, 10 H, H$_{arom}$), 4.70 (bt, 1H, J = 4.5 Hz, H-6a), 4.63-4.50 (2 ABq, 4H, 2 CH$_2$-Ph), 4.45 (m, 1H, H-3a), 4.06 (m, 2H, H-2, H-5), 3.88 (bd, 1H, J = 5.7 Hz, H-2), 3.62 (dd, 1 H, J = 10.3, 3.9 Hz, H-2'a), 3.55 (dd, 1H, J = 10.3,6.0 Hz, H-2'b), 2.80 (m, 2 H, H-1'a, H-1'b), 2.19 (m, 1 H, H-1a), 1.89 (dd, 1 H, J = 13.8, 5.4 Hz, H-1b); ^{13}C-NMR (CDCl$_3$): δ (ppm) 89.2 (C-3a), 85.1 (C-4), 85.0 (C-5), 84.0 (C-6a), 82.7 (C-2), 73.6 (CH$_2$Ph), 72.4 (CH$_2$Ph), 70.5 (C-2'), 46.7 (C-1'), 35.8 (C-1).
MS(MALDI-TOF): *m/z* 371.3 [M+H]$^+$, 393.3 [M+ Na]$^+$.
Elemental analysis calcd (%) for C$_{22}$H$_{27}$NO$_4$: C, 71.52; H, 7.37; N, 3.79, found: C, 71.54; H, 7.32; N, 3.75.

34.^{1}H-NMR (CDCl$_3$): δ (ppm) 7.3-7.1 (m, 10 H, H$_{arom}$), 4.74 (bt, 1H, H-6a), 4.60-4.45 (2 ABq, 4 H, 2 CH$_2$-Ph), 4.59 (m, 1 H, H-3a), 4.08 (m, 1 H, H-2),

4.00 (m, 1 H, H-5), 3.80 (dd, 1 H, J = 6.4, 1.3 Hz, H-4), 3.61 (dd, 1 H, J = 10.4, 3.5 Hz, H-2'a), 3.58 (dd, 1 H, J = 10.4, 6.4 Hz, H-2'b), 2.85 (dd, 1H, J = 13.2, 3.4 Hz, H-1'a), 2.72 (dd, 1 H, J = 13.0, 3.5 Hz, H-1'b), 2.11 (dd, 1H, J = 13.0, 4.8 Hz, H-1a), 1.60 (ddd, 1H, J = 12.7, 9.5, 4.7 Hz, H-1b); ^{13}C-NMR (CDCl$_3$): δ (ppm) 88.7 (C-3a), 86.0 (C-4), 83.7 (C-6a), 83.4 (C-5), 80.3 (C-2), 73.7 (CH$_2$Ph), 72.3 (CH$_2$Ph), 70.5 (C-2'), 45.6 (C-1'), 36.3 (C-1).

MS(MALDI-TOF): m/z: 370.7 [M+H]$^+$, 392.9 [M+Na]$^+$.

Elemental analysis calcd (%) for C$_{22}$H$_{27}$NO$_4$: C, 71.52; H, 7.37; N, 3.79, found: C, 71.51; H, 7.40; N, 3.71.

_____

Compound 35 and 37
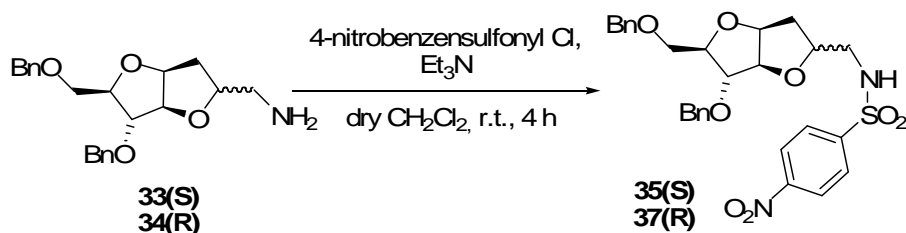
To a solution of amines **33** and **34** (400 mg, 1.1 mmol) in dry dichlorometane (30 mL), p-nitrobenzenesulfonyl chloride (365 mg, 1.65 mmol) and triethylamine (230 µL, 1.65 mmol) were added at 0 ℃ under argon atmosphere. The reaction mixture was allowed to warm at r.t. and stirred for 4 h, after this time the solvent was evaporated and the residue was purified by flash column chromatography (increasing polarity of the eluent from petroleum ether/AcOEt 6:4). Sulfonamides **35** and **37** were obtained as yellow oils (respectively, 585 mg of **35**, 96% yield, 530 mg of **37**, 87% yield).

35. ^{1}H-NMR (CDCl$_3$): δ (ppm) 8.19, 7.95 (A$_2$X$_2$, 4H, H$_{arom}$), 7.44-7.20 (m, 10 H, H$_{arom}$), 6.20 (m, 1H, N*H*), 4.62 (m, 1H, H-6a), 4.60-4.40 (2 ABq, 4 H, 2 C*H$_2$*-Ph), 4.39 (d, 1 H, J = 3.2 Hz, H-3a), 4.24 (m, 1 H, H-2), 4.10-4.00 (m, 2 H, H-5, H-4), 3.79 (dd, 1 H, J = 10.6, 2.3 Hz, H-2'a), 3.48 (dd, 1 H, J = 10.6, 3.6 Hz, H-2'b), 3.19 (m, 1H, H-1'a), 3.09 (m, 1 H, H-1'b), 2.17 (m, 1H, H-1a), 1.98 (dd, 1H, J = 13.4, 3.6 Hz, H-1b); ^{13}C-NMR (CDCl$_3$): δ (ppm) 89.3 (C-3a), 85.9 (C-4), 83.7 (C-6a), 83.6 (C-5), 78.8 (C-2), 73.4 (CH$_2$Ph), 72.6 (CH$_2$Ph), 69.4 (C-2'), 46.7 (C-1'), 34.0 (C-1).
MS(MALDI-TOF): m/z: 577.9 [M+Na]$^+$, 593.7 [M+K]$^+$.
Elemental analysis calcd (%) for C$_{28}$H$_{30}$N$_2$O$_8$S: C, 60.64; H, 5.45; N, 5.05; S, 5.78, found: C, 60.68; H, 5.42; N, 5.03; S, 5.79.

37. ^{1}H-NMR (CDCl$_3$): δ (ppm) 8.30., 8.00 (A$_2$X$_2$, 4H, H$_{arom}$), 7.40-7.20 (m, 10 H, H$_{arom}$), 5.25 (bt, 1H, J = 6.0 Hz, N*H*), 4.73 (bt, 1H, J = 4.4 Hz, H-6a), 4.60-4.40 (2 ABq, 4 H, 2 C*H*$_2$-Ph), 4.52 (m, 1 H, H-3a), 4.12 (m, 1 H, H-2), 3.97 (m, 1 H, H-5), 3.71 (dd, 1 H, J = 6.5, 1.3 Hz, H-4), 3.61 (dd, 1 H, J = 10.5, 3.4 Hz, H-2'a), 3.50 (dd, 1 H, J = 10.4, 6.2 Hz, H-2'b), 3.24 (ddd, 1H, J = 12.8, 5.7, 3.2 Hz, H-1'a), 3.0 (ddd, 1 H, J = 12.5, 6.0, 6.0 Hz, H-1'b), 2.11 (dd, 1H, J = 13.3, 4.9 Hz, H-1a), 1.60 (ddd, 1H, J = 13.5, 10.5, 4.6 Hz, H-1b); ^{13}C-NMR (CDCl$_3$): δ (ppm) 89.0 (C-3a), 85.7 (C-4), 83.5 (C-6a), 83.4 (C-5), 77.0 (C-2), 73.7 (CH$_2$Ph), 72.4 (CH$_2$Ph), 70.2 (C-2'), 46.2 (C-1'), 36.0 (C-1). MS(MALDI-TOF): m/z: 577.9 [M+Na]$^+$, 593.7 [M+K]$^+$.

Elemental analysis calcd (%) for C$_{28}$H$_{30}$N$_2$O$_8$S: C, 60.64; H, 5.45; N, 5.05; S, 5.78, found: C, 60.62; H, 5.48; N, 5.01; S, 5.72.

Compounds 36 and 38

To a solution of amines **33** and **34** (400 mg, 1.1 mmol) in DMF (30 mL), diisopropylamine (564 µL, 3.3 mmol), *N*-hydroxybenzotriazole (220 mg, 1.65 mmol), diisopropylcarbodiimide (260 µL, 1.65 mmol) and *p*-nitrobenzoic acid (220 mg, 1.3 mmol) were added. After stirring for 2 h at r.t., solvent was evaporated *in vacuo* and the residue was purified by flash column chromatography (gradient of polarity starting from petroleum ether/AcOEt 6:4). Amides **36** and **38** were obtained as yellow oils (respectively, 558 mg of **36**, 98% yield and 496 mg of **38**, 87% yield).

36. ^{1}H-NMR (CDCl$_3$): δ (ppm) 8.23, 7.92 (A$_2$X$_2$, 4H, H$_{arom}$), 7.4-7.0 (m, 10 H, H$_{arom}$), 7.40 (bd, 1H, NH), 4.69 (bt, 1H, H-6a), 4.64-4.45 (2 ABq, 4 H, 2 CH_2-Ph), 4.50 (m, 1 H, H-3a), 4.0 (m, 1 H, H-2), 4.05 (m, 2 H, H-5, H-4), 3.77 (m, 2 H, H-1'a, H-2'a), 3.40 (m, 2H, H-1'b, H-2'b), 2.22 (m, 1H, H-1a), 2.11 (dd, 1H, J = 14.7, 4.7 H-1b); ^{13}C-NMR (CDCl$_3$): δ (ppm) 88.8 (C-3a), 86.2 (C-4), 84.4 (C-6a), 83.5 (C-5), 78.5 (C-2), 73.4 (CH$_2$Ph), 72.7 (CH$_2$Ph), 68.8 (C-2'), 43.7 (C-1'), 33.5 (C-1).
MS(MALDI-TOF): *m/z* 502.9 [M-O+H]$^+$, 518.4 [M]$^+$, 541.3 [M+Na]$^+$, 557.8 [M+K]$^+$.
Elemental analysis calcd (%) for C$_{29}$H$_{30}$N$_2$O$_7$: C, 67.17; H, 5.83; N, 5.40, found: C, 67.19; H, 5.81; N, 5.38.

38. ^{1}H-NMR (CDCl$_3$): δ (ppm) 8.23, 7.92 (A$_2$X$_2$, 4H, H$_{arom}$), 7.4-7.2 (m, 10 H, H$_{arom}$), 6.79 (bt, 1H, N*H*), 4.73 (bt, 1H, H-6a), 4.64-4.45 (2 ABq, 4 H, 2 C*H$_2$*-Ph), 4.52 (m, 1 H, H-3a), 4.25 (m, 1 H, H-2), 3.98 (m, 1 H, H-5), 3.80 (bd, 1 H, J = 6.4 Hz, H-4), 3.76 (m, 2 H, H-1'a, H-2'a), 3.52-3.45 (m, 2H, H-1'b, H-2'b), 2.22 (dd, 1H, J = 13.3, 4.8 Hz, H-1a), 1.62 (ddd, 1H, J=13.3, 10.4, 4.8 Hz, H-1b); ^{13}C-NMR (CDCl$_3$): δ (ppm) 89.0 (C-3a), 85.8 (C-4), 83.5 (C-6a), 83.4 (C-5), 77.7 (C-2), 73.7 (CH$_2$Ph), 72.4 (CH$_2$Ph), 70.3 (C-2'), 43.3 (C-1'), 36.6 (C-1).

MS(MALDI-TOF): *m/z*: 502.9 [M-O+H]$^+$, 518.4 [M]$^+$, 541.3 [M+Na]$^+$, 557.8 [M+K]$^+$.

Elemental analysis calcd (%) for C$_{29}$H$_{30}$N$_2$O$_7$: C, 67.17; H, 5.83; N, 5.40, found: C, 67.12; H, 5.87; N, 5.43.

_____

Compound 24-27
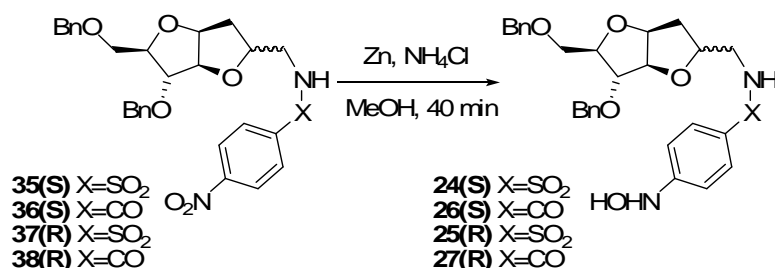
To a solution of nitro-derivatives **35**, **36**, **37,** or **38** (1.1 mmol) in methanol (20 mL), zinc (143 mg, 2.2 mmol) and ammonium chloride (87 mg, 1.65 mmol) were added, the suspension was stirred for 40 min, then filtered on sintered glass with celite layer, solvent were evaporated and the residue was purified by flash column chromatography (increasing polarity of the eluent from petroleum ether/THF 6:4). Compounds **24**, **25**, **26**, **27** were obtained as oils (respectively, 529 mg of **24**, 89% yield, 552 mg of **25**, 93% yield, 482 mg of **26**, 87% yield, 300 mg of **27**, 54% yield).

24. ^{1}H-NMR (CDCl$_3$): δ (ppm) 7.48, 6.80 (A$_2$X$_2$, 4H, H$_{arom}$), 7.40-7.20 (m, 10 H, H$_{arom}$), 5.45 (bt, 1H, J = 5.4 Hz, N*H*), 4.52 (m, 1H, H-6a), 4.60-4.40 (2 ABq, 4 H, 2 C*H*$_2$-Ph), 4.49 (m, 1 H, H-3a), 4.19 (m, 1 H, H-2), 4.01 (m, 1 H, H-5), 3.83 (d, 1 H, J= 5.8 Hz, H-4), 3.62 (dd, 1 H, J = 10.5, 3.3 Hz, H-2'a), 3.42 (dd, 1 H, J = 10.5, 5.4 Hz, H-2'b), 3.10 (m, 1H, H-1'a), 2.98 (m, 1 H, H-1'b), 2.09 (m, 1H, H-1a), 1.90 (dd, 1H, J = 13.5, 4.6 Hz, H-1b); ^{13}C-NMR (CDCl$_3$): δ (ppm) 89.4 (C-3a), 85.4 (C-4), 84.5 (C-6a), 83.8 (C-5), 79.2 (C-2), 73.5 (CH$_2$Ph), 72.4 (CH$_2$Ph), 69.8 (C-2'), 46.9 (C-1'), 34.7 (C-1). (MALDI-TOF): *m/z* 563.6 [M+Na]$^+$, 579.5 [M+K]$^+$. Elemental analysis calcd (%) for C$_{28}$H$_{32}$N$_2$O$_7$S: C, 62.21; H, 5.97; N, 5.18; S, 5,93, found: C, 62.42; H, 6.02; N, 5.20; S, 5.92.

25. ^{1}H-NMR (CDCl$_3$): δ (ppm) 7.50, 6.70 (A$_2$X$_2$, 4H, H$_{arom}$), 7.40-7.20 (m, 10 H, H$_{arom}$), 4.61 (bt, 1H, J = 4.6 Hz, H-6a), 4.60-4.40 (2 ABq, 4 H, 2 CH_2-Ph), 4.42 (m, 1 H, H-3a), 4.01 (m, 1 H, H-2), 3.85 (m, 1 H, H-5), 3.60 (dd, 1 H, J = 7.5, 1.4 Hz, H-4), 3.51 (dd, 1 H, J = 10.4, 3.6 Hz, H-2'a), 3.43 (dd, 1 H, J = 10.4, 6.3 Hz, H-2'b), 3.09 (m, 1H, H-1'a), 2.85 (m, 1 H, H-1'b), 1.99 (dd, 1H, J = 13.6, 5.1 Hz, H-1a), 1.60 (m, 1H, H-1b); ^{13}C-NMR (CDCl$_3$): δ (ppm) 88.9 (C-3a), 85.8 (C-4), 83.6 (C-6a), 83.3 (C-5), 77.1 (C-2), 73.7 (CH$_2$Ph), 72.4 (CH$_2$Ph), 70.2 (C-2'), 46.0 (C-1'), 36.0 (C-1). MS(MALDI-TOF): m/z 563.3 [M+Na]$^+$, 579.1 [M+K]$^+$. Elemental analysis calcd (%) for C$_{28}$H$_{32}$N$_2$O$_7$S: C, 62.21; H, 5.97; N, 5.18; S, 5,93, found: C, 62.16; H, 6.01; N, 5.15; S, 5.93.

26. ^{1}H-NMR (d$_6$-DMSO): δ (ppm) 8.66 (bd, 1 H, NHOH), 7.70 (bd,1 H, NHOH), 7.70-6.80 (A$_2$X$_2$, 4H, H$_{arom}$), 7.40-7.20 (m, 10 H, H$_{arom}$), 5.47 (bd, 1H, NH), 4.56 (m, 1H, H-6a), 4.60-4.40 (2 ABq, 4 H, 2 CH_2-Ph), 4.47 (m, 1 H, H-3a), 4.12 (m, 1 H, H-2), 3.83 (m, 1 H, H-5), 3.74 (dd, 1 H, J = 6.2, 1.5 Hz, H-4), 3.60-3.30 (m, 4 H, H-2'a, H-2'b, H-1'a, H-1'b), 2.03 (dd, 1H, J = 13.3, 4.9 Hz, H-1a), 1.60 (ddd, 1H, J = 13.5, 10.5, 4.6 Hz, H-1b); ^{13}C-NMR (d$_6$-DMSO): δ (ppm) 88.7 (C-3a), 85.6 (C-4), 83.4(C-6a), 83.4 (C-5), 78.0 (C-2), 73.0 (CH$_2$Ph), 71.7 (CH$_2$Ph), 70.6 (C-2'), 42.6 (C-1'), 35.2 (C-1). MS(MALDI-TOF): m/z 505.2 [M+H]$^+$, 527.1 [M+Na]$^+$, 543.3 [M+K]$^+$. Elemental analysis calcd (%) for C$_{29}$H$_{32}$N$_2$O$_6$: C, 69.03; H, 6.39; N, 5.55, found: C, 69.07; H, 6.41; N, 5.56.

27. ^{1}H-NMR (d$_6$-DMSO): δ (ppm) 8.66 (bs, 1 H, NHO), 8.49 (bs, 1H, NOH), 7.70-6.80 (A$_2$X$_2$, 4H, H$_{arom}$), 7.30 (m, 10 H, H$_{arom}$), 5.47 (bd, 1H, NH), 4.56 (m, 1H, H-6a), 4.46 (m, 1H, H-3a), 4.60-4.40 (2 ABq, 4 H, 2 CH_2-Ph), 4.12 (m, 1 H, H-2), 3.83 (m, 1 H, H-5), 3.74 (dd, 1 H, J = 6.2, 1.5 Hz, H-4), 3.60-3.30 (m, 4 H, H-2'a, H-2'b, H-1'a, H-1'b), 2.01 (dd, 1H, J = 13.3, 4.9 Hz, H-1a), 1.60 (m, 1H, H-1b); ^{13}C-NMR (d$_6$-DMSO): δ (ppm) 88.2 (C-3a), 85.6 (C-4), 83.4(C-6a), 83.4 (C-5), 78.0 (C-2), 72.9 (CH$_2$Ph), 71.7 (CH$_2$Ph), 70.6 (C-2'), 41.5 (C-1'), 35.2 (C-1). MS(MALDI-TOF): m/z 505.5 [M+H]$^+$, 527.4 [M+Na]$^+$, 543.5 [M+K]$^+$. Elemental analysis calcd (%) for C$_{29}$H$_{32}$N$_2$O$_6$: C, 69.03; H, 6.39; N, 5.55, found: C, 69.02; H, 6.37; N, 5.53.

5.1.3. Synthesis of compounds 39-44
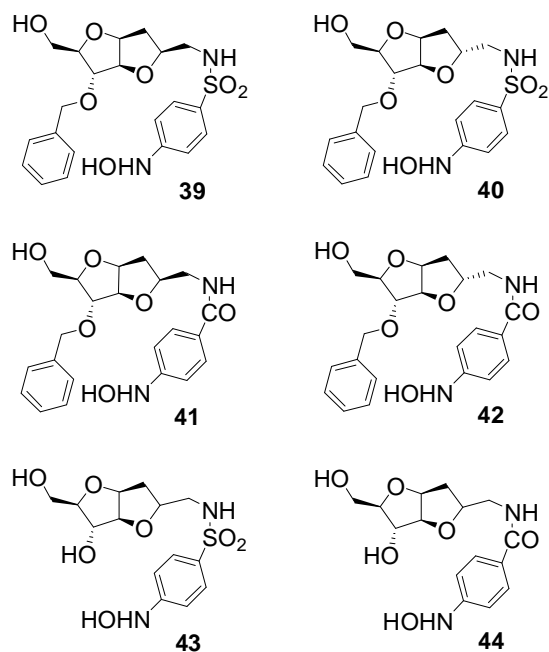
Figure 5-5. Structures of compounds **39**-**44**.
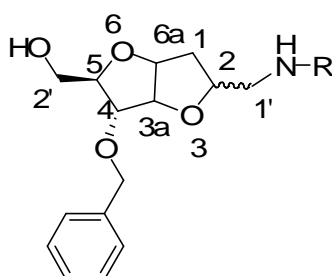
Figure 5-6. Carbon and hydrogen numbering in bicycles **39-44**.

Compound 46
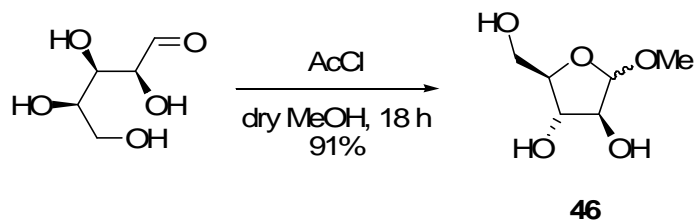
To a stirred suspension of **D-arabinose** (5 g, 33.304 mmol) in dry CH_3OH (200 ml), acetyl chloride was added dropwise at room temperature under argon atmosphere. After 24 h, Amberlite IRN78 OH⁻ resin was added to neutralise the acid and the mixture was stirred for 5 min. The resin was removed by filtering and the solvent was evaporated. The product was purified by flash column chromatography (9.75:0.25 EtOAc:CH_3OH) affording **46** (4.96 g, 90% yield) as a yellow oil (mixture of α and β anomers).[87]

---

[87] A. S. Seriani, R. Barker, *J. Org. Chem.* **1984**, 49, 3292–3300.

_____

Compound 47

46 → **47**

a. BTSFA, dry CH₃OH, 100 ℃, 3 h
b. ATMS, TMSOTf, dry CH₃OH, r.t., 1h

c. H₂O, r.t., 30 min
97%
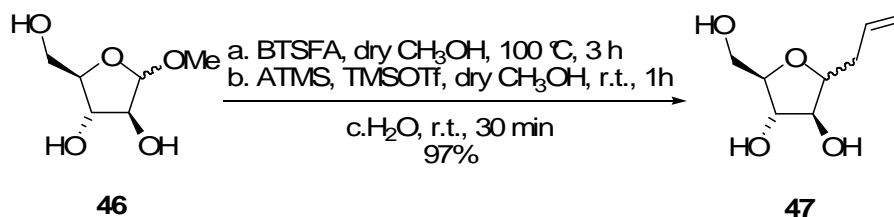
To a stirred solution of methyl D-arabinofuranoside **46** (4.5 g, 27.41 mmol) in dry CH$_3$CN (9 ml), BTSFA (16.3 mL, 61.670 mmol) was added at 100 ℃ under argon atmosphere (balloon). After 3 h, the reaction mixture was allowed to cool to room temperature; ATMS (6.5 ml, 41.115 mmol) and trimethylsilyl trifluorometanesulfonate (TMSOTf) (2.5 ml, 13.705 mmol) were added at 0℃ and reaction was stirred at room tempe rature for 1 h. Water (120 mL) was added slowly to hydrolyze TMS ethers, than the mixture was neutralised with 1M NaOH and concentrated *in vacuo.* The product was purified by flash column chromatography (1:9 petroleum ether:EtOAc) providing **47** (4.65 g, 97% yield) as a light green oil (mixture of α and β anomers; α:β 1:1.5, as determined from the integration ratio of the ¹H-NMR signals).

α anomer: ¹H-NMR (CD$_3$OD) δ (ppm) 5.88 (tdd, 1 H, J = 16.0, 6.9, 2.1 Hz), 5.12 (ddd, 1H, J = 17.2, 3.6, 1.5 Hz), 5.06 (m, 1H), 3.95 (m, 1H), 3.79 (m, 3H), 3.68 (dd, 1H, J = 11.7, 3.4Hz), 3.60 (dd, 1H, J = 11.8, 5.4Hz), 2.39 (m, 2H); ¹³C-NMR (100 MHz, CD$_3$OD) δ (ppm) 135.5, 117.4, 84.7, 83.6, 81.6, 78.8, 63.3, 38.7.

β anomer: ¹H-NMR (CD$_3$OD): δ (ppm) 5.87 (tdd, 1H, J = 17.2, 10.2, 7.0 Hz), 5.13 (ddd, 1H, J = 17.2, 3.5, 1.5Hz), 5.03 (m, 1H), 3.97 (m, 1H), 3.95 (dd,

1H, J=7.0, 3.2Hz), 3.82 (dd, 1H, J = 1.0Hz, 3.0Hz), 3.75 (ddd, 1H, J = 2.6Hz, 3.8Hz, 4.8Hz), 3.67 (dd, 1H, J = 3.8Hz, 11.4Hz), 3.64 (dd, 1H, J = 4.9Hz, 11.4Hz), 2.40 (m, 2H); ^{13}C-NMR (CD$_3$OD): δ (ppm) 135.9, 117.1, 87.3, 82.5, 80.3, 78.5, 63.5, 34.3.

HRMS (FT-ICR): calcd for C$_8$H$_{14}$O$_4$Na: 197.0790; found:197.0811 [M + Na]$^+$. The following signal attributions were obtained from the spectra of the mixture.

_____

Compound 48
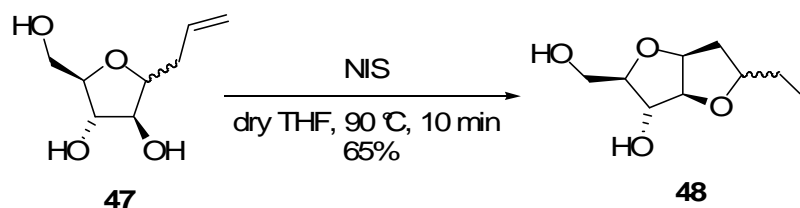
To a stirred solution of **47** (mixture of anomers, 4 g, 22.96 mmol) in dry THF (200 mL) NIS (7.7 g, 34.44 mmol) was added at 90℃ under argon atmosphere. After 10 min, β anomer reacted completely according to TLC analysis (eluent: 3:7 petroleum ether/EtOAc), while α anomer did not, as expected. The mixture was allowed to cool to room temperature, $Na_2S_2O_3$ was added to reduce excess iodine and the suspension was vigorously stirred until it became colourless. The product was purified by flash column chromatography (2:8 petroleum ether/EtOAc) to give **48** (4 g, 58% yield) as a light green oil (mixture of diastereomers, R/S 2.5:1, as determined from the integration ratio of the ^{1}H-NMR signals). The α anomer was recovered unreacted. The following signal attributions were obtained from the spectra of the mixture.

(48-R) ^{1}H-NMR (CD₃OD) δ (ppm) 4.73 (bt, 1H, J = 4.3 Hz, 6a-H), 4.47 (dd, 1H, J = 4.2, 1.6 Hz, 3a-H), 4.04 (m, 1H, 2-H), 3.94 (dd, 1H, J = 5.3, 1.4 Hz, 4-H), 3.70 (m, 2H, 5-H, 2'a-H), 3.58 (dd, 1H, J = 12.5, 7.1 Hz, 2'b-H), 3.32 (m, 2H, 1'a-H, 1'b-H), 2.28 (dd, 1H, J = 13.6, 5.3 Hz, 1a-H), 1.67 (ddd, 1H, J = 13.7, 9.6, 4.6 Hz, 1b-H); ^{13}C-NMR (CD₃OD) δ (ppm) 92.6, 87.9, 84.3, 79.2, 78.6, 63.0, 40.5, 9.7.

(48-S) ^{1}H-NMR (CD₃OD), selected signals: δ (ppm) 4.35 (dd, 1H, H-3a, J =

4.3, 1.1 Hz), 4.20 (m, 1H, H-2), 3.63 (dd, 1H, J = 12.5, 7.0 Hz, 2'b-H), 2.03 (dd, 1H, J = 14.0, 4.4 Hz, 1b-H); ^{13}C-NMR (CD$_3$OD) δ (ppm) 93.7, 89.3, 84.5, 82.1, 78.5, 63.2, 38.8, 10.3.

HRMS (FT-ICR): calcd for C$_8$H$_{13}$IO$_4$Na: 322.9756; found:.322.9743 [M+Na]$^+$. Elemental anal. calcd for C$_8$H$_{13}$IO$_4$ (322.97): C 32.02%; H 4.37%; found: C 32.11%; H 4.30%.

_____

Compound 49
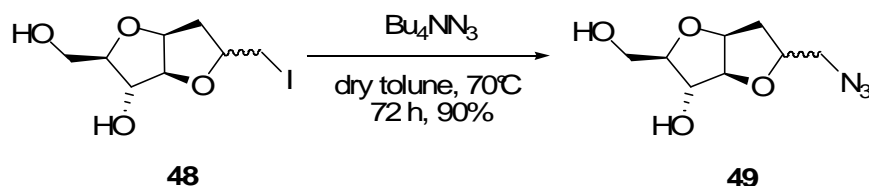
To a stirred solution of **48** (mixture of diastereomers, 2.2 g, 7.33 mmol) in dry DMF (35 mL) tetrabutylammonium azide was added at 70 ℃ under argon atmosphere. After 72 h, the reaction mixture was concentrated in vacuo without heating. The product was purified by flash column chromatography (2:8 petroleum ether/EtOAc) recovering **49** (1.41 g, 90% yield) as a yellow oil (mixture of diastereomers, R:S 2.5:1, as determined from the integration ratio of the ^{1}H-NMR signals).

(49-R) ^{1}H-NMR (CD$_3$OD): δ (ppm) 4.73 (bt, 1H, J = 4.4Hz, 6a-H), 4.44 (dd, 1H, J = 4.2, 1.6 Hz, 3a-H), 4.28 (m, 1H, 2-H), 3.97 (dd, 1H, J = 5.3, 1.4 Hz, 4-H), 3.73-3.69 (m, 2H, H-2'a, 5-H), 3.59 (dd, 1H, J = 12.5, 7.0 Hz, 2'b-H), 3.48 (dd, 1H, J = 13.1, 3.3 Hz, 1'a-H), 3.21 (dd, 1H, J = 13.1, 5.4 Hz, 1'b-H) 2.10 (dd, 1H, J = 13.4, 5.4 Hz, 1a-H), 1.78 (ddd, 1H, J = 13.4, 10.0, 4.7 Hz, 1b-H); ^{13}C-NMR (CD$_3$OD): δ (ppm) 92.3, 88.0, 84.2, 79.1, 78.6, 63.1, 54.7, 36.7.

(49-S) ^{1}H-NMR (CD$_3$OD): δ (ppm) 4.69 (bt, 1H, J = 5.0 Hz, 6a-H), 4.32 (d, 1H, J = 4.1 Hz, 3a-H), 4.18 (m, 1H, 2-H), 4.04 (d, 1H, J = 5.5 Hz, 4-H), 3.73-3.69 (m, 2H, 2'a-H, 5-H), 3.65 (dd, 1H, J = 11.8, 6.4 Hz, 2'b-H), 3.49 (dd, 1H, 1'a-H), 3.27 (dd, 1H, J = 12.9, 3.8 Hz, 1'b-H), 2.25 (ddd, 1H, J = 14.1, 8.4, 6.0 Hz, 1a-H) 1.88 (dd, 1H, J = 14.1, 5.3 Hz, 1b-H); ^{13}C-NMR (CD$_3$OD): δ (ppm) 93.4, 89.7, 84.3, 81.0, 78.3, 63.2, 55.8, 36.4.

HRMS (FT-ICR): calcd for $C_8H_{13}N_3O_4Na$: 238.0804; found: 238.0789 $[M+Na]^+$.

Elemental anal. calcd for $C_8H_{13}N_3O_4$ (238.08): C 44.65%; H 6.09%; N 19.53%; found: C 44.59%; H 6.12%; N 19.49%.

_____

Compound 50
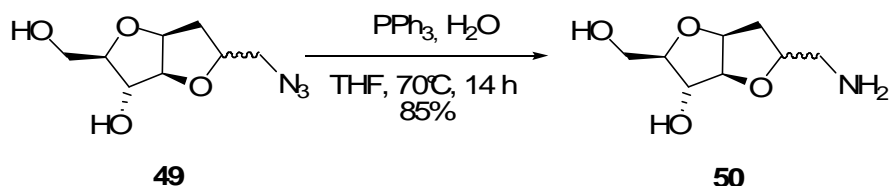
A solution of **49** (mixture of diastereomers, 500 mg, 2.35 mmol) in THF (20 ml) was treated with triphenylphosphine (1.86 g, 6.97 mmol) and H_2O (1.7 ml, 93 mmol) and was stirred at 60 °C overnight. Th e reaction mixture was concentrated in vacuo. The product was purified by flash column chromatography (8:2 EtOAc/CH_3OH, 1% TEA) affording **50** (377 mg, 85% yield) as a yellow oil (mixture of diastereomers, R:S 2:1, as determined from the integration ratio of the ^{1}H-NMR signals).

(50-R) ^{1}H-NMR (CD$_3$OD): δ (ppm) 4.71 (bt, 1H, J = 4.6 Hz, 6a-H), 4.42 (dd, 1H, J = 4.3, 1.8 Hz, 3a-H), 4.09 (m, 1H, 2-H), 3.94 (dd, 1H, J = 5.8, 1.8 Hz, 4-H), 3.88-3.57 (m, 3H, 2'a-H, 2'b-Hb, 5-H), 2.81 (dd, 1H, J = 13.1, 3.9 Hz, 1'a-H), 2.68 (dd, 1H, J = 13.1, 6.8 Hz, 1'b-H), 2.09 (dd, 1H, J = 13.4, 5.1 Hz, 1a-H), 1.61 (ddd, 1H, J = 13.5, 10.3, 4.8 Hz, 1b-H); ^{13}C-NMR (CD$_3$OD): δ (ppm) 91.9, 87.6, 84.1, 80.3, 78.6, 63.0, 45.8, 37.2.

(50-S) ^{1}H-NMR (CD$_3$OD) selected signals: δ (ppm) 4.68 (bt, 1H, J = 4.4 Hz, 6a-H), 4.28 (d, 1H, J = 4.3 Hz, 3a-H), 2.85 (dd, 1H, J = 13.2, 6.2 Hz, 1'a-H), 2.27 (ddd, 1H, J = 14.2, 8.4, 6.0 Hz, 1a-H) 1.85 (dd, 1H, J = 14.4, 5.9 Hz, 1b-H). ^{13}C-NMR (CD$_3$OD): δ (ppm) 92.9, 89.8, 84.4, 81.7, 77.8, 63.0, 46.3, 36.3.

HRMS (FT-ICR): calcd for $C_8H_{15}NO_4Na$: 212.0899; found: 212.0911

$[M+Na]^+$.

Elemental anal. calcd for $C_8H_{15}NO_4$ (212.08): C 50.78%; H 7.99%; N 7.40%; found: C 50.82%; H 7.90%; N 7.49%.

_____

Compound 51

To a stirred solution of **49** (mixture of diastereomers, 700 mg, 3.25 mmol) in dry DMF, benzyl bromide (1.55 ml, 13.018 mmol) and NaH (60% in oil, 520 mg, 13.01 mmol) were added in three portions, over a period of 20 min, at room temperature. After 15 min, the reaction was quenched by adding ethanol and the solvents were evaporated. The product was purified by flash column chromatography (9.25:0.75 petroleum ether/EtOAc) obtaining **51** (1.25 g, 90.5% yield) as yellow oils (mixture of distereomers, R:S 2:1 as determined from the integration ratio of the ^{1}H-NMR signals).

(51-R) ^{1}H-NMR (CDCl$_3$): δ (ppm) 7.4-7.2 (m, 10H, aromatic protons), 4.79 (bt, 1 H, J = 5.2Hz, 6a-H), 4.71 (m, 1H, 3a-H), 4.7-4.5 (2AB$_q$, 4H, benzyl), 4.29 (m, 1H, 2-H), 4.03 (ddd, 1H, J = 6.2, 6.2, 3.8 Hz, 5-H), 3.86 (dd, 1H, J = 6.2, 1.2 Hz, 4-H), 3.61 (dd, 1H, J = 10.5, 3.8 Hz, 2'a-H), 3.59 (dd, 1H, J = 10.5, 6.2 Hz, 2'b-H), 3.52 (dd, 1H, J = 13.0, 3.5 Hz, 1'a-H), 3.24 (dd, 1H, J = 13.0, 3.5 Hz, 1'b-H), 2.19 (dd, 1H, J = 13.4, 5.2 Hz, 1a-H), 1.78 (ddd, 1H, J = 13.4, 10.2, 6.3 Hz, 1b-H); ^{13}C-NMR (CDCl$_3$): δ (ppm) 88.72, 85.60, 83.53, 83.35, 77.70, 73.41, 72.10, 70.18, 53.60, 35.82.

(51-S) ^{1}H-NMR (CDCl$_3$): δ (ppm) 7.4-7.2 (m, 10H, aromatic protons), 4.72 (bt, 1H, J = 4.4 Hz, 6a-H), 4.65-4.45 (m, 5H, 3a-H, benzyl), 4.24 (m, 1H, 2-H), 4.03 (ddd, 1H, J = 6.0, 3.7 Hz, 5-H), 3.94 (bd, 1H, J = 6.0 Hz, 4-H), 3.65 (dd, 1H, J = 10.3, 3.0 Hz, 2'a-H), 3.58 (dd, 1H, J = 10.3, 5.9 Hz, 2'b-H), 3.48

(dd, 1H, J = 12.5, 8.1 Hz, 1'a-H), 3.16 (dd, 1H, J = 12.5, 4.0 Hz, 1'b-H), 2.20 (ddd, 1H, J = 14.1, 8.4, 5.6 Hz, 1a-H) 1.91 (m, 1H, 1b-H); ^{13}C-NMR (CDCl$_3$): δ (ppm) 90.00, 85.40, 85.03, 83.63, 80.23, 73.64, 72.57, 70.00, 55.28, 35.80.

HRMS (FT-ICR): calcd for C$_{22}$H$_{25}$N$_3$O$_4$Na: 418.1743; found: 418.1735 [M+Na]$^+$.

Elemental anal. calcd for C$_{22}$H$_{25}$N$_3$O$_4$ (418.17): C, 66.82%; H, 6.37%; N, 10.63%; found: C, 67.53%; H, 7.01%; N, 11.21%.

_____

Compound 52
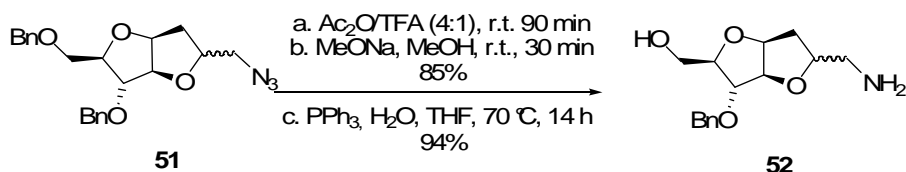
A solution of **51** (740 mg, 1.87 mmol) in 4:1 Ac$_2$O/TFA (16 mL) was stirred at room temperature for 90 min. After this time, reaction was quenched by adding a mixture of ice and 1M NaOH and the product extracted with AcOEt. After usual workup, the crude mixture was recovered as a yellow oil. The crude mixture was in dry MeOH (30 mL) and Na metallic was added in catalytic amount under argon atmosphere. The solution was stirred at room temperature for 30 min. After this time Amberlite IRA-120 H$^+$ resin was added and the mixture was stirred for 10 min. Then resin was removed by filtering and the solvent was evaporated. After usual workup and chromatography (5.5:4.5 petroleum ether/AcOEt), a mixture of **(2R, 3aS, 4R, 5R, 6aS) and (2S, 3aS, 4R, 5R, 6aS)-2-Azidomethyl-4-benzyloxy-5-methoxy-hexahydro-furo[3,2-b]furan** (R:S 2:1, as determined from the integration ratio of the ^{1}H-NMR signals) was provided as a colourless oil (463 mg, 84.5% yield for the two steps). To a solution of this diastereomeric mixture (450 mg, 1.473 mmol) in THF (15 mL), triphenylphosphine (1.18 g, 4.420 mmol) and water (1 ml, 59 mmol) were added and the reaction was stirred at 60 °C overnight. The reaction mixture was concentrated *in vacuo*. The product was purified by flash column chromatography (gradient of polarity from 7.5.2.5 EtOAc/MeOH with 1% TEA, to 1:1 EtOAc/MeOH with 1% TEA), affording **52** (377 mg, 94% yield) as colourless oil (mixture of diastereomers, R:S 2:1, as determined from the integration ratio of the ^{1}H-NMR signals).

(52-R) ^{1}H-NMR (CD$_3$OD): δ (ppm) 7.34-7.32 (m, 5H, aromatic protons), 4.71 (t, 1H, J = 4.5 Hz, 6a-H), 4.68, 4.55 (ABq, 2H, J = 11.7 Hz, benzyl), 4.59 (dd, 1H, J = 1.1, 4.3 Hz, 3a-H), 4.09 (m, 1H, 2-H), 3.90-3.79 (m, 2H, 4-H, 5-H), 3.69 (dd, 1H, J = 11.8, 3.2 Hz, 2'a-H), 3.58 (dd, 1H, J = 11.7, 5.4 Hz, 2'b-H), 2.78 (dd, 1H, J = 13.2, 3.9 Hz, 1'a-H), 2.66 (dd, 1H, J = 13.2, 6.6 Hz, 1'b-H), 2.08 (dd, 1H, J = 13.4, 5.0 Hz, 1a-H), 1.61 (ddd, 1H, J = 13.5, 10.3, 4.7 Hz, 1b-H); ^{13}C-NMR (CD$_3$OD): δ (ppm) 139.1, 129.2, 128.8, 128.6, 128.6, 89.6, 86.3, 86.0, 84.6, 80.9, 72.89, 63.1, 45.9, 37.1.

(52-S) ^{1}H-NMR (CD$_3$OD) selected signals: δ (ppm) 4.44 (d, 1H, J = 4.0 Hz, 3a-H), 2.24 (ddd, 1H, J = 14.0, 8.3, 6.1 Hz, 1a-H), 1.83 (dd, 1H, J = 13.9, 4.9 Hz, 1b-H); ^{13}C-NMR (CD$_3$OD) selected signals: δ (ppm) 139.06, 90.1, 87.9, 85.6, 84.9, 82.7, 72.94, 63.2, 46.7, 36.3.

HRMS (FT-ICR): calcd for C$_{15}$H$_{21}$NO$_4$Na: 302.1368; found: 302.1354 [M+Na]$^+$.

Elemental anal. calcd for C$_{15}$H$_{21}$NO$_4$ (302.13): C 64.50%; H 7.58%; N 5.01%; found: C 64.45%; H 7.53%; N 5.08%.

Compound 53
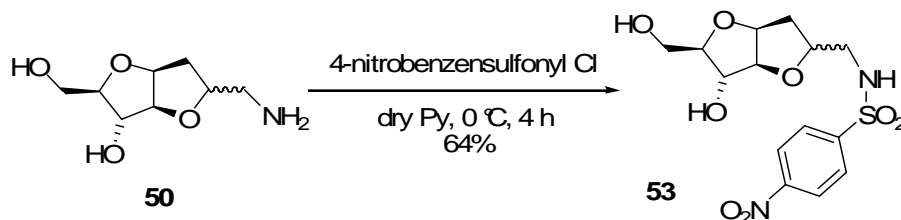
To a stirred solution of **50** (180 mg, 0.951 mmol) in dry Pyridine (13.5 ml) *p*-nitrobenzensulfonyl chloride were added at 0°C unde r argon atmosphere. After 6 h, the reaction was quenched by adding CH_3OH. The solvents were evaporated *in vacuo* and, after flash-chromatography (1:9 petroleum ether/EtOAc), **53** (228 mg, 64% yield) was recovered as pale yellow oil (diastereomeric mixture, R:S 3:1, as determined from the integration ratio of the ^{1}H-NMR signals).

(53-R) ^{1}H-NMR (CD$_3$OD): δ (ppm) 8.39, 8.07 (AA'XX', 4H, J = 8.8 Hz, aromatic protons), 4.65 (bt, 1H, J = 4.5 Hz, 6a-H), 4.28 (dd, 1H, J = 4.3, 1.8 Hz, 3a-H), 4.06 (m, 1H, 2-H), 3.81 (dd, 1H, J = 5.5, 1.5 Hz, 4-H), 3.68-3.61 (m, 2H, 2'a-H, 5-H), 3.50 (dd, 1H, J = 12.5, 7.1 Hz, 2'b-H), 3.15 (dd, 1H, J = 13.6, 3.9 Hz, 1'a-H), 3.02 (dd, 1H, J = 13.6, 5.8 Hz, 1'b-H), 2.04 (dd, 1H, J = 13.5, 5.2 Hz, 1a-H), 1.65 (ddd, 1H, J = 13.5, 10.1, 4.8 Hz, 1b-H); ^{13}C-NMR (CDCl$_3$): δ (ppm) 151.1, 147.9, 129.2, 125.2, 92.1, 87.8, 84.0, 78.6, 78.5, 63.0, 47.2, 37.0.

(53-S) ^{1}H-NMR (CD$_3$OD) selected signals: δ (ppm) 4.62 (bt, 1H, J = 4.6 Hz, 6a-H), 4.22 (d, 1H, J = 4.0 Hz, 3a-H), 3.95 (d, 1H, J = 5.3 Hz, 4-H), 3.54 (dd, 1H, J = 11.7, 5.8 Hz, 2'b-H), 2.18 (ddd, 1H, J = 14.1, 8.4, 5.8 Hz, 1a-H), 1.84 (dd, 1H, J = 14.1, 4.8 Hz, 1b-H); ^{13}C-NMR (CDCl$_3$) selected signals: δ (ppm) 129.2, 93.2, 89.7, 84.4, 80.4, 78.1, 63.2, 36.3.

HRMS (FT-ICR): calcd for $C_{14}H_{18}N_2O_8SNa$: 397.0682; found: 397.0674 $[M+Na]^+$.

Elemental anal. calcd for $C_{14}H_{18}N_2O_8S$ (397.06): C 44.92%; H 4.85%; N 7.48%; found: C 44.95%; H 4.89%; N 7.39%.

Compound 54
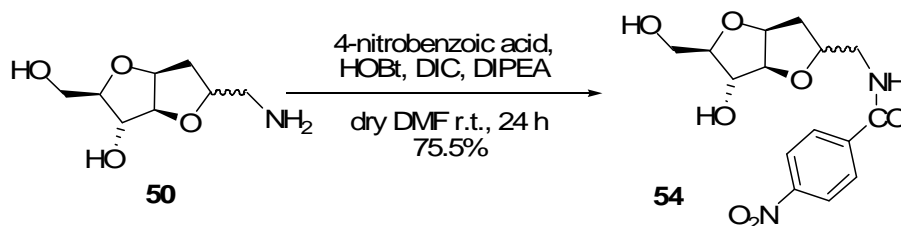
To a stirred solution of **50** (200 mg, 1.057 mmol) in dry DMF (16 ml) HOBt (214 mg, 1.585 mmol), DIPEA (545 μl, 3.171 mmol) and *p*-nitrobenzoic acid (212 mg, 1.268 mmol) were added under argon atmosphere; DIC (246 μl, 1.585 mmol) was added at 0°C and the reaction was stirred at room temperature for 24 h. After this time, the solvent was concentrated *in vacuo* and the product was purified by flash column chromatography (8.5:1.5 toluene:CH$_3$OH) affording **54** (270 mg, 75.5% yield) as a pale yellow oil (mixture of diastereomers, *R*:*S* 2:1, as determined from the integration ratio of the ^{1}H-NMR signals).

(54-R) ^{1}H-NMR (CD$_3$OD): δ (ppm) 8.27, 7.99 (AA'XX', 4H, *J*=8.9 Hz, aromatic protons), 4.72 (bt, 1H, *J*=4.7 Hz, 6a-H), 4.47 (dd, 1H, *J*=4.4, 1.9 Hz, 3a-H), 4.29 (m, 1H, 2-H), 3.96 (dd, 1H, *J*=5.8, 1.8 Hz, 4-H), 3.74-3.65 (m, 3H), 3.62-3.47 (m, 2H, 1'a-H, 1'b-H), 2.17 (dd, 1H, *J*=13.4, 5.2 Hz, 1a-H), 1.68 (ddd, 1H, J=13.5, 10.1, 4.8 Hz, 1b-H); ^{13}C-NMR (CDCl$_3$): δ (ppm) 167.8, 150.6, 140.9, 129.4, 124.3, 92.0, 87.6, 83.9, 78.5, 78.4, 62.9, 44.4, 37.6.

(54-S) ^{1}H-NMR (CD$_3$OD) selected signals: δ (ppm) 4.69 (bt, 1H, *J*=5.2Hz, 6a-H), 4.12 (d, 1H, *J*=5.1 Hz, 3a-H), 2.28 (ddd, 1H, *J*=14.1, 8.5, 5.8 Hz, 1a-H), 1.95 (dd, 1H, J=14.1, 5.2 Hz, 1b-H); ^{13}C-NMR (CDCl$_3$): δ (ppm) 168.1,

150.5, 141.2, 129.6, 124.2, 93.0, 89.7, 84.5, 80.0, 77.9, 62.9, 45.2, 36.0.

HRMS (FT-ICR): calcd for $C_{15}H_{18}N_2O_7Na$: 361.1012; found: 361.1033 $[M+Na]^+$.

Elemental anal. calcd for $C_{15}H_{18}N_2O_7$ (361.10): C 53.25%; H 5.36%; N 8.28%; found: C 53.19%; H 5.29%; N 8.36%.

Compounds 55 and 56
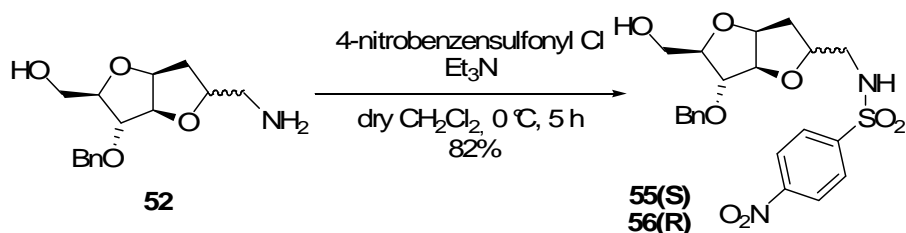
To a stirred solution of **52** (15 mg, 0.053 mmol) in dry CH_2Cl_2 (0.7 ml) TEA (9 µl, 0.064 mmol) and *p*-nitrobenzensulfonyl chloride were added at 0℃ und er argon atmosphere. After 5 h, the reaction was quenched by adding MeOH. The solvents were evaporated in vacuo and, after flash-chromatography (1:1 petroleum ether/EtOAc), pure compounds **55** (*S* diastereomer, 5 mg, 20% yield) and **56** (*R* diasteremer, 15 mg, 60% yield) were purified and separated as pale yellow oils.

(55) ^{1}H-NMR (CDCl₃): δ (ppm) 8.31, 8.04 (AA'XX', 4H, J = 8.8 Hz, aromatic protons), 7.30-7.22 (m, 5H, aromatic protons), 6.38 (dd, 1H, J = 6.8, 2.8 Hz, NH), 4.65, 4.52 (ABq, 2H, J = 11.8 Hz, benzyl), 4.65 (dd, 1H, J = 5.5, 3.5 Hz, 6a-H), 4.40 (d, 1H, J = 3.4 Hz, 3a-H), 4.31-4.26 (m, 1H, 2-H), 4.07 (d, 1H, J = 5.4 Hz, 4-H), 4.00-3.94 (m, 2H, 2'a-H, 5-H), 3.72 (dd, 1H, J = 11.6, 2.0 Hz, 2'b-H), 3.18 (dt, 1H, J = 12.6, 3.0 Hz, 1'a-H), 3.10 (ddd, 1H, J = 12.6, 6.9, 3.4 Hz, 1'b-H), 2.63 (bs, 1H, OH), 2.24 (ddd, 1H, J = 14.6, 9.4, 5.6 Hz, 1a-H), 1.99 (dd, 1H, J=14.6, 4.6 Hz, 1b-H); ^{13}C-NMR (CDCl₃): δ (ppm) 149.65, 145.6, 137.1, 128.4, 128.2, 127.9, 127.5, 124.1, 89.2, 86.5, 83.5, 83.0, 77.9, 72.4, 61.3, 46.0, 33.9

$[\alpha]^{20}_D$: +14.6 (c 0.5, CHCl₃).

HRMS (FT-ICR): calcd for $C_{21}H_{24}N_2O_8S$ Na: 487.1151; found: 487.1143

$[M+Na]^+$.

Elemental anal. calcd for $C_{21}H_{24}N_2O_8S$ (487.11): C 54.30%; H 5.21%; N 6.03%; found: C 54.22%; H 5.29%; N 5.97%.

(56) ^{1}H-NMR (CDCl$_3$): δ (ppm) 8.32, 8.03 (AA'XX', 4H, J = 8.6 Hz, aromatic protons), 7.37-7.29 (m, 5H, aromatic protons) 5.33 (t, 1H, J = 6.1 Hz, NH), 4.72 (bt, 1H, J = 4.5 Hz, 6a-H), 4.63, 4.50 (ABq, 2H, J = 11.6 Hz, benzyl), 4.55 (dd, 1H, J = 4.4, 1.5 Hz, 3a-H), 4.12 (m, 1H, 2-H), 3.86-3.76 (m, 3H, 2'a-H, 4-H, 5-H), 3.60 (dd, 1H, J = 12.0, 4.8 Hz, 2'b-H), 3.27 (ddd, 1H, J = 13.0, 6.2, 3.3 Hz, 1'a-H), (btd, 1H, 1'b-H), 2.10 (dd, 1H, J = 13.5, 5.0 Hz, 1a-H), 2.05 (bs, 1H, OH), 1.68 (ddd, 1H, J = 13.5, 10.3, 4.7 Hz, 1b-H); ^{13}C-NMR (CDCl$_3$): δ (ppm) 149.8, 145.5, 137.1, 128.4, 128.0, 127.8, 127.5, 124.3, 88.8, 84.4, 84.1, 83.0, 76.8, 72.2, 62.1, 45.9, 35.7

$[\alpha]^{20}_D$: +7.8 (c 0.5, CHCl$_3$).

HRMS (FT-ICR): calcd for $C_{21}H_{24}N_2O_8S$ Na: 487.1151; found: 487.1164 $[M+Na]^+$.

Elemental anal. calcd for $C_{21}H_{24}N_2O_8S$ (487.11): C 54.30%; H 5.21%; N 6.03%. Found: C 54.26%; H 5.25%; N 6.00%.

___

Compounds 57 and 58

To a stirred solution of **52** (200 mg, 0.716 mmol) in dry DMF (10 ml) HOBt (145 mg, 1.074 mmol), DIPEA (368 μl, 2.148 mmol) and 4-nitrobenzoic acid were added under argon atmosphere; DIC (166 μl, 1.074 mmol) was added at 0°C and the reaction was stirred at room tempera ture for 24 h. After this time, the solvent was concentrated *in vacuo* and, after flash-chromatography (4.5:5.5 toluene/EtOAc), pure compounds **57** (*S* diastereomer, 59 mg, 20% yield) and **58** (*R* diastereomer, 150 mg, 50% yield) were purified and separated as pale yellow oils.

(57) ^{1}H-NMR (CDCl$_3$): δ (ppm) 8.23, 8.01 (AA'XX', 4H, J = 8.9 Hz, aromatic protons), 7.65 (dd, 1H, J = 6.8, 2.8 Hz, NH), 7.35-7.28 (m, 5H, aromatic protons), 4.69 (dd, 1H, J = 5.0, 3.3 Hz, 6a-H), 4.66, 4.53 (ABq, 2H, J = 11.7 Hz, benzyl), 4.41 (m, 2H, 2-H, 3a-H), 4.09 (d, 1H, J = 5.0 Hz, 4-H), 4.02 (m, 1H, 5-H), 3.80 (m, 2H, 1'a-H, 2'a-H), 3.69 (dd, 1H, J = 11.9, 2.9 Hz, 2'b-H), 3.53 (td, 1H, J = 14.3, 3.0 Hz, 1'b-H), 2.82 (bs, 1H, OH), 2.27 (ddd, 1H, J = 14.4, 9.0, 5.6 Hz, 1a-H), 2.07 (dd, 1H, J = 14.4, 4.8 Hz, 1b-H); ^{13}C-NMR (CDCl$_3$): δ (ppm) 166.3, 149.1, 140.2, 137.2, 128.514, 128.35, 127.8, 127.5, 123.2, 88.5, 86.8, 83.8, 83.2, 78.6, 72.3, 61.6, 43.4, 33.7.

$[\alpha]^{20}_D$: -18.4 (c 0.5, CHCl$_3$).

HRMS (FT-ICR): calcd for C$_{22}$H$_{24}$N$_2$O$_7$Na: 451.1481; found: 451.1498 [M+Na]$^+$.

_____

Elemental anal. calcd for $C_{22}H_{24}N_2O_7$ (451.14): C 61.67%; H 5.65%; N 6.54%; found: C 61.64%; H 5.61%; N 6.59%.

(58) ^{1}H-NMR (CDCl$_3$): δ (ppm) 8.26, 7.94 (AA'XX', 4H, J = 8.7 Hz, aromatic protons), 7.35-7.28 (m, 5H, aromatic protons), 6.77 (t, 1H, J = 4.9Hz, NH) 4.75 (bt, 1H, J = 4.5Hz, 6a-H) 4.68, 4.54 (ABq, 2H, J = 11.6Hz, benzyl) 4.63 (d, 1H, J = 4.4 Hz, 3a-H), 4.28 (m, 1H, 2-H), 3.89 (m, 2H, 4-H, 5-H), 3.82 (dd, 1H, J = 12.0, 2.2 Hz, 2'a-H), 3.80 (m, 1H, 1'a-H), 3.65 (dd, 1H, J = 12.0, 4.0 Hz, 2'b-H), 3.49 (td, 1H, J = 13.8, 5.9 Hz, 1'b-H), 2.50 (bs, 1H, OH), 2.19 (dd, 1H, J = 13.5, 4.9 Hz, 1a-H), 1.64 (ddd, 1H, J = 13.6, 10.5, 4.7 Hz, 1b-H); ^{13}C-NMR (CDCl$_3$): δ (ppm) 165.3, 149.5, 139.6, 137.2, 128.3, 128.1, 127.8, 127.5, 123.6, 88.8, 84.5, 84.2, 83.1, 77.4, 72.1, 62.2, 43.0, 36.1.

$[\alpha]^{20}_D$: -17.2 (c 0.5, CHCl$_3$).

HRMS (FT-ICR): calcd for $C_{22}H_{24}N_2O_7Na$: 451.1481; found: 451.1476 [M+Na]$^+$.

Elemental anal. calcd for $C_{22}H_24N_2O_7$ (451.14): C 61.67%; H 5.65%; N 6.54%; found: C 61.69%; H 5.60%; N 6.57%.

_____

Compound 39-44
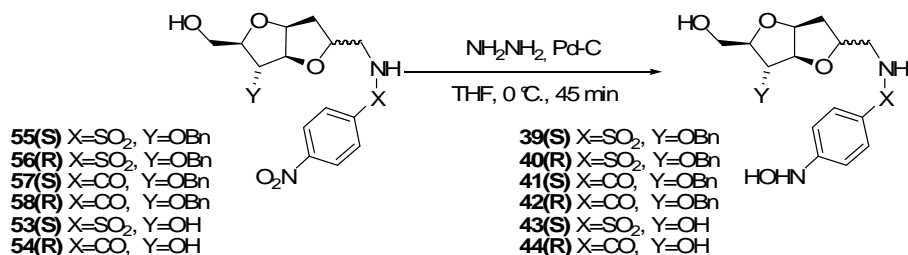

55(S) X=SO₂, Y=OBn
56(R) X=SO₂, Y=OBn
57(S) X=CO, Y=OBn
58(R) X=CO, Y=OBn
53(S) X=SO₂, Y=OH
54(R) X=CO, Y=OH

39(S) X=SO₂, Y=OBn
40(R) X=SO₂, Y=OBn
41(S) X=CO, Y=OBn
42(R) X=CO, Y=OBn
43(S) X=SO₂, Y=OH
44(R) X=CO, Y=OH

To a stirred solution of **55** (40 mg, 0.086 mmol) in THF (3.7 mL) Pd/C (3.7 mg) was added at 0°C; after 15 min, the suspension was treated with hydrazine hydrate (8.4 μl, 0.172 mmol) and stirred at 0°C for 45 min. The reaction was quenched by adding acetone. Then Pd/C was removed by filtering and the solvents were concentrated in vacuo. The product was purified by flash column chromatography (9.5:0.5 toluene/CH₃OH) to give **39** (35.5 mg, 92% yield) as a pale yellow amorphous solid.

(39) ^{1}H-NMR (9:1 D₂O:CD₃OD): δ (ppm) 7.62, 7.00 (AA'XX', 4H, J = 8.8 Hz, aromatic protons), 7.38-7.32 (m, 5H, aromatic protons), 4.64 (bt, 1H, J = 5.0 Hz, 6a-H), 4.59, 4.47 (ABq, 2H, J = 11.6 Hz, benzyl), 4.48 (bd, 1H, J = 4.7 Hz, 3a-H), 4.11 (m, 1H, 2-H), 3.76 (m, 1H, 5-H) 3.61 (bd, 1H, J = 6.1 Hz, 4-H), 3.49 (dd, 1H, J = 12.2, 3.4 Hz, 2'a-H), 3.26 (dd, 1H, J = 12.2, 6.6 Hz, 2'b-H), 2.93 (dd, 1H, J = 13.3, 3.9 Hz, 1'a-H), 2.87 (dd, 1H, J = 13.3, 8.0 Hz, 1'b-H), 2.18 (ddd, 1H, J = 14.4, 8.7, 5.9 Hz, 1a-H), 1.75 (dd, 1H, J = 14.6, 4.0 Hz, 1b-H); ^{13}C-NMR (CD₃OD): δ (ppm) 156.7, 139.0, 131.05, 129.2, 129.1, 128.8, 128.6, 113.1, 90.4, 87.7, 85.9, 84.7, 80.6, 72.9, 63.4, 48.8, 36.3.
$[\alpha]^{20}_D$: -12.65 (c 0.7, DMSO).
HRMS (FT-ICR): calcd for C₂₁H₂₆N₂O₇SNa: 473.1358; found: 473.1367 [M+Na]⁺.

Elemental anal calcd for $C_{21}H_{26}N_2O_7S$ (473.13): C 55.99%; H 5.82%; N 6.22%; found: C 56.07%; H 5.77%; N 6.29%.

Compound **56** (50 mg, 0.107 mmol) was reacted in the described conditions to afford compound **40** (45 mg, 92% yield) as a pale yellow amorphous solid.

(40) ^{1}H-NMR (9:1 D_2O:CD_3OD): δ (ppm) 7.68, 7.02 (AA'XX', 4H, J = 8.1 Hz, aromatic protons), 7.39-7.34 (m, 5H, aromatic protons), 4.67 (bt, 1H, J = 5.0 Hz, 6a-H), 4.60, 4.48 (ABq, 2H, J = 11.5 Hz, benzyl), 4.42 (bd, 1H, J = 4.7 Hz, 3a-H), 3.95 (m, 1H, 2-H), 3.75 (m, 1H, 5-H) 3.65 (bd, 1H, J = 5.7 Hz, 4-H), 3.59 (dd, 1H, J = 12.5, 3.4 Hz, 2'a-H), 3.42 (dd, 1H, J = 12.5, 5.8 Hz, 2'b-H), 3.14 (dd, 1H, J = 13.7, 3.9 Hz, 1'a-H), 2.97 (dd, 1H, J = 13.7, 5.3 Hz, 1'b-H), 1.95 (dd, 1H, J = 14.3, 3.6 Hz, 1a-H), 1.61 (ddd, 1H, J = 14.3, 8.7, 5.9 Hz, 1b-H); ^{13}C-NMR (CD_3OD): δ (ppm) 155.6, 138.6, 129.9, 128.8, 128.4, 128.2, 128.1, 112.1, 88.4, 85.7, 85.6, 83.2, 77.9, 71.6, 62.2, 46.7, 36.9.
$[\alpha]^{20}_D$: -4.75 (c 0.5, DMSO).
HRMS (FT-ICR): calcd for $C_{21}H_{26}N_2O_7SNa$: 473.1358; found: 473.1342 [M+Na]$^+$.Elemental anal. calcd for $C_{21}H_{26}N_2O_7S$ (473.13): C 55.99%; H 5.82%; N 6.22%. Found: C 56.04%; H 5.76%; N 6.25%.

Compound **57** (70 mg, 0.163 mmol) was reacted in the described conditions and, after purification by flash column chromatography (9:1 toluene/MeOH), afforded **41** (62 mg, 92% yield) as a pale yellow amorphous solid.

(41) ^{1}H-NMR (9:1 D_2O:CD_3OD): δ (ppm) 7.60, 6.99 (AA'XX', 4H, J = 8.7 Hz, aromatic protons), 7.28 (m, 5H, aromati protons), 4.72 (bt, 1H, 6a-H), 4.61, 4.48 (ABq, 2H, J = 11.6Hz, benzyl), 4.52 (bd, 1H, J = 4.2Hz, 3a-H), 4.27 (m, 1H, 2-H), 3.84 (m, 2H, 4-H, 5-H), 3.61 (dd, 1H, J = 12.3, 3.6 Hz, 2'a-H), 3.54 (dd, 1H, J = 13.9, 7.1 Hz, 1'a-H), 3.51 (m, 1H, 2'b-H), 3.38 (dd, 1H, J = 14.0, 3.8 Hz, 1'b-H), 2.27 (ddd, 1H, J = 14.5, 8.0, 6.3 Hz, 1a-H), 1.86 (dd, 1H, J = 14.6, 4.0 Hz, 1b-H). ^{13}C-NMR (CD_3OD): δ (ppm) 170.1, 156.0, 139.1, 129.3, 129.2, 128.8, 128.6, 126.4, 113.3, 90.4, 87.9, 85.8, 84.9, 80.7, 73.0, 63.3,

_____

45.3 36.3.

$[\alpha]^{20}_D$: -3.91 (c 0.7, DMSO).

HRMS (FT-ICR): calcd for $C_{22}H_{26}N_2O_6Na$: 437.1689; found: 437.1678 $[M+Na]^+$.

Elemental anal calcd for $C_{22}H_{26}N_2O_6$ (437.16): C 63.76%; H 6.32%; N 6.76%; found: C 63.73%; H 6.29%; N 6.81%.

The procedure was carried out as described for the preparation of **39**, starting from **58** (90 mg, 0.209 mmol) and, after purification by flash column chromatography (9:1 toluene/CH₃OH), affording **42** (82 mg, 95% yield) as pale yellow amorphous solid.

(42) ^{1}H-NMR (9:1 D₂O:CD₃OD): δ (ppm) 7.65, 7.02 (AA'XX', 4H, J = 8.8 Hz, aromatic protons), 7.32-7.26 (m, 5H, aromatic protons), 4.74 (1H, 6a-H), 4.63, 4.53 (ABq, 2H, J = 11.6 Hz, benzyl), 4.62 (1H, 3a-H), 4.23 (m, 1H, 2-H), 3.82 (dd, 1H, J = 6.4, 1.4 Hz, 4-H), 3.79 (m, 1H, 5-H), 3.65 (dd, 1H, J = 12.3, 3.1 Hz, 2'a-H), 3.51 (dd, 1H, J = 13.3, 5.8 Hz, 2'b-H), 3.48 (1H, 1'a-H), 3.43 (dd, 1H, J = 14.2, 6.4Hz, 1'b-H), 2.11 (dd, 1H, J = 13.9, 5.3 Hz, 1a-H), 1.68 (ddd, 1H, J = 14.2 10.2, 4.9 Hz, 1b-H); ^{13}C-NMR (CD₃OD): δ (ppm) 170.0, 156.1, 139.0, 129.2, 129.2, 128.8, 128.6, 126.3, 113.3, 89.7, 86.0, 86.0, 84.5, 79.1, 72.9, 63.1, 44.1, 37.6.

$[\alpha]^{20}_D$: -13.59 (c 0.7, DMSO).

HRMS (FT-ICR): calcd for $C_{22}H_{26}N_2O_6Na$: 437.1689; found: 437.1698 $[M+Na]^+$.

Elemental anal calcd for $C_{22}H_{26}N_2O_6$ (437.16): C 63.76%; H 6.32%; N 6.76%; found: C 63.75%; H 6.28%; N 6.83%.

The procedure was carried out as described for the preparation of **39**, starting from **52** (100 mg, 0.267 mmol) and, after purification by flash column chromatography (7.5:2.5 toluene/MeOH), affording **43** (95 mg, 98% yield) as pale yellow amorphous solid (mixture of diastereomers, R:S 3:1, as determined from the integration ratio of the ^{1}H-NMR signals).

(43-R) ^{1}H-NMR (D$_2$O): δ (ppm) 7.70, 7.09 (AA'XX', 4H, J = 8.8 Hz, aromatic protons), 4.70 (bt, 1H, 6a-H), 4.29 (dd, 1H, J = 4.3, 1.8 Hz, 3a-H), 4.02 (m, 1H, 2-H), 3.82 (dd, 1H, J = 5.8, 1.7 Hz, 4-H), 3.71 (ddd, 1H, J = 6.4, 6.2, 3.5 Hz, 5-H), 3.65 (dd, 1H, J = 12.3, 3.5, 3.5Hz, 2'a-H), 3.49 (dd, 1H, J = 12.2, 6.6 Hz, 2'b-H), 3.11 (dd, 1H, J = 14.1, 3.6 Hz, 1'a-H), 3.02 (dd, 1H, J = 13.6, 5.8 Hz, 1'b-H), 1.98 (dd, 1H, J = 14.0, 5.4 Hz, 1a-H), 1.64 (ddd, 1H, J = 14.3, 10.2, 4.8 Hz, 1b-H); ^{13}C-NMR (CD$_3$OD): δ (ppm) 156.6, 131.3, 129.1, 113.1, 92.1, 87.7, 84.1, 78.6, 78.5, 63.2, 47.2, 37.2.

(43-S) ^{1}H-NMR (D$_2$O) selected signals: δ (ppm) 4.33 (dd, 1H, H3a, J = 4.2, 0.8 Hz), 4.11(m, 1H, H-2) 3.85 (dd, 1H, J = 5.5, 0.7 Hz, 4-H), 3.75 (m, 1H, 5-H), 3.60 (dd, 1H, J = 12.1, 3.7 Hz, 2'a-H), 3.42 (dd, 1H, J = 12.1, 6.7 Hz, 2'b-H), 2.21 (ddd, 1H, J = 14.3, 8.5, 5.8 Hz, 1a-H), 1.75 (dd, 1H, H-1b, J = 14.6, 4.6Hz); ^{13}C-NMR (CD$_3$OD) selected signals: δ (ppm) 131.1, 129.2, 113.0, 93.1, 89.6, 84.4, 80.4, 78.3, 63.5, 36.5.

HRMS (FT-ICR): calcd for C$_{14}$H$_{20}$N$_2$O$_7$SNa: 383.0889; found: 383.0877 [M+Na]$^+$.

Elemental anal calcd for C$_{14}$H$_{20}$N$_2$O$_7$S (383.08): C 46.66%; H 5.59%; N 7.77%; found: C 46.59%; H 5.63%; N 7.81%.

The procedure was carried out as described for the preparation of **39**, starting from **53** (120 mg, 0.355 mmol) and, after purification by flash column chromatography (7.5:2.5 toluene/CH$_3$OH), pure **44** (113 mg, 98% yield) was obtained, as a pale yellow amorphous solid (mixture of diastereomers, R:S 2:1, as determined from the integration ratio of the ^{1}H-NMR signals) by flash column chromatography.

(44-R) ^{1}H-NMR (D$_2$O): δ (ppm) 7.65, 7.02 (AA'XX', 4H, J = 8.8 Hz, aromatics), 4.77 (bt, 1H, J = 4.6Hz, 6a-H), 4.49 (dd, 1H, J = 4.3, 1.7 Hz, 3a-H), 4.29 (m, 1H, 2-H), 3.98 (dd, 1H, J = 5.8, 1.7 Hz, 4-H), 3.76 (ddd, 1H, J = 6.2, 6.2, 3.4 Hz, 5-H), 3.71 (dd, 1H, J = 12.2, 3.4 Hz, 2'a-H), 3.58 (dd, 1H, J = 12.2, 6.5 Hz, 2'b-H), 3.49 (m, 2H, 1'a-H, 1'b-H), 2.14 (dd, 1H, 1a-H, J =

_____

14.4, 5.2 Hz), 1.72 (ddd, 1H, J = 14.4, 10.2, 4.9 Hz, 1b-H); ^{13}C-NMR (CD$_3$OD): δ (ppm) 169.0, 155.0, 128.2, 125.4, 112.2, 91.0, 86.6, 82.9, 77.9, 77.6, 62.0, 43.1, 36.6.

(44-S) ^{1}H-NMR (D$_2$O) selected signals: δ (ppm) 4.49 (dd, 1H, J = 4.3, 1.7Hz, 3a-H), 4.05 (bd, 1H, J = 5.2 Hz, 4-H), 3.82 (ddd, 1H, J = 6.5, 5.4, 4.0 Hz, 5-H), 3.68 (dd, 1H, J = 12.1, 3.8 Hz, 2'a-H), 3.58 (dd, 1H, J = 12.1, 6.7 Hz, 2'b-H), 3.53 (m, 2H, 1'a-H, 1'b-H), 2.32 (ddd, 1H, J = 8.3, 6.2 Hz, 1a-H) 1.86 (dd, 1H, J = 14.4, 5.7 Hz, 1b-H); ^{13}C-NMR (CD$_3$OD): δ (ppm) 169.1, 154.9, 128.2, 125.4, 112.2, 92.0, 88.7, 83.5, 79.4, 77.1, 62.3, 44.2, 35.4.

HRMS (FT-ICR): calcd for C$_{15}$H$_{20}$N$_2$O$_6$Na: 347.1219; found: 347.1234 [M+Na]$^+$.

Elemental anal calcd for C$_{15}$H$_{20}$N$_2$O$_6$ (347.12): C 55.55%; H 6.22%; N 8.64%; found: C 55.63%; H 6.29%; N 8.57%.

5.1.3. Synthesis of compound SCH-54292
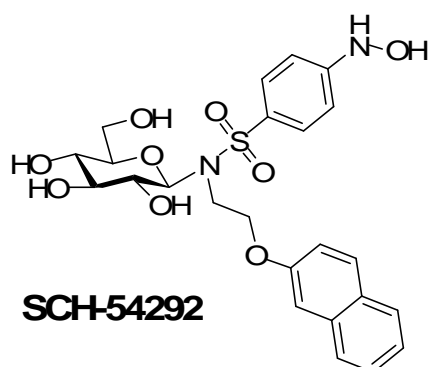

Figure 5-7. Structure of **SCH-54292**.
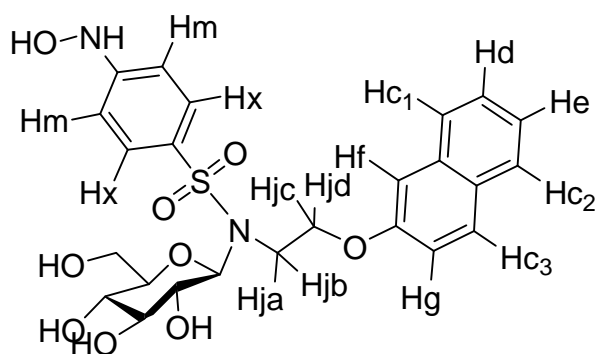
Figure 5-8. Carbon and hydrogen numbering in **SCH-54292**.

_____

Compound 59
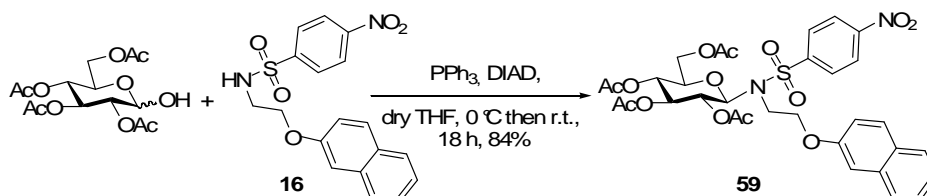
To a stirred solution of **16** (500 mg, 1.344 mmol) and 2,3,4,6-*O*-tetraacetyl glucopyranoside (608 mg, 1.747 mmol) in dry THF (13.4 mL) PPh$_3$ (528.8 mg, 2.016 mmol) was added under argon atmosphere; the reaction was cooled at -80°C and, after 15 min, DIAD (390.5 µl, 2.016 mmol) was added very slowly. After 1 h, the reaction was allowed to reach room temperature and stirred overnight. The solvent was evaporated *in vacuo* and the product was purified by flash column chromatography (9.5:0.5 toluene/EtOAc) giving **59** (840.5 mg, 84% yield) as a yellow crystalline solid.

^{1}H-NMR (CDCl$_3$): δ (ppm) 8.23, 8.05 (AA'XX', 4H, J = 8.6 Hz, arom), 7.73-7.66 (m, 3H, arom), 7.42 (bt, 1H, J = 6.9 Hz, arom), 7.32 (bt, 1H, J = 7.0 Hz, arom), 7.00 (s, 1H, arom), 6.93 (bd, 1H, J=8.9 Hz, arom), 5.45 (d, 1H, J = 8.6Hz), 5.31 (m, 2H), 5.07 (t, 1H, J = 9.3 Hz), 4.18-4.04 (m, 4H), 3.82-3.79 (m, 2H), 3.59-3.54 (m, 1H), 2.04 (s, 3H, CH$_3$), 2.02 (s, 3H, CH$_3$), 2.00 (s, 3H, CH$_3$), 1.91 (s, 3H, CH$_3$); ^{13}C-NMR (CDCl$_3$): δ (ppm) 170.3, 170.0, 169.6, 169.4, 155.8, 150.3, 145.3, 134.5, 129.7, 129.3, 129.0, 127.8, 126.9, 126.8, 124.4, 124.1, 118.5, 107.0, 85.6, 74.5, 73.7, 68.5, 68.0, 66.2, 61.9, 43.8, 21.0; $[\alpha]^{20}_D$: -12.8 (c 0.5, DMSO). HRMS (FT-ICR): calcd for C$_{32}$H$_{34}$N$_2$O$_{14}$SNa: 725.1628; found: 725.1635 [M+Na]$^+$. Elemental anal calcd for C$_{32}$H$_{34}$N$_2$O$_{14}$S (725.16): C 54.70%; H 4.88%; N 3.99%; found: C 54.65%; H 4.92%; N 3.95%.

Compound 60
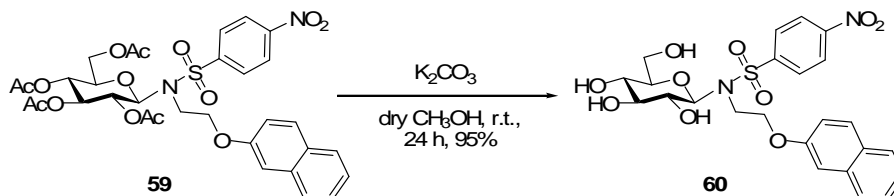
To a stirred solution of **59** (68 mg, 0.096 mmol) in dry CH_3OH (0.5 mL) K_2CO_3 (27 mg, 0.193 mmol) was added under argon atmosphere at room temperature. After a few minutes, a yellow precipitate appeared and the suspension was stirred at room temperature for 24 h. The reaction was filtered and the solid residue dissolved in boiling methanol and then filtered when hot to eliminate salts. The filtrate was concentrated *in vacuo* and the product was purified by flash column chromatography (8.5:1.5 toluene/CH_3OH) providing **60**[51] (49 mg, 95% yield) as a yellow amorphous solid, resulting to be only the β-anomer.

_____

45 (SCH-54292)
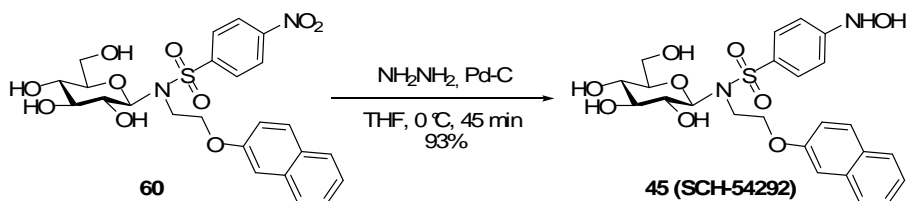
The procedure was carried out as described for the preparation of **1**, starting from **60** (40 mg, 0.075 mmol) and, after purification by flash column chromatography (9:1 toluene/CH$_3$OH), affording **SCH-54292** (36.5 mg, 93% yield) as a pale yellow amorphous solid.

^{1}H-NMR (9:1 D$_2$O/CD$_3$OD): δ (ppm) 7.88 (d, 1H, J = 7.3 Hz, c2-H), 7.86 (d, 1H, J = 8.8 Hz, c3-H), 7.84 (d, 1H, J = 8.4 Hz, c1-H), 7.82, 7.06 (AA'XX', 4H, J = 8.8 Hz, arom), 7.53 (t, 1H, J = 7.6 Hz, d-H), 7.43 (t,1H, J = 7.5 Hz), 7.30 (d, 1H, J = 2.4 Hz, f-H), 7.16 (dd, 1H, J = 8.9, 2.6 Hz, f-H), 5.07 (d, 1H, J = 9.2 Hz, 1-H), 4.33 (m, 2H, jc-H, jd-H), 3.78 (ddd, 1H, J = 16.0, 8.0, 5.0 Hz, ja-H), 3.67 (t, 1H, J = 9.0 Hz, 2-H), 3.60 (dd, 1H, J = 12.3, 2.1 Hz, 6a-H), 3.59 (ddd, 1H, J = 16.0, 8.0, 5.0 Hz, jb-H), 3.58 (t, 1H, J = 8.9 Hz, 3-H), 3.51 (dd, 1H, J = 12.3, 5.4 Hz, 6b-H), 3.41 (m, 1H, 5-H), 3.33 (m, 1H, 4-H); ^{13}C-NMR (d6-DMSO): δ (ppm) 155.7, 155.4, 134.1, 129.4, 129.2, 128.5, 127.5, 127.4, 126.6, 126.5, 123.8, 118.4, 111.3, 106.6, 86.7, 78.3, 77.2, 70.1, 69.1, 66.2, 60.4, 40.8; $[\alpha]^{20}_D$: -42.6 (c 0.5, DMSO); HRMS (FT-ICR): calcd for C$_{24}$H$_{28}$N$_2$O$_9$SNa: 543.1413; found: 543.1432 [M+Na]$^+$. Elemental anal calcd for C$_{24}$H$_{28}$N$_2$O$_9$S (543.14): C, 55.38%; H, 5.42%; N, 5.38%; found: C, 55.58%; H, 5.89%; N, 4.76%.

5.1.3. Synthesis of compounds 62 and 62
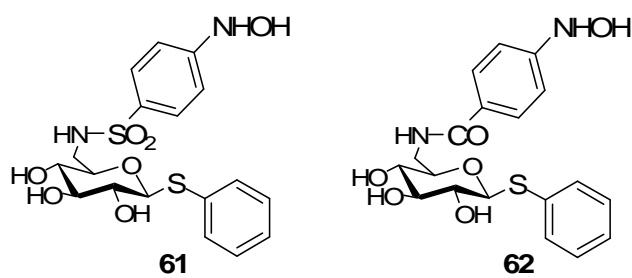
Figure 5-9. Structures of compounds **61** and **62**.

Compound 64
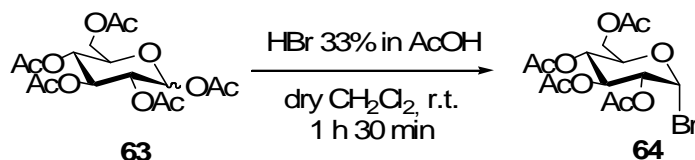
To a stirred solution of **pentaacetyl-D-glucopyranoside (63)** (19.7 gr, 50.04 mmol) in CH_2Cl_2 (30 ml) a 33% solution of HBr in AcOH (53 ml) was added and the reaction mixture was stirredat room temperature for 1 h 30 min. The reaction was quenched by adding a mixture of ice and aqueous satureted $NaHCO_3$ until pH neutralization. The product was extracted with CH_2Cl_2 and, after usual workup, the crude was recovered as a colorless oil.

Compound 65
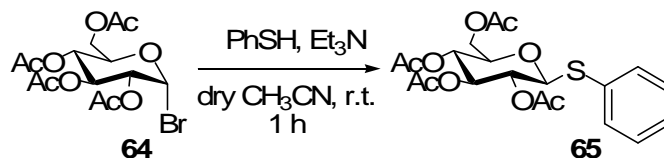
To a stirred solution of crude **64** (50.04 mmol) in CH$_3$CN (30 ml) thiophenol (7.72 ml, 75.06 mmol) was added and the reaction mixture was stirred at room temperature for 1 h. The solvent was evaporated *in vacuo* and the product was purified by crystallization from ethanol, giving crude **65** (23 gr) as a white solid.

_____

Compound 66
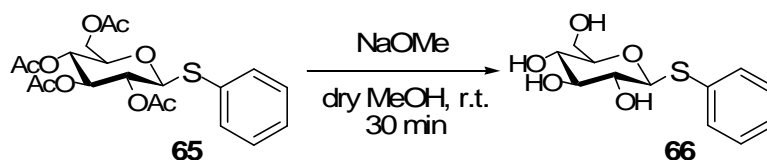
To a stirred solution of crude **65** (10 gr, 22.703 mmol) in CH_3OH (50 ml) Na metallic was added in catalytic amount and the reaction mixture was stirred at room temperature for 30 min. After this time Amberlite IRA-120 H$^+$ resin was added and the mixture was stirred for 10 min. Then resin was removed by filtering and the solvent was evaporated. After usual workup crude **66** (7.81 gr) was obtained as pale yellow oil.

Compound 67
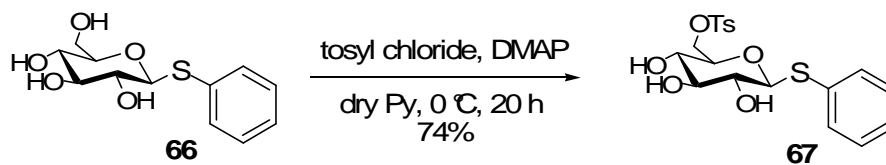
To a stirred solution of crude **66** (5.2 gr, 19.09 mmol) in pyridine (50 ml) tosyl chloride (4 gr, 21.00 mmol) and dimethylaminopyridine (cat. amount) were added and the reaction mixture was stirred at room temperature for 20 h. The solvent was evaporated *in vacuo* and the product was purified by flash column chromatography (9.5:0.5 EtOAc/MeOH), affording **67** (6 gr, 74% yield) as green oil.

Compound 68
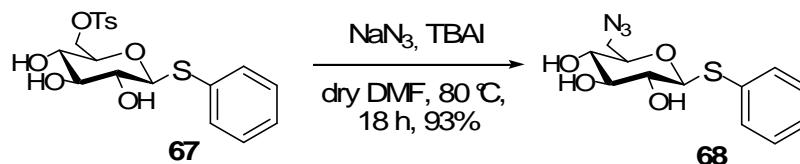
To a stirred solution of **67** (3.5 gr, 8.21 mmol) in DMF (40 ml) sodium azide (1.6 gr, 24.62 mmol) and tetrabutylamoniun iodine (cat. amount) were added and the reaction mixture was stirred at 80 °C for 1 8 h. The solvent was evaporated *in vacuo* and the residue was dissolved in EtOAc and washed with aqueous saturated NaHCO$_3$ to eliminate NaN$_3$ excess. After usual workup the product was purified by flash column chromatography (EtOAc), affording **68** (2.3 gr, 93% yield) as yellow oil.

Compound 69
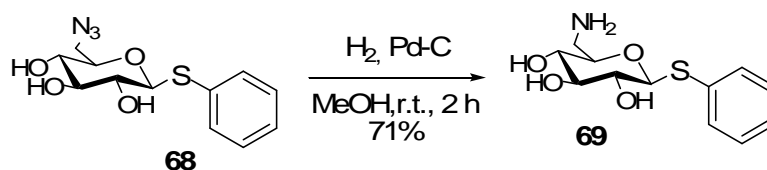
To a solution of **68** (200 mg, 0.673 mmol) in MeOH (12 mL), palladium on charcoal (catalytic) was added under H_2 atmosphere (vacuum/H_2 cycles). After 2 h, crude was filtered and solvents evaporated *in vacuo*. The residue was purified by flash column chromatography (9.5:0.5 AcOEt/MeOH) affording **69** as a yellow oil (130 mg, 71%).

^{1}H-NMR (CD$_3$OD) δ (ppm) 7.42 (m, 2H, arom), 7.24-7.13 (m, 3H, arom), 4.51 (d, 1H, J = 9.72 Hz, H-1), 3.28 (t, 1H, J = 8.81 Hz, H-3), 3.23-3.14 (m, 1H, H-5), 3.12 (dd, 1H, J = 9.72, 8.81 Hz, H-2), 3.05 (t, 1H, J = 9.24 Hz, H-4), 2.94 (dd, 1H, J = 13.38, 2.80 Hz, H-6a), 2.64 (dd, 1H, J = 13.42, 7.77 Hz, H-6b); ^{13}C-NMR (CD$_3$OD) δ (ppm) 134.3, 133.0, 129.7, 128.4, 88.8, 81.1, 79.3, 73.8, 72.9, 43.8.

_____

Compound 70
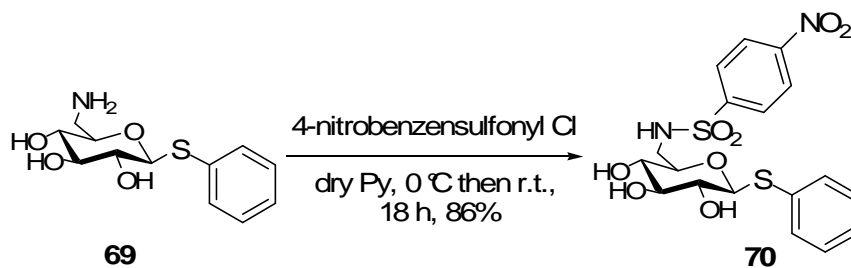
To a stirred solution of **69** (200 mg, 0.74 mmol) in dry pyridine (5 ml) *p*-nitrobenzensulfonyl chloride were added at 0°C under argon atmosphere. After a night, the reaction was quenched by adding CH_3OH. The solvents were evaporated *in vacuo* and, after flash-chromatography (1.5:8.5 petroleum ether/EtOAc), **70** (289 mg, 86% yield) was recovered as pale yellow oil.

^{1}H-NMR (CDCl$_3$) δ (ppm) 8.11, 7.87 (AA'XX', 4H, J = 8.78 Hz, arom), 7.22 (m, 5H, arom) 5.78 (t, 1H, J = 5.45 Hz, NH), 4.60 (d, J = 9.73 Hz, 1H, H-1), 4.04 (dd, 1H, J = 7.13 Hz), 3.64 (dd, 1H, J = 14.02, 7.01 Hz), 3.57 (dd, 1H, J = 16.24, 6.96 Hz), 3.48-3.27 (m, 2H), 3.21 (dd, 1H, J = 10.04, 3.68 Hz); ^{13}C-NMR (CDCl$_3$) δ (ppm) 151.0, 148.0, 134.8, 132.3, 129.7, 129.1, 128.1, 125.1, 88.9, 79.7, 79.2, 73.5, 72.4, 45.5.

Compound 71

To a stirred solution of **69** (1.13 gr, 4.17 mmol) in dry DMF (54 ml) HOBt (846 mg, 6.263 mmol), DIPEA (2.148 ml, 12.52 mmol) and 4-nitrobenzoic acid (837 mg, 5.01 mmol) were added under argon atmosphere; DIC (970 µl, 6.26 mmol) was added at 0℃ and the reaction was st irred at room temperature for 2 h. After this time, the solvent was concentrated *in vacuo* and, after flash column chromatography (4.5:5.5 toluene/EtOAc), pure compounds **71** (873 mg, 50% yield) was purified as a yellow solid.

^{1}H-NMR (CD$_3$OD): δ (ppm) 8.31, 7.98 (AA'XX', 4H, J = 8.95 Hz, arom), 7.50-7.43 (m, 2H, arom), 7.18-7.03 (m, 3H, arom), 4.62 (d, 1H, J = 9.78 Hz, H-1), 3.90 (m, 1H,), 3.61-3.47 (m, 2H), 3.41 (t, 1H, J = 8.83 Hz), 3.22 (m, 2H).

_____

Compound 61 and 62
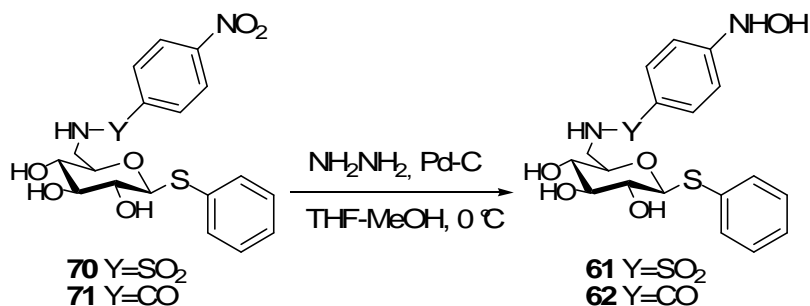
To a stirred solution of **70** (30 mg, 0.065 mmol) in THF (3.7 mL) Pd/C (3.7 mg) was added at 0°C; after 15 min, the suspension was treated with hydrazine hydrate (8.4 µl, 0.172 mmol) and stirred at 0°C for 45 min. The reaction was quenched by adding acetone. Then Pd/C was removed by filtering and the solvents were concentrated in vacuo. The product was purified by flash column chromatography (0.5:9.5 petroleum ether/EtOAc) to give **61** (23 mg, 79% yield) as a pale yellow oil.

^{1}H-NMR (CD$_3$OD): δ (ppm) 7.57, 6.9 (AA'XX', 4H, J = 8.84 Hz, arom), 7.50 (m 2H, arom), 7.33-7.13 (m, 3H), 4.39 (d, 1H, J = 9.72 Hz, H-1), 5.27-3.23 (m, 2H), 3.18-3.01 (m, 3H), 2.85 (dd, 1 H, J = 13.6, 7.9 Hz, H-6b); ^{13}C-NMR (CD$_3$OD): δ (ppm) 156.7, 134.4, 133.3, 132.9, 131.1, 129.8, 129.2, 128.5, 89.0, 79.6, 79.2, 73.6, 72.6, 45.6,

Compound **71** (43 mg, 0.102 mmol) was reacted in the described conditions to afford compound **62** (28 mg, 68% yield) as a pale yellow amorphous solid after flash column chromatography (0.5:9.5 petroleum toluene/MeOH).

^{1}H-NMR (CD$_3$OD): δ (ppm) 7.69, 6.96 (AA'XX', 4H, *J* = 8.90 Hz, arom), 7.47 (m, 2H, arom), 7.17-7.02 (m, 3H), 6.96 (d, 1H, J = 8.90 Hz), 4.60 (d, 1H, J = 9.80 Hz), 3.86 (m, 1H), 3.53-3.44 (m, 2H), 3.41 (t, 1H, t, J = 8.86 Hz), 3.22 (m ,2 H, H-2, H6b).

5.2. Molecular Modelling

5.2.1. Protein modelling

Before applying virtual ligand docking, the X-ray crystal structure of the Ras-GDP complex was optimized and prepared for the docking program. The X-ray structure of the human p21-hRas in its inactive form was taken from the Protein Data Bank (code: 4Q21) and optimized by applying the program Impact of Schrödinger and the OPLS-AA force field.[88] The protein was solvated in an explicit solvent box (65x65x65 Å) with 7991 water molecules. The protein was allowed to relax slowly in several steps in order to orient the added hydrogens correctly and in order to relieve steric clashes. In the first optimization step force constraints were placed on all the heavy atoms of the protein, In the second step the force constraints on the heavy atoms of the protein side chains were decreased in five sub-steps, but the constraints on the backbone atoms were kept constant, Then in the third step these force constraints on the backbone atoms of the protein were also decreased in five substeps and finally in the last step no force constraints were applied and all the atoms of the system were flexible. Every step in this minimization procedure was splitted into a steepest descent step and a conjugate gradient step; this is a general procedure within protein homology modelling. The protein structure obtained after this thorough minimization procedure could be applied in the subsequent docking procedure. The root mean square deviation of the minimized protein structure in comparison with the X-ray structure is 0.46 Å for the backbone atoms, 0.62 Å for the heavy atoms

---

[88] Jorgensen W. L., Maxwell D. S., Tirado-Rives J., "Development and Testing of the OPLS All-Atom Force Field on Conformational Energetics and Properties of Organic Liquids", *J. Am. Chem. Soc.*, **1996**, 118, 11225-11236.

_____

of the side chains, and 0.55 Å for all protein heavy atoms.

5.2.2. Ligand modelling

In order to ensure the complete coverage of conformational space for the ligands we applied a conformational search for each designed ligand using the Monte Carlo method (MCMM) implemented in the program MacroModel of Schrödinger. Random changes were made in the torsion angles during the search and the OPLS-AA force field was used. The obtained conformations of the compounds were clustered with the program NMRCLUST,[89] in order to obtain the most representative conformations of the structures for the subsequent docking studies.

5.2.3. Ligand docking

The virtual ligand docking studies were performed with the GLIDE method implemented in the Impact program of Schrödinger. The model of the Ras-GDP complex was not modified further as is recommended by Schrödinger, but all protein charged groups were kept charged and were not neutralized.

GLIDE requires as a first step the generation of an initial grid. The center of the box enclosing this grid was defined by the Mg^{2+}-ion, the β-phosphate group of the bound GDP, and the two residues identified by NMR to be involved in interactions with the ligand: residues Arg-68 and Leu-100. The box dimensions were set to 26x26x26 Å. In the second step, the actual docking step, the dimensions for the box for placing the ligand center were set to 12x12x12 Å and the same center was used as for the grid box. In this

_____

[89] A. Kelley, S.P. Gardner, M.J. Sutcliffe, "An automated approach for clustering an ensemble of NMR-derived protein structures into conformationally related subfamilies", *Protein Engineering* , **1996**, 9, 1063-1065.

way the complete cavity in close proximity of Switch region II was included in the box where GLIDE would try to place the ligands. A scaling factor of 0.9 was applied to van der Waals radii of protein and ligand atoms. For the other parameters of Glide the default values were applied.

As a proof-of-concept, we first looked at the series of characterized compounds from the Schering-Plough Research Institute[51] in order to assess the validity of our computer-aided design approach.

The poses depicted in Figure 1 were selected on the same criteria as applied by Schafferhans et al.[90] When several docking solutions are suggested for each ligand as is the case when several conformations of one ligand are docked, is it a hard problem to efficiently discriminate between the solutions and to select the most relevant one. Considering several case studies done by Schafferhans et al., the best solution (the solution with the best score) is not always the one with the most similarity to the experimentally determined structure. However, if more than two ligands are considered, an optimal overall set of solutions for all ligands can be recognized by extracting those orientations that correspond to an optimal mutual similarity among the considered ligands. This additional criterion helps to select a set of relevant ligand placements, provided of course, that the ligands bind to the same binding site.

Furthermore, it can be analyzed how often each of the four new designed compounds is recovered within the top scoring poses. For this purpose, the 20 best scoring poses of each compound were selected. Subsequently, of these 80 poses the 40 best scoring poses were selected and the recovery rate for each compound was calculated.

---

[90] Schafferhans A., Klebe G., "Docking Ligands onto Binding Site Representations Derived from Proteins built by Homology Modelling", *J Mol Biol.* **2001**, *307*, 407-427.

_____

5.3. Biological procedures

5.3.1. Biological assay

5.3.1.1. Expression and isolation of proteins

The C-Cdc25^{Mm} (GEF from Mouse; portion of *CDC25*^{Mm} that contains the catalytic domain of the protein)[91, 92] was expressed in *Escherichia coli* using the pGEX-2T expression vector and then purified by affinity chromatography using a Glutathione Sepharose 4B resin, while the p21 h-Ras was expressed in *E. coli* using the pQE-30 expression vector and then purified by affinity as a 6xHis-tagged protein using an Ni-NTA resin.[92]

5.3.1.2. Measurement of C-Cdc25^{Mm}-stimulated Guanine Nucleotide Exchange on p21 h-Ras

To investigate the ability of putative Ras inhibitors to inhibit or to reduce the C-Cdc25^{Mm}-stimulated nucleotide exchange on purified human Ras proteins we used a technique described by Lenzen et al.[93] with some modifications. This approach utilises guanine nucleotides carrying an N-methylanthranoyl fluorophore (mant-GDP or mant-GTP). p21-hRas (100 nM) and mant -GTP (0.5 μM) were incubated in buffer A (50 mM Tris/HCl, pH 7.5, 1mM MgCl$_2$, 100 mM NH$_4$Cl, 1 mM DTE) in the absence and in the presence of

_____

[91] Coccetti P., Mauri L., Alberghina L., Martegani E., Parmeggiani A., "The Minimal Active Domain of the Mouse Ras Exchange Factor CDC25^{Mm}", *Biochem. Biophys. Res. Commun*, **1995**, 206, 253-259.
[92] Thomas B. J. and Rothstein R., *Cell*, **1989**, *56*, 619-630.
[93] Lenzen C., Cool R. H., Wittinghofer A., *Methods in Enzymology*, **1995**, 255, 95-109.

increasing concentrations of the putative inhibitors. The exchange reaction was started by the addition of 25 nM C-Cdc25^{Mm}. The reaction was monitored at an excitation wavelength of 370 nm and emission wavelength of 450 nm using a Perkin-Elmer Luminescence Spectrometer. Measurements have been taken every second.

Starting from the slope of each curve, IC$_{50}$ values were calculated.

5.3.1.3. Measurement of C-Cdc25^{Mm}-stimulated dissociation rate of p21-hRas-mant-GDP complex

To investigate the ability of Ras inhibitors to influence the C-Cdc25^{Mm}-stimulated dissociation rate of p21-hRas–mant-GDP complexes, we used the method described by Lenzen *et al.*[70] with some modifications. The complex p21-hRas.MANT-GDP (200 nM) and an excess of GDP (500 μM) were incubated in buffer B (40 mM Hepes, pH 7.5, 2 mM DTT, 100 μM MgCl$_2$) in the absence and in the presence of the inhibitors. The dissociation reaction was started by addition of 100 nM C-Cdc25^{Mm}. The reaction was monitored at an excitation wavelength of 370 nm and emission wavelength of 450 nm using a Perkin-Elmer Luminescence Spectrometer. Measurements have been taken every second.

The slope of each curve was calculated assuming a single exponential decay.

5.3.1.4. Yeast strain and growth conditions

Yeast strains used in this study were: W303-1A (*MAT*a *leu2-3,112 ura3-1 trp1-92 his3-11, 15 ade2-1 can1-100 GAL SUC mal*)[94] and T23-13B (*MAT*α *his3, leu2, ura3, trp1, ras1ΔHIS3, ras2ΔURA3, bcy1*) (M. Wigler, Cold Spring Harbor Laboratory). Both strains were grown in 1% yeast extract, 2% Bacto-

---

[94] Milburn M. V., Tong L., de Vos A. M., Brunger A., Yamaizumi Z., Nishimura S., Kim S. H., "Molecular switch for signal transduction: structural differences between active and inactive forms of protooncogenic ras proteins", *Science*, **1990**, 247, 939-945.

peptone (YP) supplemented with 2% glucose and 50 mg/l adenine (YPDA). Growth was monitored by counting the cell number/ml with a Coulter Counter.

5.3.1.5. Cell Cultures and growth conditions

Normal NIH3T3 and NIH3T3 activated k-Ras (Arg12)[94] mouse fibroblast were grown in Dulbecco's modified Eagle's medium supplemented with 10% newborn calf serum, 100 units/ml penicillin, 100 μg/ml streptomycin. Cells were detached by treating them with 0.05% trypsin and 0.15 mM EDTA and growth was monitored by counting the cell number/ml with a Coulter Counter.

5.3.1.6. Assay of MAPK activation

Cells were scraped, and ice-cold Lysis buffer (25 m HEPES, pH 7.5, 150 mM NaCl, 1% NP-40, 0.25% Na deoxycholate, 10% glycerol, 25 mM NaF, 10 mM $MgCl_2$, 1 mM EDTA, 1mM Na vanadate, one tablet of Protease Inhibitor Mixture from Roche Applied Science in 50 mM of extraction medium) was added. The lysates were transferred to a microfucentrifuge tube on ice and centrifuged. Proteins were separated by SDS-PAGE, transferred to nitrocellulose, and immunodecorated with anti-p42/44 MAPK antibody and anti-phospho-p42/44 MAPK antibody (Cell Signalling Technology). Bound antibodies were revealed with ECL Western blotting analysis system (Amersham Pharmacia Biotech).

5.3.1.7. Two-hybrid system

A two-hybrid assay was performed in the Y190 strain (*MATα ura3-52 his3-200 lys2-801 ade2-101 trp1-901 leu2-3,112 gal4Δ gal80Δ cyh2 LYS2::GAL1*$_{UAS}$-*GAL1*$_{TATA}$-*lacZ*) (Clontech) carrying the pGBT9-RAS2^{N24} plasmid and either the pGADGH plasmid (as a negative control) or the

pGADGH-CDC25y plasmid. The pGBT9-RAS2[N24] plasmid carries a fusion of Gal4 DNA binding domain with a dominant negative version of *S. cerevisiae* Ras2, while the pGADGHCDC25y plasmid encodes a fusion of Gal4 trans-activation domain with the catalytic domain of the yeast RasGEF, Cdc25.[95]

The assay was performed essentially as described in Kiechle et al.[96] Cells were grown overnight in selective complete medium in the presence of a sub-lethal concentration of Ras inhibitor, then 1 OD-aliquots of cells were collected by centrifugation, resuspended in 500 µl Z-buffer (75 mM Na_2HPO_4, 50 mM NaH_2PO_4, 10 mM KCl, 1 mM $MgSO_4$) and immediately frozen at -80 °C. For detection, all samples were simultaneously thawed, a 50 µl-aliquot was removed and used to determine the OD_{600}. The remaining cells were incubated for 1 h at 37 °C with 100 µl zymolyase solution (zymolyase T20, ICN, USA; 0.5 mg/ml in Z-buffer). After the lysis step, 100 µl CPRG solution (Chloro Phenol-Red-Galactopyranosid, SIGMA; 4 mg/ml in Z-buffer) were added and incubated at 37 °C for suitable incubation time. Reactions were stopped by adding 200 µl 1M Na_2CO_3. After a 15 min centrifugation at 13000 rpm, the optical density of the supernatant was measured at 574 nm and 634 nm.

The β-galactosidase activity in Miller Units was calculated as: $[MU]=[(OD_{574} - OD_{634}) \times 1000]/(OD_{600} \times t_{inc})$, where t_{inc} is the incubation time in min.

5.3.2. Espression of p21-hRas(1-166)

The *Escherichia coli* expression vector pTACCrasC',[83] encoding the first 166 residues of the human Ras p21 protein [Ras p21(1-166)], was kindly provided A. Wittinghofer. The plasmid were transformed into *E. coli* strain JM109. Uniformly enriched ^{15}N samples were obtained by growing bacteria on a minimum medium with $^{15}NH_4Cl$ as the sole nitrogen source. At a

---

[95] Mosteller R. D., Park W., Broek D., *Methods Enzymol.*, **1995**, 255, 135-148.
[96] Kiechle M., Manivasakam P., Eckardt-Schupp F., Schiestl R. H., Friedl A. A., *Nucleic Acids Res.*, **2002,** 30(24), 136-143.

turbidity of 1.0 OD$_{600nm}$, expression of the protein was induced over night by the addition of 1 mM isopropyl β-D-thiogalactoside (IPTG) and culture was transferred at 30 ℃. The cells were then harvested pelleting at 4000 rpm for 20 min and stored at -80 ℃.

5.3.2.2. Protein Purification

All the procedures described below were performed at 4 ℃. The cells were resuspended to 0.1 g of cell paste/mL with sonication buffer (20 mM Tris-HC1, pH 7.2, 100 mM NaCl, 5 mM MgC12, 1 mM DTT, and 1 mM PMSF). The cells were then broken by sonication and submitted to digestion by 30 min incubation with DNase (0.1 mg/mL) at room temperature. The soluble and insoluble fractions were separated by centrifugation at 20000g for 30 min. The resultant pellet containing inclusion bodies was resuspended to 10 mg of protein/mL with solubilization buffer (5.0 M guanidine hydrochloride, 50 mM Tris-HC1, pH 8.0,50 mM NaCl, 5 mM MgCl$_2$, 1 mM EDTA, 1 mM DTT, 1 mM PMSF, and 30 μM GDP) and stirred for 2 h. The insoluble material was pelleted by centrifugation at 20000g for 2x20 min, and the supernatant was diluted 100-fold with dilution buffer (solubilization buffer without the guanidine hydrochloride) to give a final protein concentration of 100 μg/mL. The diluted solubilized protein was incubated without stirring for a further 3 h. The sample was then dialyzed for 4 h and then overnight against 2 volumes of dialysis buffer (20 mM Tris-HC1, pH 8.0,5 mM MgClz, 1 mM DTT, 1 mM PMSF, 5% glycerol, and 30 pM GDP). The dialyzed material was concentrated using Amicon Centricon-10000 and then loaded onto a Amersham Hi-Trap QFF anion-exchange column (2x5 mL for 4 L culture) preequilibrated with dialysis buffer containing 10 mM NaCl at a flow rate of 2mL min. The protein was eluted using a 165 mL 10-300 mM NaCl gradient. The fractions were analyzed using 12% polyacrylamide gel electrophoresis, and those containing the protein were pooled, concentrated and desalted using Amicon Centricon-10000, lyophilized and stored at -20

°C. The Bio-Rad protein assay [97] (Bradford, 1976) was used to determine protein concentrations using bovine serum albumin (BSA, Sigma) as the standard.

---

[97] Bradford M., *Anal. Biochem.*, **1976**, 72, 248-254.

_____

5.4. SPR analysis

The wild type fusion protein between glutathione S-transferase (GST) and the catalytic domain of the C-Cdc25^{Mm} (GEF from Mouse; portion of $CDC25^{Mm}$ that contains the catalytic domain of the protein) and the recombinant N-terminal His-tagged p21 h-Ras protein (GDP-bound) were purified as previously described [5.3.1.1.].

An NTA sensor chip, presenting high affinity for hystidine residues after activation with $NiCl_2$ was employed for p21 h-Ras protein immobilization. In particular, the chip was activated through injection on both the cells of 30µl of 500 µM $NiCl_2$ in the running / eluent buffer (10 mM Na HEPES, pH 7.4, 150 mM NaCl, 5 mM $MgCl_2$, 0.005% Tween 20, 0.3% TFE) with a flow of 30 µL/min.

Ras-GDP was immobilized on the chip on the FC2 with a concentration of 100 nM by an injection of 70 µL (flow 30 µL/min). After 5 min, injection of 50 µl of 50 nM C-Cdc25^{Mm} (flow of 10 µL/ min) on FC1 and FC2 was made. In order to study our inhibitor effect on Ras-GDP Cdc25 interaction, each molecule (diluted immediately before use in the running buffer) was injected immediately after Ras-GDP on both the cells with a with the concentrations of 0.5 µM, 1 µM, 3 µM, 5 µM and 10 µM (flow of 10 µL/min for 5 min), followed by C-Cdc25^{Mm} injection. Cdc25 binding to Ras was measured as a change in the resonance signal in time.

After every Ras-GDP-Cdc25 or Ras-GDP-inhibitor-Cdc25 injection, the chip was completely regenerated injecting the regeneration buffer (Hepes 10mM, NaCl 150 mM, EDTA 350 mM, Tween 20 0.005% pH 8.2). Every 10 interaction experiment, further a regeneration of the chip was performed with protease K 1 ug/mL in SDS 0.5%.

5.5. NMR Ras-inhibitor binding studies

5.5.1. Ligand-based binding studies

NMR spectra for compounds **39**-**44** and **SCH-54292** were recorded at 293 K on a Bruker Avance 500 MHz spectrometer; NMR spectra for compounds **61** and **62** were recorded at 293 K on a Varian 400 MHz MERCURY instrument.

5.5.1.1. Sample preparation

For the experiments with the free ligand, compounds **43** and **44** were dissolved in a d_{11}-Tris buffer at pH=7.3, containing 100 mM NaCl and 5 mM MgCl$_2$; for compounds **39**-**42, SCH-54292** and **61** and **62** 10% CD$_3$OD was added. COSY, TOCSY, and HSQC experiments were performed by using the standard sequences. A mixing time of 800 ms was employed for NOESY experiments.

For the binding experiments, p21 h-Ras, expressed and purified as previously described [5.3.1.1.] was dissolved in 405 µL of the same d_{11}-Tris buffer, containing an amount of GDP equimolar to the protein, and transferred into a 5 mm NMR tube; 45 µL of the ligand solution (molecules **39**-**42, SCH-54292** and **61** and **62** were dissolved in CD$_3$OD, molecules **43** and **44** in D$_2$O) were added slowly, and the mixture was incubated at 4 °C overnight.

_____

5.5.1.2. Binding experiments

trNOESY experiments were carried out without saturation of the residual HDO signal. Optimized mixing times of 200 and 250 ms and molar ratios between 15:1 and 30:1 of compound/protein were employed.

In _relaxation-edited experiments_, T_1 and $T_{1\rho}$ values were calculated for the same ligand protons in the free state and in the presence of p21 h-Ras-GDP complex. Selective ^{1}H T_1 relaxation times were measured using the standard inversion recovery method with selective pulses at the resonance of interest. $T_{1\rho}$ experiments used a spin-lock period of ca. 4000 Hz. In both cases, fourteen different delays were used to monitor the decay of the magnetization. The experiments were repeated for the free molecules and in the presence of Ras-GDP. The relaxation delays for selective T_1 were chosen to cover values between 0.1 and 3 s, while those for $T_{1\rho}$ covered values between 0.05 and 2 s. All the spectra were processed using the program Mestre-C. T_1 and $T_{1\rho}$ values were extracted from fitting the integral of a given proton signal as a function of the relaxation delay, according to a single exponential decay: $y=-a*exp(-x/b)$ where $b=T_1$ or $T_{1\rho}$.

STD experiments were performed, without saturation of the residual HDO signal, for molar ratios between 15:1 and 50:1 of compound/protein. A train of Gaussian-shaped pulses of 50 ms each was employed, with a total saturation time of the protein envelope of 2 s. MaxB$_1$ field strength : 50 Hz. An off-resonance frequency of 40 ppm and on-resonance frequencies between δ=0.8 and -1.5 ppm (protein aliphatic signals region) were applied.

In all cases, line broadening of ligand protons was monitored before and after every binding experiment in order to check our compounds stability.

_____

5.5.2. Protein-based binding studies

All NMR spectra were recorded at 293 K on a Bruker Avance 500 MHz spectrometer. They were processed and assigned using the programs Mestre-C and TopSpin.

5.5.2.1. Sample preparation

4.1 mg of ^{15}N p21h-Ras(1-166), expressed and purified as previously described [5.3.2.], was dissolved in 500 µL of NMR buffer (95% H_2O/5% D_2O containing 20 mM d_{11}-Tris-HCl, pH (or pD) 6.7, 40 mM NaCl, 5 mM $MgCl_2$, 0.01% sodium azide, and 30 µM GDP), obtaining a final protein concentration of 0.434 mM.

In order to perform the ^1H/^{15}N-HSQC titration, compound **41** was dissolved in CD_3OD and added in portions to the protein solution, according to the quantities reported in Table 5-1. After every addition, the mixture was incubated at room temperature for 1 h before spectra recording.

P:L	q.ty of L	added L q.ty	added vol.*
1:0.25	0,05425 umol = 22,48 ug	22,48 ug	3,75 ul
1:0.50	0,10850 umol = 44,97 ug	22,48 ug	3,75 ul
1:0.75	0,16275 umol = 67,45 ug	22,48 ug	3,75 ul
1:1.00	0,21700 umol = 89,93 ug	22,48 ug	3,75 ul
1:1.25	0,27125 umol = 112,4 ug	22,49 ug	3,75 ul
1:2.00	0,43400 umol = 179,9 ug	67,50 ug	11,25 ul
			tot. 30 ul

*of a 6 mg/mL solution of **41** in CD_3OD.

Table 5-1. Ligand quantities (column 4) added to Ras sample according to protein:ligand ratios (P:L) (column 1) employed in ^1H/^{15}N-HSQC titration.

_____

5.5.2.2. ^{1}H/^{15}N-HSQC titration

^{1}H, NOESY, TOCSY and ^{1}H/^{15}N-HSQC spectra were recorded by using the standard Bruker sequences. ^{15}N-p21h-Ras(1-166) ^{1}H/^{15}N-HSQC spectrum assignments were compared with data present in literature.[98] To perform the titration, ^{1}H and ^{1}H/^{15}N-HSQC spectra were recorder for different protein-ligand ratios (1:0.25, 1:0.5, 1:0,75, 1:1, 1:1.25, 1:2) and they were then compared, looking for changes in protein signals chemical shifts of both ^{1}H and ^{15}N. Moreover, ^{15}N-HSQC spectra of Ras sample added of different CD$_3$OD volumes were also acquired and analyzed, to evaluate possible CD$_3$OD effects.

_____

[98] Kraulis P. J., Domaille P. J., Campbell-Burk S. L., Van Aken T., and Laue E. D., "Solution Structure and Dynamics of Ras p21-GDP Determined by Heteronuclear Three- and Four-Dimensional NMR Spectroscopy", *Biochemistry*, **1994**, 33, 3515-3531.

Papers

1. Peri F., Airoldi C., Colombo S., Martegani E., Van Neuren A. S., Stein M., Marinzi C., Nicotra F., *Design, Synthesis and Biological Evaluation of Sugar-Derived Ras Inhibitors*, ChemBioChem, **2005**, 6, 1839-1848.

2. Peri F., Airoldi C., Colombo S., Mari S., Jimenez-Barbero J., Martegani M., Nicotra F., *Sugar-derived Ras inhibitors: Group Epitope Mapping by NMR Spectroscopy and Biological Evaluation*, Eur. J. Org. Chem. **2006**, 3707–3720.

3. Colombo S., Peri F., Airoldi C., Tisi R., Fantinato S., Palmioli A., Martegani E., Nicotra F., *Structure-activity relationship in Ras inhibitors,* Bioorg. Med. Chem., submitted.

4. Nicotra F., Airoldi C., Cardona F., *Synthesis of C- and S-Glycosides*, Comprehensive Glycoscience, Elsevier Science Ltd.

Oral communications

1. Peri, F.; Airoldi, C.; Martegani, E.; Colombo, S.; and Nicotra, F., *Progettazione, sintesi e caratterizzazione biologica di potenziali inibitori di RAS derivanti da zuccheri*, IX Convegno sulla Chimica dei Carboidrati, Pontignano (SI), 20-23 Giugno **2004**;

2. Peri, F.; Airoldi, C.; Martegani, E.; Colombo, S.; and Nicotra, F., *Design, synthesis and biological evaluation of sugar-derived Ras inhibitors*, Sugar in the synthesis of natural products, Paszkowka (Krakow), June 8-13 **2005**;

_____

3. Airoldi C., Peri F., Colombo S., Martegani E., Vanoni M., Jimenez-Barbero J., Nicotra F., *A novel class of Ras protein inhibitors based on glycidic scaffolds*, X Convegno-Scuola sulla Chimica dei Carboidrati, Pontignano 25-29 Giugno **2006**.

4. Airoldi C., Peri F., Jimenez-Barbero J., Assfalg M., Molinari H., Colombo S., Nicotra F., *New Ras protein inhibitors and their interaction with the target: the NMR point of view*, XXXVI National Congress on Magnetic Resonance, Vietri sul Mare, Salerno – Italy, September 20-23 **2006**.

Communications

1. Peri F.; Airoldi C.; Martegani E.; Colombo S.; and Nicotra F., *Synthesis and biological evaluation of potent sugar-derived Ras protein inhibitors*, 22nd International Carbohydrate Symposium, 23-27 July **2004**, Glasgow, UK (Poster);

2. Colombo, S.; Tisi, R.; Airoldi, C.; Peri, F.; Nicotra, F. and Martegani E., *Studies on the mechanism of action of a new class of inhibitors of Ras activation*, The protein world, 30th FEBS Congress and 9th IUBMB Conference, 2-7 July **2005**, Budapest, Hungary (Poster);

3. Peri, F., Airoldi, C.; Colombo, S.; Marinzi, C.; Martegani, E.; Nicotra, F., *Novel Sugar-Derived molecules inhibit oncogenic Ras activation*, XVIII International Symposium on Glycoconjugates, 4-9 September **2005**, Firenze (Oral comunication);

4. Mari, S.; Airoldi, C.; Peri, F.; Nicotra, F.; Potenza, D.; Bernardi, A. and Jimenez-Barbero, J., *Small Molecules Binding to Protein Receptors: the NMR point of view*, SMASH, **2005**, Verona (Oral comunication);

5. <u>Peri F.</u>, Airoldi C., Colombo S., Martegani E., Nicotra F. *Sugar-derived inhibitors of Ras protein activation: novel compounds with anti-tumor activity*, Congresso Nazionale della Divisione di Chimica dei Sistemi Biologici della Società Chimica Italiana, Rimini, 4 Ottobre **2005** (Invited lecture);

6. <u>La Ferla B.</u>, Russo L., Airoldi C., Nicotra F. *GDP-L-Galactose mimic for affinity chromatography*, X Convegno-Scuola sulla Chimica dei Carboidrati, Pontignano 25-29 Giugno **2006** (Poster);

7. <u>Peri F.</u>, Airoldi C., Colombo S., Martegani E., Nicotra F. *Sugar-based antitumor drugs: selective inhibitors of human Ras protein derived from D-arabinose*, Targeted therapies in cancer. Myth or reality?, September 4/5 **2006**, Milan (Poster).

Il ringraziamento più grande va certamente ai miei genitori, per avermi sempre consentito, grazie al loro supporto, di realizzare ciò che desideravo e per non aver mai contrastato o anche solo influenzato le mie scelte; lode inoltre al merito di avermi "sopportato" fino ad ora.

Mi fa poi molto piacere ricordare tutti i ragazzi che ho conosciuto durante i mesi trascorsi a Madrid nel laboratorio del Prof. Jimenez Barbero, in particolare Carmen, "Super Vicky" ed Alba, che hanno reso la mia permanenza molto piacevole; coloro i quali, oltre che piacevole, l'hanno resa anche estremamente fruttuosa sono certamente Jesus e Silvia, che ringrazio per tutto quello che mi hanno consentito di imparare.

Potrei poi mai dimenticarmi di tutti gli "stranieri" che hanno popolato il nostro laboratorio in questi anni? Certo che no! Un affettuosissimo abbraccio a Iris, Ines, Isabel, Marek, ma soprattutto Marcos e Ingrid.

Grazie a tutti i tesisti e "stagisti" che hanno collaborato con me a questo progetto (Giulia, Silvia, Erika, Nicola e Marco) e a tutti coloro i quali sono passati dal lab. 4048 in questi anni.

Grazie a Cry (tra l'altro per averci recentemente annunciato che i mirabili discorsi relativi a poppate, pannolini, pappe e notti in bianco sono ben lungi dal terminare) al Krama, e alla "masnata di disgraziati" del 4018 (leggi Paolino, Maria e Chiara); spero che il clima armonioso che si è venuto a creare negli ultimi tempi grazie a tutti possa durare a lungo e spero che la nostra bella conoscenza si tramuti presto in amicizia (mi sembra che siamo sulla strada buona).

Grazie a Laura per la sua amicizia, per i bei momenti passati insieme, per la mia cameretta sempre pronta.

Un ringraziamento particolare poi agli "anziani" (come sono diplomatica!) del gruppo. Grazie a Laura perché, benchè, tra una cosa e l'altra, non siamo ancora riuscite ad approfondire bene la nostra conoscenza (rimedieremo), quando contava c'è comunque sempre stata; grazie alla mia ormai definitivamente "sorella maggiore adottiva" Barbara, per le chiaccherate, per i consigli, per le pacche sulle spalle date al momento giusto … e per mio "nipote"; grazie a Francesco per il suo aiuto, per i suoi insegnamenti e per l'entusiamo che ha sempre riversato nel lavoro che gli auguro di non perdere mai: in un momento per me cruciale per decidere che cosa volessi fare "da grande" è stato molto importante avere vicino una persona come lui; infine grazie allo "zio Nik", per tante cose, ma per una in particolare: perché per quanto una persona possa essere capace e determinata, ha sempre bisogno di qualcuno che creda in lei.

Per ultime voglio ringraziare le tre persone che mi sono state più vicine e con le quali ho avuto il piacere e la fortuna di condividere molto più che con altri timori, momenti di tensione e sconforto, difficoltà ma anche soddisfazioni, divertimenti e … sogni: Ciccio (sempre e per sempre il nostro eroe) Catarina ed Ale. La mia speranza più grande è che ovunque (in senso lato) le nostre aspirazioni e le nostre scelte ci porteranno, troveremo sempre il modo di rimanere "uniti".